

EVALUATION OF OUTDOOR LIGHTING DESIGN BASED ON MESOPIC DIMENSIONING

*A thesis submitted towards partial fulfilment
of the requirements for the degree of*

MASTER OF ENGINEERING IN ILLUMINATION ENGINEERING

Submitted by

TANMAY DAS

EXAMINATION ROLL NUMBER: M4ILN23002

REGISTRATION NO.: 160190 of 2021-22

Under the guidance of

**Mrs. SANGITA SAHANA
ASSISTANT PROFESSOR**

DEPARTMENT OF ELECTRICAL ENGINEERING

FACULTY OF ENGINEERING AND TECHNOLOGY

JADAVPUR UNIVERSITY

KOLKATA – 700032

INDIA

2023

CERTIFICATE OF RECOMMENDATION

This is to certify that the thesis entitled "**EVALUATION OF OUTDOOR LIGHTING DESIGN BASED ON MESOPIC DIMENSIONING**" is a bonafide work carried out by **TANMAY DAS** (Exam. Roll No. **M4ILN23002** Registration No. **160190 of 2021-22**) under my supervision and guidance for partial fulfilment of the requirement of Master of Engineering in Illumination Engineering, during the academic session 2022 - 2023.

(Thesis supervisor)
Mrs. SANGITA SAHANA
Assistant Professor,
Electrical Engineering Department,
Jadavpur University,
Kolkata - 700032.

Countersigned:

Prof. (Dr.) BISWANATH ROY
Head of the Department,
Electrical Engineering Department,
Jadavpur University,
Kolkata-700032.

Prof. (Dr.) SASWATI MAZUMDAR
Dean,
Faculty of Engineering Technology,
Jadavpur University,
Kolkata-700032.

CERTIFICATE OF APPROVAL

This foregoing thesis is hereby approved as a credible study of an engineering subject carried out and presented in a manner satisfactorily to warranty its acceptance as a prerequisite to the degree for which it has been submitted. It is understood that by this approval the undersigned do not endorse or approve any statement made or opinion expressed or conclusion drawn therein but approve the thesis only for purpose for which it has been submitted.

**Committee of final examination
for evaluation of Thesis**

DECLARATION OF ORIGINALITY AND COMPLIANCE OF **ACADEMIC ETHICS**

It is hereby declared that this thesis contains literature survey and original research work by the undersigned candidate, as part of his Master of Engineering in Illumination Engineering, studies during academic session 2022-2023.

All information in this document has been obtained and presented in accordance with academic rules and ethical conduct.

I also declare that, as required by this rules and conduct, I have fully cited and referred all material and results that are not original to this work.

NAME : TANMAY DAS
EXAMINATION ROLL NUMBER : M4ILN23002
REGISTRATION NUMBER : 160190 of 2021-22
THESIS TITTLE : EVALUATION OF OUTDOOR
LIGHTING DESIGN BASED
ON MESOPIC DIMENSIONING

SIGNATURE:

DATE:

ACKNOWLEDGEMENT

I take this opportunity to express my deep sense of gratitude and indebtedness to Mrs. Sangita Sahana, Assistant Professor, Electrical Engineering Department, Jadavpur University, Kolkata, without his mission and vision, this project would not have been possible.

I would like to acknowledge my sincere thanks to Prof. (Dr.) Saswati Mazumdar, Electrical Engineering Department, Jadavpur University, and Prof (Dr.) Suddhasatwa Chakraborty, Electrical Engineering Department, Jadavpur University for their constant guidance and supervision. I would also like to thank them for providing me their valuable time and helpful suggestions.

Again, I would like to acknowledge my sincere thanks to Prof. (Dr.) Biswanath Roy, HOD of Electrical Engineering Department, Jadavpur University for providing me the opportunity to carry out my project work in Illumination Engineering Laboratory, Jadavpur University.

I am also thankful to Mr. Samir Mandi and Mr. Pradip Pal of the Illumination Engineering Laboratory for their Co-operation during my project work.

Last but not least, I wish convey my gratitude to my parents, whose love, teachings and support have brought me this far.

Date:

Place : Jadavpur University

Kolkata – 700032

TANMAY DAS

LIST OF CONTENTS	PAGE NO.
Abstract	1
Chapter 1: Introduction	2-9
1.1 Literature Survey	4
1.2 Problem Definition	7
1.3 Objective	7
1.4 Methodology	8
1.5 Outline Of Dissertation	8
Chapter 2: Mesopic photometry	10-22
2.1 Introduction	11
2.2 Human eye and photometric quantities	11
2.3 Contribution of Rods and Cones to Human vision	12
2.4 Photometry & Human visual Response to light	13
2.5 Photometric vision	13
2.5.1 Photopic vision	14
2.5.2 Scotopic Vision	14
2.5.3 Mesopic vision	14
2.6 Spectral eye sensitivity	15
2.7 S/P Ratio	16
2.8 Brief description of the mesopic models	17
2.9 Application of mesopic system	19
2.10 Limitation of mesopic photometry	21
2.11 Calculation of Mesopic Luminances	22
2.12 Comparison of Light Sources	22
Chapter 3: Lamps: Classification, Construction & their Working	23-39

3.1 Different types of Lamps	24
3.1.1 Lamps Used in Outdoor Lighting	24
3.1.2 Color temperature of light sources	25
3.2 Construction & Operating Principle of Lamps used in Outdoor Lighting	27
3.2.1 Compact Fluorescent Lamps	27
3.2.1.1 Construction & working principle	27
3.2.1.2 Lamp Properties	28
3.2.2 Constructional Feature of a Metal Halide Lamp	29
3.2.2.1 Working of Metal Halide Lamp	29
3.2.2.2 Establishment of arc Inside the Metal Halide Arc Tube	31
3.2.2.3 Lamp Properties	31
3.2.3 High-Pressure Sodium Lamps	32
3.2.3.1 Construction of HPSV lamp	32
3.2.3.2 Working of HPSV lamp	33
3.2.3.3 Lamp Properties	35
3.2.4 Solid State Light or Light Emitting Diode or LED	35
3.2.4.1 Working of LED	36
3.2.4.2 Direct Band Gap	37
3.2.4.3 Indirect Band Gap	38
3.2.4.4 White LED (WLED)	38
Lighting design and standards	40-65
4.1 Introduction to Lighting Design	41
4.2 Lighting Design Parameters	41
4.3 Application of Lighting Design Parameters	44
4.4 Mesopic Vision and Lighting Design	45
4.5 Mesopic Photometry Standards and Recommendations	46
4.5.1 CIE 191:2010	46
4.5.1.1 Recommended System For Performance Based Mesopic Photometry	46

4.5.1.2 System for mesopic photometry based on	
visual task performance	49
4.5.1.2.1 USP-SYSTEM	51
4.5.1.2.2 MOVE – SYSTEM	55
4.5.1.2.3 Intermediate-System	60
Chapter 5: Lighting design in photopic region	66-85
5.1 Design using high pressure sodium vapour light (HPSV)	67
5.1.1 Luminaire Details	67
5.1.2 Design Considerations	67
5.2 Design using Metal Halide lamp (MH)	73
5.2.1 Luminaire Details	73
5.2.2 Design Considerations	73
5.2 Design using Cool White LED	79
5.3.1 Luminaire Details	79
5.3.2 Design Considerations	79
Chapter 6: Lighting design in mesopic region	86-108
6.1 Method for converting photopic data to the corresponding mesopic data	87
6.2 DIALUX design using modified photometric file	90
6.2.1 Design using high pressure sodium vapour light (HPSV)	90
6.2.1.1 Luminaire Details	90
6.2.1.2 Design Considerations	90
6.2.2 Using Metal Halide lamp (MH)	96
6.2.2.1 Luminaire Details	96

6.2.2.2 Design Considerations	96
6.2.3 Design using Cool White LED	102
6.2.3.1 Luminaire Details	102
6.2.3.2 Design Considerations	102
Chapter 7: Result analysis	109-117
7.1 Comparison of Photopic luminance (L_p), Calculated mesopic luminance (L_m) & Simulated mesopic luminance (L_{ms}) for different lamps	110
7.1.1 For High Pressure Sodium Vapour (HPSV) lamp	110
7.1.2 For Metal Halide (MH) lamp	112
7.1.3 For Cool White LED (CWLED)	114
7.2 Comparison of average luminances for different lamps	116
7.3 Validation of the proposed Model	118
Chapter 8: Conclusions & Future scope	119
References	121

Abstract

The sensitivity of the human eye varies with the different lighting conditions to which it is exposed. The cone photoreceptors perceive the color and work for illuminance conditions greater than 3.00 cd/m^2 under photopic vision. Below 0.01 cd/m^2 , the rods are the cells that assume this function under scotopic vision. Both types of photoreceptors work coordinately in the interval between these values which is known as mesopic vision. Each mechanism generates a different spectral sensibility. DIALux is a widely-used lighting design software that primarily relies on photometric values for its simulations and calculations. However, the transition from photopic to mesopic vision, especially in outdoor and transitional lighting scenarios, presents significant opportunities for improving lighting design efficiency and effectiveness. This thesis work tries to focus on transformation of the photopic luminous flux provided by the manufacturer of the luminaire into its equivalent mesopic luminous flux and simulate average mesopic luminance values by using DIALux light simulation software and tries to study comparative analysis of simulated photopic luminance, calculated mesopic luminance from CIE191:2010 and simulated mesopic luminance of different lamps.

CHAPTER 1

INTRODUCTION

INTRODUCTION

There are three categories of vision: scotopic, mesopic and photopic. The activity of the two types of light-sensitive cells in the eye, the cones and the rods, is different in each category. At very low adaptation levels only rods are active and vision is scotopic. With rising adaptation levels, from 0.005 cd/m^2 , the cones become gradually active and the rods less active. Vision is then mesopic. At adaptation levels higher than 5 cd/m^2 only the cones are active and vision is photopic. Most road lighting installations have lighting levels corresponding to mesopic vision. The cones and rods have differing spectral sensitivities: the rods are more sensitive to short wavelengths while the cones have their maximum sensitivity in the middle of the visible spectrum. ^[1]

In mesopic conditions, the human eye undergoes a transition between relying predominantly on rod cells in dim light to incorporating cone cells as light levels increase. This transition introduces several challenges in accurately assessing the brightness, color perception, and visibility of objects. Therefore, mesopic photometry seeks to bridge the gap between scotopic and photopic measurements to provide a more comprehensive understanding of visual performance in real-world situations, such as street lighting, automotive headlights, and outdoor signage.

The introduction of mesopic photometry has been driven by the need to develop lighting solutions and visual standards that optimize visibility and safety in various environments, especially during the twilight hours or in situations where artificial lighting is used. By considering the combined sensitivity of both rod and cone cells, mesopic photometry allows for more precise measurements of illuminance, luminance, and related parameters under conditions that were previously not well-understood.

In the context of integrating mesopic photometry into outdoor lighting according to the CIE 191:2010 standard^[2], this study introduces two streamlined approaches for quantifying mesopic luminance. These methodologies are designed to facilitate practical implementation. The first method, referred to as the Adaptation Spectral Power Distribution (ASPD) method, operates on the premise that the spectral power

distributions (SPDs) of light reflected from designated test locations on the road surface closely resemble the SPD of the adaptation field. In contrast, the second method, denominated the Source Spectral Power Distribution (Source SPD) method, posits that the SPDs of the reflected light are essentially equivalent to the SPD of the primary light source being utilized in the lighting system. These methods present simplified frameworks for mesopic luminance assessment, which can be instrumental in ensuring the effective deployment of mesopic photometry in outdoor lighting applications adhering to the CIE 191:2010 standard.^[7]

In the realm of mesopic photometry, it's crucial to consider the Scotopic/Photopic (S/P) ratio of a light source. This ratio is essential for calculating mesopic luminance. Essentially, the S/P ratio tells us how well a light source performs in terms of mesopic design. A higher S/P ratio indicates that the light source is more effective for mesopic vision. When the S/P ratio is greater than 1, it means that the light source emits more light in the shorter wavelength range. This characteristic is particularly advantageous for road lighting applications, as it contributes to energy-efficient design. In practical terms, many white light sources have a higher S/P ratio, making them well-suited for road lighting where energy efficiency is a key consideration. LED technology has emerged as a promising solution in mesopic applications. LEDs can produce light with varying spectral properties, and they tend to have high mesopic luminous efficacy functions. This makes them an attractive choice for energy-efficient mesopic lighting design.^[2]

1.1 Literature survey

- **Adjustment of Lighting Parameters from Photopic to Mesopic Values in Outdoor Lighting Installations Strategy and Associated Evaluation of Variation in Energy Needs.** Enrique Navarrete-de Galvez 1 , Alfonso Gago-Calderon 1,* , Luz Garcia-Ceballos 2,Miguel Angle Contreras-Lopez 2 and Jose Ramon Andres-Diaz .^[8]

In this paper, the emission spectra of common sources in present public lighting installations are analyzed. Based on a common street urban configuration (ME6), a large set of simulations are generated to determine the ideal light point setup configuration (luminance and light point height vs. poles distance ratio) for each case of spectrum source and analyze the derived energy variation from each design possibility. The results obtained may contribute to improving the criterion of light source selection and adapting the required regulatory values to the human eye vision process under normalized artificial street lighting condition, reaching an average energy saving of 15% and a reduction of 8% in terms of points of light required. They also offer a statistical range of energy requirements for lighting installation that can be used to generate accurate electrical designs or estimations without the necessity of defining the exact lighting configuration, which is 77.5% lower than conventional design criteria.

- **Simplified field measurement methods for the CIE mesopic photometry system** by T Uchida and Y Ohno, Panasonic Corporation, Osaka, Japan, National Institute of Standards and Technology, Gaithersburg, MD, US;Lighting Res. Technol.2017;Vol.49;774-787 ^[9]

This paper delineates the implementation of a mesopic photometry system within the framework of CIE 191:2010 for outdoor lighting applications. This implementation involves the utilization of two simplified measurement methods to quantify mesopic luminance: 1. Adaptation Spectral Power Distribution Method: This method operates on the premise that the spectral power distributions (SPDs) of the light reflected from test points within the adaptation field are identical to those of the road surface. 2. Source SPD Method: In contrast, this approach posits that the SPD of reflected light matches the SPD of the light source itself. A core contribution of this study is the validation that the Source SPD method can effectively measure mesopic quantities without the necessity of specialized S/P luminance meters. The paper further engages

in an error simulation, utilizing actual spectral reflectance data from road surfaces, to assess the accuracy of both measurement techniques. The findings of this investigation reveal that the Source SPD method exhibits limited sensitivity when applied to lighting scenarios featuring multiple types of light sources. To address this limitation, the paper introduces a correction method as a potential remedy. This correction method is proposed as a means to substantially reduce measurement errors, thereby enhancing the applicability of these techniques to a wider array of road surfaces and lighting conditions.

- **Driver decision making in response to peripheral moving targets under mesopic light levels** Yukio Akashi PhD, MS Rea PhD and JD Bullough PhD Lighting Research Center, Rensselaer Polytechnic institute Troy, NY, USA ^[10]

This paper details a comprehensive field study undertaken to extend the foundational insights regarding visual performance under mesopic lighting conditions to a driving context. The study involved participants operating a motor vehicle on a well-illuminated street while concurrently engaged in a high-level decision-making task. Specifically, the subjects were required to determine the directional movement of an off-center target in relation to the street and subsequently respond by either applying brakes or accelerating accordingly.

Two distinct sets of illumination sources were compared during the study: one comprised of ceramic metal halide light sources, and the other comprised of high-pressure sodium light sources. To ensure robustness, a parallel study was conducted during daylight hours for comparative analysis.

The outcomes of the study showcased a notable trend: as the unified luminance levels increased, both the response times for braking and acceleration exhibited a consistent reduction. This trend suggests that unified luminance stands as a viable and rectifying variable for characterizing light levels across different light source types, particularly concerning intricate visual tasks, such as those encountered during driving scenarios.

- **Defining the visual adaptation field for mesopic photometry Does surrounding luminance affect peripheral adaptation?** T Uchida MEng, b and Y Ohno PhD Panasonic Corporation, Osaka, Japan National Institute of Standards and Technology, Gaithersburg, MD, USA [11]

An adaptation field to determine the adaptation state needs to be defined. To address this issue, vision experiments have been conducted to measure surrounding luminance effects on the adaptation state at a peripheral task point. The results reveal that the adaptation state depends mainly on the local luminance at the task point but there is also a small effect of the surrounding luminance. The results suggest that the surrounding luminance effect is larger than the veiling luminance predicted with existing foveal models; nevertheless, it is not significant for the mesopic luminance on uniform luminance distributions.

- **CIE Mesopic photometry –implementation for outdoor lighting** by Liisa Halonen, Grega Bizjak, laboratory of Lighting & photometry. [12]

This study encompasses an examination of the limitations associated with the MOVE and X models. It is noted that these two models share a similar foundational concept but produce divergent outcomes. The paper proceeds to underscore the significance of aligning with the CIE 191:2010-recommended system for mesopic photometry, grounded in considerations of visual performance.

A core focal point of this research is the pivotal role of Adaptation Luminance in the computation of mesopic values. It is established that mesopic photometry outcomes are substantially influenced by the Adaptation Luminance, particularly when the visual adaptation field extends beyond the confines of the road environment.

1.2 Problem Definition

Outdoor lighting installations incorporate different types of lamps such as High Pressure Sodium Vapour (HPSV), Metal Halide (MH) and CWLEDs. The luminance level generally lies in mesopic zone for different types of outdoor lighting systems. The

performance for different lamps in outdoor lighting scenario under Mesopic luminance range are studied and compared.

1.3 Objectives

The objectives of the thesis are:

- To study the behaviour of different lamps under mesopic conditions.
- Simulation of photopic and mesopic Luminance using DIALux software.
- To compare simulated photopic luminance, simulated mesopic luminance and the mesopic luminance calculated from CIE 191:2010 Table for different lamps.

1.4 Methodology

- Simulation of photopic luminance using DIALux software.
- Determination of S/P ratios.
- Calculation of Mesopic Luminance from CIE191:2010.
- Determination of M/P (mesopic/photopic) ratio.
- Original photopic luminance value is modified with the corresponding mesopic values, obtained by multiplying the source luminance values by the M/P ratio adequate in each case.
- Simulation of mesopic luminance using dialux software.
- Comparison of simulated photopic luminance, simulated mesopic luminance and calculated mesopic luminance from CIE191:2010 for different lamps.

1.5 Outline of Dissertation

- Chapter 1 gives the introduction to this thesis It also states the objective and

methodology of the thesis.

- Chapter 2 discusses the concepts of mesopic photometry.
- Chapter 3 discusses the constructional aspects working principle of different lamps used in outdoor lighting system.
- Chapter 4 discusses lighting design and standards.
- Chapter 5 deals with lighting design in photopic region.
- Chapter 6 deals with lighting design in mesopic region.
- Chapter 7 shows comparisons and analysis of the results.
- Chapter 8 draws the conclusion to the experiment and discusses the future scopes of the field of study.

CHAPTER 2

MESOPIC PHOTOMETRY

2.1 Introduction

Photometry, as a scientific discipline, concerns itself with the quantification of light in various conditions of stimulus and observation. It aims to measure and evaluate light in a precise manner. Vision can be categorized into three main types: scotopic, mesopic, and photopic. These categories are distinguished by the differential activity of two types of light-sensitive cells in the eye, namely cones and rods. Each category of vision exhibits unique characteristics. In scotopic vision, which occurs at very low adaptation levels below 0.005 cd/m^2 , only the rods are active, resulting in a limited visual capacity. Mesopic vision, on the other hand, emerges as adaptation levels increase from 0.005 cd/m^2 to 5 cd/m^2 . During this phase, the cones gradually become active, while the rods become less active. In mesopic vision, both cones and rods contribute to visual perception. Finally, at adaptation levels exceeding 5 cd/m^2 , only the cones are active, leading to photopic vision. In most road lighting installations, the lighting levels are designed to correspond to mesopic vision. This choice takes into consideration the differing spectral sensitivities of cones and rods. Rods exhibit greater sensitivity to short wavelengths, while cones are most sensitive to the middle range of the visible spectrum. Moreover, cones are predominantly concentrated in the region of the retina responsible for central or on-line vision, whereas rods are primarily located in the peripheral vision areas. As a consequence of these factors, in mesopic vision, peripheral task performance and the subjective perception of brightness improve when light sources have a relatively large short wavelength component. This effect becomes more pronounced at lower lighting levels due to the increased activity of rods. However, since photometric units are based on photopic vision, these advantages are not readily apparent. Therefore, correction factors have been determined based on the light source's spectrum, characterized by its S/P ratio, and the lighting level obtained from the road lighting installation. These correction factors help account for the differences between photopic and mesopic vision when evaluating lighting conditions.

2.2 Human eye and photometric quantities

Figure 2.1 illustrates the mechanism of color vision in the human eye. The retina, located in the innermost portion of the eyeball, is responsible for detecting light and contains two types of light-sensitive photoreceptor cells: rods and cones. Within the retina, there is a small depression known as the fovea, located at the center of the Macula Lutea, which exclusively contains cone cells and lacks rod cells. The fovea plays a crucial role in providing high visual acuity and color perception. The figure also provides an overview of the cellular structure of the retina, including the presence of rods and cones. When light enters the eye and falls on the retina, the rods and cones become stimulated and generate nerve impulses that are transmitted via the optic nerve to the brain. Upon exposure to light, the visual pigments within the retinal receptors, namely Rhodopsin and Iodopsin, undergo breakdown into their respective components. This breakdown process facilitates the generation of visual impulses within the receptors. In darkness, the pigments are synthesized again for reuse. This cyclic breakdown and synthesis of visual pigments in response to light and darkness is referred to as the photochemical cycle of the retina. The retina contains a central region called the macula, with the Fovea Centralis positioned at its exact center. The distribution of rods and cones within the retina is not uniform. The concentration of cone cells is highest at the Fovea, while the presence of rods is minimal in this area. Conversely, the peripheral zone of the retina has a high concentration of rod cells. The intermediate region between the Fovea and the peripheral zone contains both rod and cone cells.^[5]

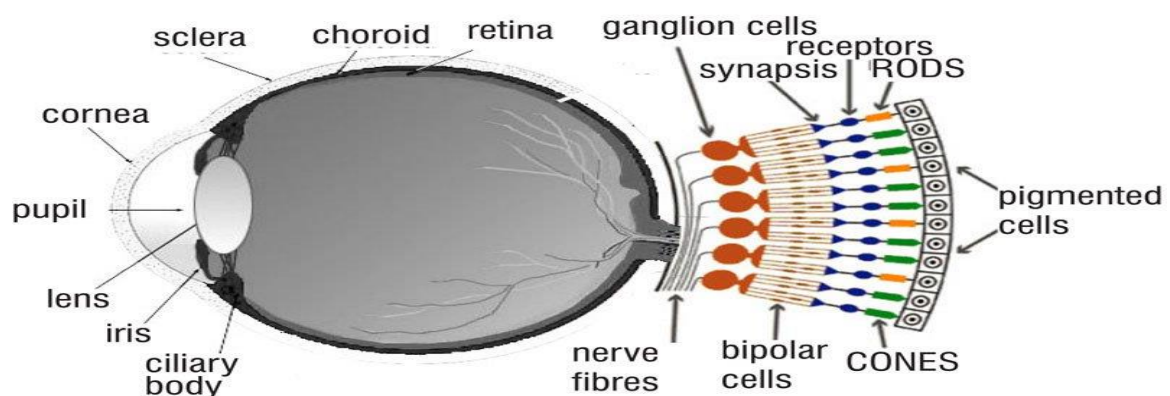


Fig 2.1 Structure of human eye

2.3 Contribution of Rods and Cones to Human vision

Within the retina of the eye, there exist two distinct types of photoreceptors: rods and cones. Rod cells, which are highly responsive to light, are distributed throughout the retina but are particularly concentrated in the peripheral region of the eyeball. Operating effectively in low light conditions, rods are responsible for facilitating night vision, a visual phenomenon known as scotopic vision. On the other hand, cone cells are predominantly found in the central region of the retina known as the fovea and are characterized by their heightened sensitivity to colors. Cones enable vision in bright light conditions and are responsible for color perception. There are three types of cones: red cones, green cones, and blue cones, each specialized in detecting specific wavelengths of light. This mechanism of vision is referred to as photopic vision. In addition to scotopic and photopic vision, there exists a third type known as mesopic vision, which occurs in lighting conditions that fall between low and bright light levels. During mesopic vision, both rod and cone cells are simultaneously active.

2.4 Photometry & Human visual Response to light

The branch of optics which deals with the measurement of light is known as 'Photometry'. ('Photo' means light and 'metry' means measurement). The primary aim of photometry is to measure visible radiation or light, in such a way that the results correlate as closely as possible with what the relevant visual sensation would be of a normal human observer exposed to that radiation. The measurement of photometric quantities referring to radiation are evaluated according to a given spectral luminous efficiency function, $V(\lambda)$ or $V'(\lambda)$.^[2]

2.5 Photometric vision

The photometric vision perceived by our eyes can be classified by following three types based on luminance range as well as presence of photoreceptors.

- Photopic Vision
- Scotopic Vision
- Mesopic Vision

2.5.1 Photopic vision

Its luminance level is more than 5 cd /m². Photopic vision provides for color perception, which is primarily cone mediated and perceptions are chromatic. In other words color vision is present in light level of daylight. Maximum efficacy of photopic vision is 683lumen/watt at a wavelength of 555 nm i.e. green light, with photosensitivity of 100%. Sensitivity of human vision in photometry region varies with different visible wavelength. Fine details can be perceived in photopic vision and is known as light adapted vision. Adaptation is faster under photopic vision.

2.5.2 Scotopic Vision

It is known as dark adaptive or night vision. This vision is produced exclusively through rod cells. Rod cells are most sensitive around 498 nm. In scotopic vision luminance level is between 0.000001 cd/m² to 0.005 cd /m² [3]. This type of vision is performed with the rods in the eye. As these are mainly located in the peripheral areas of the retina, visual acuity is low.

2.5.3 Mesopic vision

Mesopic vision is a visual phenomenon that arises from the combined contributions of both rods and cones in the human eye. It occurs in an intermediate light intensity range, lying between photopic (daytime) and scotopic (nighttime) vision regions. The luminance value during mesopic vision ranges from 0.005 cd/m² to 5 cd/m². Mesopic vision is particularly relevant in certain outdoor lighting scenarios and nighttime traffic lighting. In this region, the spectral sensitivity of the human visual system is not fixed but varies with the level of light. To standardize the measurement of mesopic vision, the CIE (Commission Internationale de l'Eclairage) introduced the international system of mesopic photometry, known as CIE 191:2010.[2] This new mesopic photometry system is a linear combination of the efficiency functions from both the photopic and scotopic systems. LED light sources are commonly used in mesopic photometry

applications. As the luminance decreases from the photopic to the mesopic region, the absolute sensitivity of the visual system declines, but there is no change in spectral sensitivity until scotopic vision is reached. During mesopic vision, the rod receptors in the eye begin to dominate over the cone receptors, resulting in a loss of color vision and a shift in spectral sensitivity towards shorter wavelengths. The transition between the sensitivities of light-adapted and dark-adapted eyes is known as the Purkinje effect. This phenomenon explains the differences in color perception between well-lit conditions and low-light conditions.

2.6 Spectral eye sensitivity

In the mechanism of vision, two different types of light-sensitive cells in the retina of the eye play a role i.e. the cones and the rods. The type of cell that is active is dependent on the lighting level to which the eyes are adapted, which in turn is dependent on the luminance level of the scene that is observed. At high adaptation levels (larger than some 5 cd/m^2) it is the cones that are active. That is photopic vision. Colour vision is possible because we have red, green and blue sensitive cones. The spectral sensitivity with photopic vision is characterized by the $V(\lambda)$ curve and reaches its maximum sensitivity at a wavelength of around 555 nm , corresponding to a green-yellow colour as shown in Fig.2.2. All photometric units (luminous flux, luminous intensity, illuminance, luminance, etc.) are based on the $V(\lambda)$ function. At very low adaptation levels, lower than some 0.005 cd/m^2 only the rods are active and we speak of scotopic vision.

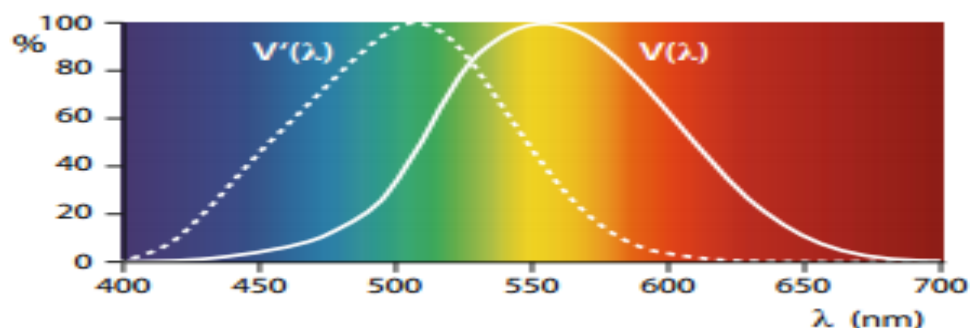


Fig.2.2 Spectral eye sensitivity curves for photopic vision (CIE 1926) and scotopic vision (CIE 1951) ^[1]

The rods have a higher sensitivity to light i.e. 1700 lumen/Watt than do the cones. 683 lumen/Watt. With scotopic or rod vision, colour vision is impossible. The spectral sensitivity with scotopic vision is characterized by the $V'(\lambda)$ curve. It reaches its maximum sensitivity at a wavelength of around 505 nm, corresponding to the colour blue-green whereas in the $V(\lambda)$ curve, there is a clear shift towards the blue end of the spectrum as shown in fig.2.2. At adaptation luminance levels between approximately 5 and 0.005 cd/m² both the cones and the rods are active. That is mesopic vision. In the mesopic vision range, the activity of the rods becomes more important from high to low adaptation levels. As a result, the spectral sensitivity gradually shifts into the direction of small wavelengths—that is to say in the direction of blue as shown in Fig.2.3. The sensitivity scale here is not relative as is commonly the case (Fig.2.2), but in terms of absolute spectral luminous efficacy values, so that the effect of the larger sensitivity of rods, as mentioned above, also becomes apparent. Because of the shift towards the green-blue end of the spectrum, it can be claimed that under road-lighting conditions, where we are mostly in the mesopic vision range, light sources containing more green-blue light (cool-white light) than yellow-red light (warm-white light) are more efficient for vision. Claims are sometimes exaggerated and sometimes made when they are not valid at all. Such claims are valid for peripheral vision but not for on-line vision. [1]

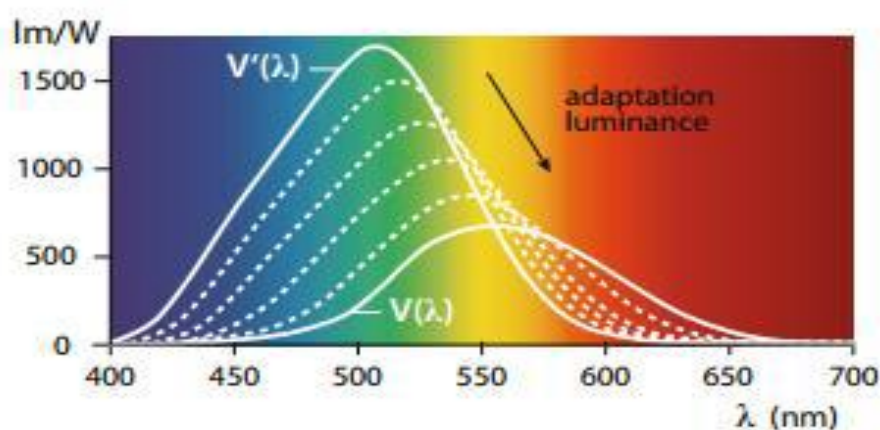


Fig.2.3 Spectral luminous efficacy curves for scotopic $V'(\lambda)$, photopic $V(\lambda)$ and mesopic vision $V_{mes}(\lambda)$ (broken lines). [1]

2.7 S/P Ratio

The human eye exhibits distinct responses to light levels during the day and night. Vision scientists have designated specific names for these responses, known as photopic (for daytime light levels) and scotopic (for nighttime light levels) sensitivities. Recent research has shed light on how to combine these sensitivities to obtain a reliable measure of brightness. To achieve this, scientists have discovered that for any light source, there exists a constant ratio between its scotopic and photopic output. This ratio remains fixed and independent of the light's intensity, and it can be accurately measured using appropriate instruments. Once this ratio is determined, obtaining a scotopic value becomes a straightforward process. One simply needs to multiply the known ratio by the measured or given photopic value (lumens), and this yields the scotopic value.

2.8 Brief description of the mesopic models

In the past many attempts were made to develop a model for mesopic vision. Several authors have measured the spectral sensitivity functions in the mesopic domain (Walters and Wright, 1943; Kinney, 1958; Palmer, 1968; Kokoschka and Bodmann, 1975; Ikeda and Shimozone, 1981; Yaguchi and Ikeda, 1984; Sagawa and Takeichi, 1986; Sagawa and Takeichi, 1987; He et al., 1998). All these studies proposed a specific spectral sensitivity as a function of the adaptation light level in the mesopic range. However, it appeared to be difficult to establish a consistent mesopic model. In 1989 the CIE published a report on the status of mesopic photometry, without actually establishing a standard model for mesopic vision (CIE, 1989). After that publication new methods and refinements of the existing models were proposed. In 2001 a new CIE report was published (CIE, 2001), updating the CIE publication of 1989. Seven mesopic models were addressed in this publication, which are based on 100 visual field and heterochromatic brightness matching (HCBM). Table 2.1 lists these mesopic models and their most important parameters, together with four mesopic models based on reaction time (RT) which were published elsewhere. With these models it is possible to calculate the so-called equivalent luminance, using various types of input variables. The equivalent luminance is defined as the luminance of the reference

stimulus (formally with wavelength of nearly 555 nm, but also often a broadband white light) that appears equal to the test stimulus in brightness (CIE, 2001). The equivalent luminance has a better correlation to the visual impression or task performance than the common photopic luminance based on the $V(\lambda)$ function. Instead of the more formal term equivalent luminance, the term mesopic luminance will be used in this study to designate the output of mesopic models. The seven models are based on HCBM experiments in which the task of the subjects was to match the brightness of two parts of a static stimulus with a diameter of 10 degrees. The currently widely-used luminous efficiency function for photopic vision, $V(\lambda)$, is mainly based on flicker photometry using a 2-degreelfield in which the two parts of the stimulus are compared by presenting them in an alternating mode. These differences in the tasks and conditions result in different shapes of the spectral sensitivity function in photopic conditions. A stimulus with a saturated colour (e.g. monochromatic blue or red) that has the same luminance as a white stimulus is perceived as brighter than the white stimulus. This effect is known as the Helmholtz–Kohlrausch effect (Wyszecki and Stiles, 1982). Therefore the spectral sensitivity functions based on photopic brightness matching are wider than the luminous efficiency function $V(\lambda)$ which is incorporated in the vast majority of all luminance meters and illuminance meters. The spectral luminous efficiency function for scotopic vision, $V'(\lambda)$, is determined by HCBM using a 20-degree field (CIE, 1983). Thus, because of differences in task and stimulus diameter, it is difficult to merge the sensitivity functions to a single model. There is no smooth connection between the existing spectral sensitivity data in the mesopic domain and the current spectral sensitivity standards for scotopic, $V'(\lambda)$, at the lower end of the mesopic range, and for photopic vision, $V(\lambda)$, at the higher end of the mesopic range. The problem of the difference in the field size can be solved by applying the spectral luminous efficiency function for the 10 degree CIE-observer, $V_{10}(\lambda)$, for the photopic domain, instead of the more generally used spectral luminous efficiency function for the 2-degree CIE-observer, $V(\lambda)$. Another problem is that the spectral sensitivity functions based on brightness matching suffer from a failure of additive feature. Additive feature is essential for photometry (Abney's law). The additive problem can be tackled by using flicker photometry or a similar method. The $V(\lambda)$ and $V_{10}(\lambda)$ functions are based on flicker photometry and have been shown to obey Abney's law (Wyszecki and Stiles, 1982). The models 8 and 9 are based on

RT. The authors claim that these models do not suffer from the problems of models which are based on brightness matching (He et al., 1997, 1998). They state that in a reaction time task, just as in flicker photometry, the fast magnocellular channel, rather than the slow parvocellular channel, is being used. It is thought that the magnocellular channel is used for the fast transportation of the brightness signal; the parvocellular channel is slower and transports both the brightness and colour signals. Only the magnocellular channel appears to obey Abney's law of additivity. Therefore, the results of the reaction time experiments can be directly compared with luminance data obtained with the spectral luminous efficiency functions for photopic vision, $V(\lambda)$ and $V_{10}(\lambda)$. As both He models include peripheral measurements these models make use of the wide field $V_{10}(\lambda)$ rather than the $V(\lambda)$ for describing the luminance at photopic light levels. Foveal vision measured by reaction times might be modelled by $V(\lambda)$ for any light level (He et al., 1997).

The reaction time task is directly linked to the performance task of driving a vehicle. One of the tasks of driving a vehicle is avoiding a potential hazard on the road and therefore a fast reaction is essential. Potential hazards, such as cars, pedestrians, and animals, do not always appear in front of the car, often they can come into view from the side. For that reason, off-axis detection is also important. The rods play an important role for off-axis detection, so the photopic luminance based on the $V(\lambda)$ function is inadequate. It should be noted that the first seven models in Table 3.a. do not account for the eccentricity of the stimulus, i.e. eccentricity is not a parameter in the model.

Models 8, 9, 10, and 11 are all based on reaction time measurements of two studies (He et al., 1997, 1998).

$$V_{mes}(\lambda, L_{mes}) = k \{ x(L_{mes}) V_{10}(\lambda) + [1 - x(L_{mes})] V'(\lambda) \}$$

Which ensures that the maximum value of $V_{mes}(\lambda)$ is unity. The mesopic luminance, L_{mes} , is calculated by applying the calculated spectral luminous efficiency function for mesopic vision in the integration over the visual part of the spectrum.

$$L_{mes} = K_{mes} \int V_{mes}(\lambda, L_{mes}) L_e(\lambda) d\lambda$$

The factor K_{mes} is equal to 683 lm/W divided by the value of $V_{mes}(\lambda)$ for a wavelength of $\lambda = 555$ nm and $L_e(\lambda)$ is the spectral radiance in $W\ m^{-2}\ s^{-1}$. Note that the light level used to calculate the weighting factor x in turn is used as mesopic luminance. Hence, the calculation of the mesopic luminance is a complicated iterative algorithm that must be repeated until a sufficiently accurate value of L_{mes} is obtained.

Model 9 differs from model 8 because of a slightly different function for the weighting factor. The algorithm is also iterative and more complicated because the light level is expressed as mesopic retinal illuminance rather than as mesopic luminance. Model 9 also determines the spectral luminous efficiency function for mesopic vision, $V_{mes}(\lambda)$, by weighting the spectral luminous efficiency functions $V'(\lambda)$ and $V_{10}(\lambda)$. Model 10 is designed according to the same weighting principle as applied in models 8 and 9. The difference is that now the more common efficiency function for photopic vision for a 2-degree field size, $V(\lambda)$, is used instead of $V_{10}(\lambda)$. The second simplification is that the weighting factor is a function of the photopic luminance L and the ratio of scotopic and photopic luminance, S/P (2-degree observer). Therefore, the calculation procedure is not iterative. Model 11, the unified luminance model, is the simplest model (Rea et al., 2004), which only needs the photopic luminance and scotopic luminance as input, rather than the spectral radiance data as in previous models. The model consists of a closed form equation and the calculation is not iterative. As the reaction time task is highly relevant for traffic, and additivity is preserved, it can be concluded that spectral Model 8 is based on the calculation of the spectral luminous efficiency function for mesopic vision, $V_{mes}(\lambda)$, by weighting the spectral luminous efficiency function for scotopic vision, $V'(\lambda)$, and the spectral luminous efficiency function for photopic vision with 10 degrees' field size, $V_{10}(\lambda)$ according to equation:

The weighting factor, x , depends on the light level. The factor k is a normalization constant sensitivity determined with a reaction time task would seem to be a promising candidate for a mesopic model.

Table 2.1 A list of Mesopic models in the 2001 CIE report (No. 1–7) and the models of He and Rea (No. 8–11) [6]

No.	Model	Field diameter (degrees)	Task	Eccentricity (degrees)	Input variables	References
1.	Palmer 1	10	HCBM	0	L_{10}, L'	Palmer, 1968
2.	Palmer 2	10	HCBM	0	L_{10}, L'	CIE, 1989, 2001
3.	Sagawa-Takeichi	10	HCBM	0	L_{10}, L', X, Y, Z	Ikeda and Shimozono, 1981; CIE 1989
4.	Nakano-Ikeda	10	HCBM	0	$L', X_{10}, Y_{10}, Z_{10}$	Sagawa and Takeichi, 1987, 1992
5.	Kokoschka-Bodmann	10	HCBM	0	$L', X_{10}, Y_{10}, Z_{10}$	Kokoschka and Bodmann, 1975; Kokoschka 1980
6.	Trezona	10	HCBM	0	$L', X_{10}, Y_{10}, Z_{10}$	Trezona, 1987, 1990
7.	Ashizawa	10	HCBM	0	$V_{10}(\lambda), V'(\lambda)$	Ashizawa et al, 1985
8.	He 1	2	RT	15	$Le(\lambda)$	He et al 1997
9.	He 2	2	RT	12	$Le(\lambda)$	He et al 1998
10	Rea	2	RT	Non-foveal	$Le(\lambda)$	Rea et al 2003
11	Unifl	2	RT	Non-foveal	Le, L	Rea et al 2004

2.9 Application of mesopic system

Mesopic photometry offers a standardized approach to compare light sources under low light conditions, providing a common criterion for assessment. It is expected that the lighting community will strongly embrace and adopt this photometric method for mesopic applications, given its validity and justification.

The implementation of mesopic design will enable the optimization of outdoor lighting, considering both human visual performance and energy consumption. By utilizing mesopic photometry, the lighting industry can develop products that are specifically tailored for low light level scenarios. This optimization will lead to improved energy efficiency and enhanced visual effectiveness in outdoor lighting conditions. Ultimately, the use of mesopic photometry will drive the development of more efficient and effective lighting solutions.

2.10 Limitation of mesopic photometry

Though mesopic photometry system is based on visual task performance, it cannot be applicable to all tasks. The limitations of mesopic photometry system is given below.

- 1) Mesopic photometry system cannot be applied to tasks seen by retina at all the angles.
- 2) It cannot be used for situations where high light levels are used. This is because the experiments performed by CIE 191 system mainly used white light.
- 3) Mesopic photometry cannot be applied to light sources with extremely high S/P ratio.

2.11 Calculation of Mesopic Luminances

For the calculation of the mesopic luminance, the S/P ratio of the light source is needed. The higher the S/P ratio, the higher is the luminous efficacy of the light source in terms of mesopic design.

2.12 Comparison of Light Sources

The use of mesopic dimensioning changes the luminous output and consequently the luminous efficacy orders of lamps.

Table 2.1 lists the S/P ratios of light sources used in outdoor lighting. Light sources with $S/P > 1$ have higher content of their spectral output in the short wavelength region and are thus mesopically more efficient than light sources with $S/P < 1$.

Light source	R_{sp}
Low pressure sodium	0.23
High pressure sodium	0.4
Mercury vapour lamp	0.8
Incandescent	1.41
Quartz halogen	1.5
Fluorescent	1.5–2.4
Cool white LED	2.3
LED – red (635 nm)	0.06
LED – blue (470 nm)	14.3
LED – royal blue (450 nm)	28
Diode laser – red (650 nm)	0.016
Diode laser – blue (445 nm)	32

Fig 2.4 Typical S/P ratio of different light sources

CHAPTER 3

Lamps: Classification, Construction & Working Principles

3.1 Different types of Lamps

Various types of lamps are available for a range of lighting needs, including:

1. Incandescent Lamps

- Traditional lamps emitting warm, soft light.

2. Tungsten Halogen Lamps

- Provide bright, white light; often used for focused lighting.

3. Fluorescent Lamps

- Energy-efficient options producing bright, white light.

4. Compact Fluorescent Lamps

- Energy-saving versions of fluorescent lamps; compact in size.

5. Low Pressure Mercury Vapour Lamps

- Emit bluish light; used for outdoor and industrial lighting.

6. High Pressure Mercury Vapour Lamps

- Produce bluish-green light; commonly used for street lighting.

7. Metal Halide Lamps

- Offer high-quality, white light; used for various applications.

8. High Pressure Sodium Vapour Discharge Lamps

- Emit orange-yellow light; used for outdoor and industrial lighting.

9. Low Pressure Sodium Vapour Lamps

- Emit monochromatic yellow light; used for specific outdoor lighting.

10. LED Lamps

- Highly energy-efficient and long-lasting lamps with adjustable color temperatures.

Each type of lamp serves specific purposes, from providing ambient lighting to offering focused illumination. Consider the unique characteristics of each lamp when selecting the right option for your indoor or outdoor lighting needs.

3.1.1 Lamps Used in Outdoor Lighting

The following types of lamps are used in outdoor lighting .They are

1. High pressure sodium lamp (HPSV)
2. Metal Halide Lamps (MH)
3. White Light Emitting Diodes (WLED)
4. Cool White Light Emitting Diodes(CWLED).

3.1.2 Color temperature of light sources

Color Temperature: Color temperature plays a pivotal role in outdoor lighting applications and serves various other purposes. The color emitted by a black body, defined by its temperature, results in a specific hue range, collectively referred to as color temperature. This measurement is denoted in Kelvins (K). Traditional lamps such as tungsten halogen and incandescent lamps emit a warm, yellowish light, limiting the choice of emitted light color.

However, with the introduction of LED technology, the range of available colors has expanded, enabling the selection of specific colors to establish the desired ambiance within a space. Color temperatures exceeding 5000 K fall under the "cool colors" category, showcasing bluish tones. On the contrary, lower color temperatures (2700–3000 K) fall within the "warm colors" range, radiating a yellowish glow. As the scale ascends, the light increasingly resembles the blue hues of natural daylight, illustrated in Figure 3.1.



Fig.3.1 Objects under lamps with different CCT

➤ Correlated Colour Temperature (CCT)

The Color Correlated Temperature (CCT) of a lamp denotes the temperature at which a hypothetical black body, when heated, emits radiation or light with the same color characteristics as that radiated by the lamp under consideration. The unit used for measuring CCT is the Kelvin (K). When the CCT of a fluorescent lamp, for instance, is specified as 4500K, it signifies that heating a black body to 4500K will yield radiation or light exhibiting identical color attributes as the fluorescent lamp.

Lamps are categorized into warm white, neutral white, or cool white based on their CCT values. A lamp boasting a CCT below 3000K imparts a yellowish-reddish hue to the emitted light, engendering a sensation of warmth in the environment. Consequently, lamps possessing CCT values less than 3000K are classified as warm white. In instances where the lamp's CCT falls within the range of 3000K to 4000K, the resulting light assumes a white coloration, earning the label of neutral white. Conversely, a lamp with a CCT surpassing 4000K projects a whitish light, generating a perceptible coolness in the surroundings. As such, lamps characterized by CCT values exceeding 4000K are denoted as cool white.

➤ Warm & Cool Light

The Correlated Color Temperature (CCT) specification for warm light lamps resides at levels below 3000 K. This CCT range engenders perceptible colors ranging from yellowish to red, akin to the illumination produced by conventional incandescent and halogen lamps. In contrast, cool white lamps are characterized by a CCT exceeding 4500 K, evoking a bluish-white chromatic perception. The utilization of either warm or cool light is contingent upon user preferences and specific contexts. Warm white lighting finds prominence in conventional residential settings, while it is favored in bakery environments. Cool white light, on the other hand, bestows a serene and tranquil atmosphere. The judicious selection of the appropriate color temperature assumes paramount importance in the realm of commercial lighting design, where desired emotional and aesthetic impacts are sought.

It's noteworthy that cool white bulbs exhibit a higher lumen output in comparison to their warm white counterparts when their equivalency is taken into account. This luminous intensity disparity further underscores the multifaceted considerations entailed in light source selection for achieving intended illumination objectives.^[2]

3.2 Construction & Operating Principle of Lamps used in Outdoor Lighting

3.2.1 Compact Fluorescent Lamps

Low-pressure mercury lamps of the compact type, normally referred to as compact fluorescent lamps (CFLs), were originally developed at the beginning of the 1980s for use in those applications where incandescent lamps were traditionally in use. Today, the application of “twin-leg” compact fluorescent lamps has been widened to include those residential streets where relatively low lighting levels suffice. Alternatives are lowwattage high pressure sodium, metal halide and to an increasing extent solid-state lamps.

3.2.1.1 Construction & working principle

The operating principle of compact fluorescent lamps is exactly the same as that in tubular fluorescent lamps. A tube made out of glass is filled with an inert gas and a little mercury. To facilitate starting, the electrodes sealed into each end of the tube are pre-heated prior to ignition by a high-voltage pulse. Once the mercury is completely vaporised, an operating gas pressure of slightly less than 1 Pa ($\pm 10^{-5}$ atm) is reached. The radiation emitted from the low-pressure mercury discharge contains a large amount of ultraviolet radiation and a small amount of blue light. The inside of the tube is therefore coated with a mixture of fluorescent powders that convert the ultraviolet radiation into visible light as it passes through this coating. The final result is white light, the colour properties of which depend on the mix of fluorescent powders employed. The compactness of these lamps is achieved by reducing their length by folding a longer tube into a U-tube, or by joining together two (or more) parallel tubes by means of a welded bridge so that one open pathway is obtained where free electrons and ions can move from one electrode to the other (Fig.3.2). A great variety

of tube shapes are available. Versions with the electric gear integrated in the lamp itself and with a lamp cap as in normal incandescent lamps are produced as energy-saving retro-fits for incandescent lamps. The compact fluorescent lamps employed in road lighting are normally of the non-integrated type and the gear needs to be installed in the luminaire. They are of the twin-leg or circular versions. The twin leg versions have a length, depending on wattage, of between 100 and 600 mm.

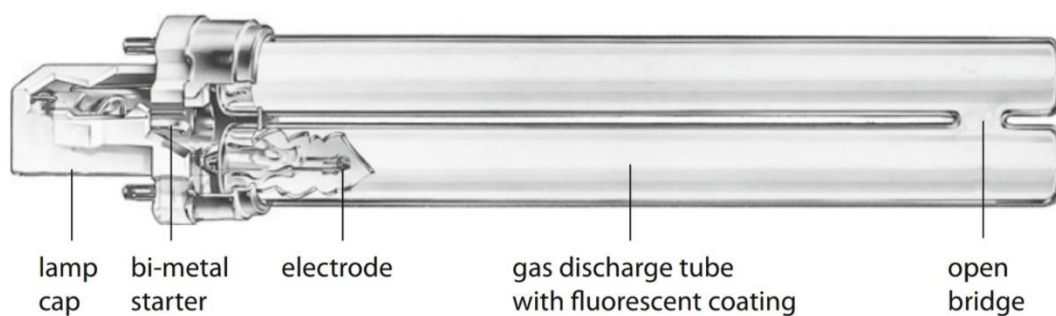


Fig 3.2 Main parts of a compact fluorescent lamp (welded-bridge version)

3.2.1.2 Lamp Properties

Lumen Range Non-integrated compact fluorescent lamps are available in the range from some 250–6000 lm, corresponding to the wattage range of 5–80W.

System Efficacy The higher-wattage versions, which are most suited for street lighting, reach efficacies up to some 70 lm/W.

Lifetime Non-integrated CFLs have lifetimes, based on L20 between 7000 and 20,000 h, with the better values for the higher wattages.

Run-Up and Re-ignition Fluorescent lamps operated on present-day electronic gear start within 1.5 s and without flickering. When a hot lamp is switched off, the vapour pressure drops so quickly that re-ignition is instantaneous.

Dimming Non-integrated compact fluorescent lamps with four-pin lamp cap can be dimmed.

Ambient-Temperature Sensitivity The luminous flux of a fluorescent lamp is determined by the mercury vapour pressure during operation. The mercury vapour pressure is in turn determined by the coldest spot in the tube, which, because

fluorescent lamps have no outer bulb, is dependent on the ambient temperature. With a compact lamp the coldest spot is also dependent on its tube shape. In all cases the luminous efficacy decreases with temperatures lower than some 20–30 °C ambient temperature. In completely-open luminaires, at –10°, the remaining light output may be lower than 20% of the nominal value. So, in colder regions, fluorescent lamps should never be used in open luminaires.^[1]

3.2.2 Constructional Feature of a Metal Halide Lamp

Metal halide lamp consists of

1. Outer Glass bulb
2. Arc tube
3. Screw Base
4. Ballasts
5. Arc tube
6. Quartz discharge tube
7. Argon gas
8. Mercury vapor
9. Indium, thallium and sodium iodide



Fig 3.3. Metal Halide Lamps

3.2.2.1 Working of Metal Halide Lamp

Metal halide (MH) lamps operate through a structured arrangement involving essential components. The core setup comprises an arc tube, enclosed within an outer

envelope or bulb. The arc tube is meticulously fabricated from either quartz or ceramic materials. Its internal composition encompasses a blend of initiating gas, typically argon, alongside mercury and metal halide salts. It is noteworthy that conventional quartz MH arc tubes bear resemblances to mercury vapor (MV) arc tubes in shape. However, their operation takes place at elevated temperatures and pressures.

The initiation of MH lamps is facilitated by the ballast, which administers a heightened starting voltage surpassing the customary levels supplied to the lamp's electrodes. This voltage is delivered through a gas amalgam present in the arc tube. The critical precondition for lamp ignition is the ionization of the gas content within the MH arc tube, a process that paves the way for the passage of electric current, subsequently leading to lamp activation. The ballast assumes a dual role by not only providing the requisite starting voltage but also governing the starting and operational currents of the lamp.

With a surge in pressure and temperature within the arc tube, the materials enclosed therein undergo vaporization. This transformation generates the emission of light and ultraviolet (UV) radiation. An outer bulb, typically fashioned from borosilicate glass, serves multifaceted functions. Primarily, it establishes a thermally stable milieu for the arc tube's functionality. Furthermore, it maintains an inert atmosphere that prevents oxidation of arc tube components under elevated temperatures. Simultaneously, the outer bulb curtails the extent of UV radiation emitted by the lamp. Notably, some MH lamps incorporate an inner bulb coating, designed to diffuse the light produced. This coating often includes phosphor elements, which contribute not only to light diffusion but also to alterations in the lamp's color characteristics.

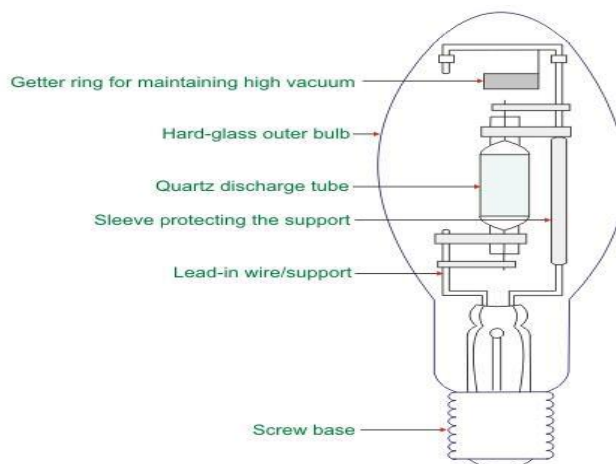


Fig 3.4 Constructional Feature of a Metal Halide Lamp

3.2.2.2 Establishment of arc Inside the Metal Halide Arc Tube

During the deactivated state of the lamp, the metal iodides (such as indium, thallium, and sodium iodides) situated within the lamp are present along the interior surface of the bulb. As the temperature of the arc increases, these metal iodides undergo vaporization and disperse from the bulb's surface into the arc's flow. Subsequently, they experience dissociation, leading to the liberation of unbound metal and iodine atoms. In a manner akin to this process, the mercury atoms within the bulb encounter excitation and ionization. It's important to note that not all iodide salts exhibit simultaneous vaporization within the metal halide lamp.

- Initially, argon gas undergoes vaporization, followed by the vaporization of mercury to initiate the formation of the arc.
- Specifically, indium is the first to vaporize, generating a blue envelope around the mercury arc.
- Subsequently, thallium vaporizes, creating a yellow envelope encompassing the thallium.
- Lastly, the vaporization of sodium iodides takes place, rendering the lamp exceedingly responsive to variations in lamp wattage.

3.2.2.3 Lamp Properties

Lumen Range Typical versions of the metal-halide lamps developed for use in road lighting are available in lumen packages from some 5000 to 50,000 lm. The versions for floodlighting range from some 20,000 to more than 200,000 lm.

System Efficacy The road-lighting versions range from 80 to 110 lm/W, and the floodlight versions from 75 to slightly more than 105 lm/W.

Lifetime The ceramic metal halide lamps specifically developed for use in road lighting have lifetimes of up to 20,000 h (basis L80). The floodlight types have shorter lifetimes ranging from 4000 to 10,000 h.

Run-Up and Re-ignition The metal halides in the discharge tube need time to heat up, evaporate and dissociate into metal and halide. During this process, which takes about 2–3 min, the light output and colour gradually change until the final stable condition is reached. If there is an interruption in the power supply, medium and high-wattage lamps will take approximately 10–20 min for the pressure in the lamp to decrease enough for it to re-ignite. Compact ceramic lamps reignite faster: after some 3–10 min.

Dimming Dimming of metal halide is difficult because with the resulting decrease in temperature some of the metal halides may condense, so changing the colour properties of the lamp. Only by employing specially shaped burners can this phenomenon be avoided. Most metal halide lamps specifically developed for road lighting can indeed be dimmed to at least 50% of their light output. The lamp types used mainly for floodlighting cannot be dimmed.^[1]

3.2.3 High-Pressure Sodium Lamps

High-pressure sodium (HPS) gas-discharge lamps belong to the group of high intensity discharge HID lamps. HPS lamps, in common with all high-pressure discharge lamps, are relatively compact. By increasing the vapour pressure in a sodium lamp, the spectrum around the typical yellow sodium line broadens. The result is that colour rendering improves and the colour appearance changes from yellow to yellow-white, albeit at the cost of a decrease in efficacy. However, the resulting efficacy is more than double that of a high-pressure mercury lamp. At its introduction in the late 1960s, a very efficient alternative was thus obtained for the many high-pressure mercury lamps employed at that time, and which are still sometimes employed today, in road lighting. Since then, road-lighting installations all over the world very often use high-pressure sodium lamps. LED solutions have now become an alternative.

3.2.3.1 Construction of HPSV lamp

- The HPSV lamp consists of compact arc tube which contains mixture of xenon, sodium and mercury.

- The arc tube containing sodium mercury amalgam provides proper environment for producing light.
- The electrodes are made of tungsten and carry high voltage, high frequency pulse to strike the arc and vapourize mercury and sodium.
- The base of lamp provides means of electrical connection.
- The outer bulb shields the arc tube from drafts, outer temperature.
- Some lamps have phosphor coating on inner surface of outer bulb to diffuse the light.
- The lamp is powered with ac voltage source in series with inductive ballast in order to supply constant voltage.
- The HPSV lamp is commercially called 'SON'.
- This Type Of Lamp Is Used In Area And Outdoor Lighting.

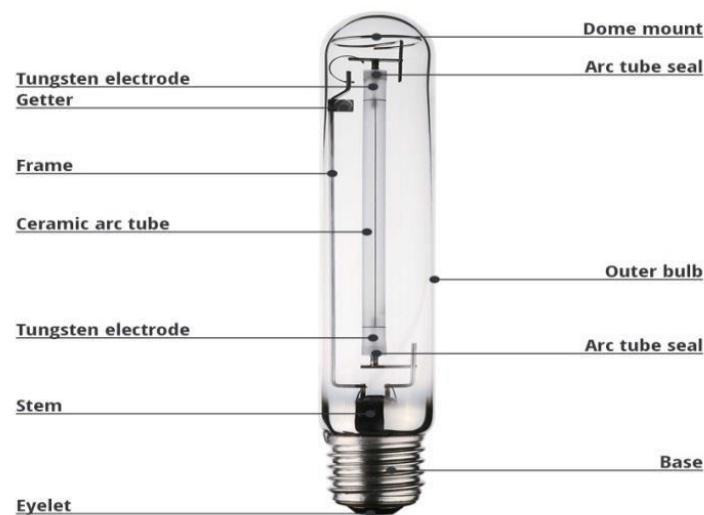


Fig 3.4 Constructional features of HPSV lamp

3.2.3.2 Working of HPSV lamp

The functionality of the HPSV lamp involves intricate processes driven by temperature variations and vapor pressure dynamics:

- Within the lamp, an amalgam composed of metallic sodium and mercury resides in the coolest region, facilitating the generation of sodium and mercury

vapors essential for arc formation. Notably, the temperature of the amalgam rises in proportion to the lamp's power, directly influencing mercury and sodium vapor pressures as well as terminal voltage.

- The temperature escalation initiates a sequence where steady current accompanied by increasing voltage leads to escalating energy consumption until the operational power level is attained. The lamp's operational modes are primarily delineated by voltage parameters:
 1. Lamp extinguished with no current flow.
 2. Lamp operation with liquid amalgam present within the tube.
 3. Lamp operation with complete amalgam evaporation.
- Stable states are the initial and final ones, owing to the weak connection between lamp resistance and voltage. In contrast, the second state is inherently unstable.
- Any unusual current surge triggers a rise in power, elevating the amalgam temperature, subsequently lowering resistance, and further intensifying current flow. This culminates in an uncontrollable escalation, driving the lamp into a high-current state.
- Analogously, an abnormal current decline propels the lamp towards extinction. The sought-after operational state is the second mode, characterized by stable lamp operation.
- Consequently, the HPSV lamp demonstrates an average lifespan exceeding 20,000 hours.

In practical applications, the lamp operates in tandem with an AC voltage source connected to an inductive "ballast," ensuring a near-constant current supply to the lamp for stable functioning. The preference for inductive ballasts over resistive counterparts stems from the intention to mitigate energy wastage due to resistive

losses. Given the lamp's extinguishing at each zero-current point in the AC cycle, the inductive ballast aids in re-ignition by inducing a voltage spike at these junctures.

The lamp's emitted light predominantly comprises atomic emission lines of mercury and sodium, with the sodium D-line emission (589nm) taking prominence. This specific emission line, renowned for its pronounced characteristics, contributes significantly to the lamp's improved color rendering capabilities.

3.2.3.3 Lamp Properties

Lumen Range High-pressure sodium lamps are produced in the approximate range of 4000 (50 W)–150,000 lm (1000 W).

System Efficacy The efficacy goes from 80 lm/W, for the lower wattages, to 140 lm/W for the higher wattages.

Lifetime High-pressure sodium lamps have a lifetime, based on L80, of up to 20,000 h.

Run-Up and Re-ignition The nominal pressure and full light output is reached after 3–5 min. Re-ignition of the hot lamp requires the lamp to cool down for about 1 min to allow the pressure to decrease far enough for the ignition pulse to again ionise the sodium atoms.

Dimming Lower wattages (100–150 W) can be dimmed to 20% of light output with special electronic gear. Higher lamp wattages can be switched to some 50% of light output, by including an extra inductive coil (ballast) in the lamp circuit, Lamp colour remains virtually constant and lifetime is not affected. ^[1]

3.2.4 Solid State Light or Light Emitting Diode or LED

Solid State Lighting, also referred to as Light Emitting Diode (LED) technology, relies on the utilization of specific semiconductors to achieve its illuminating properties. Among these semiconductors, Aluminum Indium Gallium Phosphide (AlInGaP) and Indium Gallium Nitride (InGaN) stand out as the most widely employed. In the past, LED technologies relied on Gallium Arsenide Phosphide (GaAsP), Gallium Phosphide (GaP), and Aluminum Gallium Arsenide (AlGaAs) as their semiconductor materials.

The fundamental principle underlying the LED's light emission lies in the phenomenon of electroluminescence. This process involves the generation of visible radiation when a low-voltage direct current is applied to a suitably doped crystal containing a p-n junction within its structure. This controlled manipulation of electrons and holes at the p-n junction results in the emission of light, making LEDs a reliable and efficient source of illumination in various applications.

3.2.4.1 Working of LED

The operational functionality of Light Emitting Diodes (LEDs) parallels that of conventional diodes, functioning under forward bias. In this context, the n-type semiconductor substrate is intentionally doped with higher concentrations relative to the p-type counterpart, consequently constituting a p-n junction. Upon imposition of a forward bias, the potential barrier within the junction undergoes diminution, permitting the amalgamation of electrons and holes within the depletion layer (referred to as the active layer). This intricate process culminates in the emission of photons, radiated omnidirectionally. A visual representation of this phenomenon is showcased in Figure 3.5, encapsulating the emission of light due to electron-hole recombination following forward biasing.

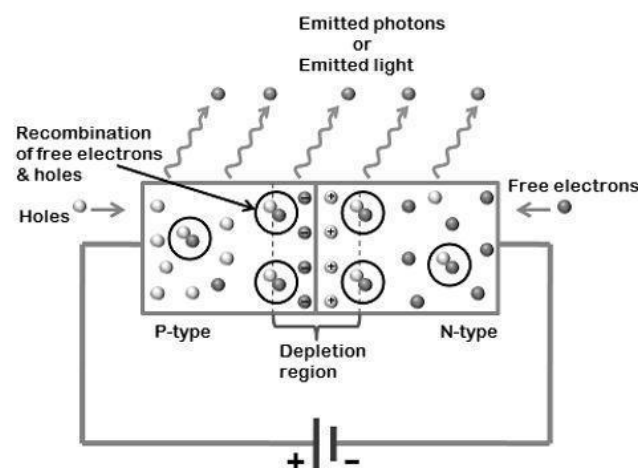


Fig 3.5 Working of LED

The crux of photon emission within an LED diode is embedded within the energy band theory of solids. According to this theoretical framework, the propensity of electron-hole pairs to release photons hinges on the nature of the material's energy band gap - whether it is direct or indirect. Semiconductors exhibiting a direct band gap inherently emit photons upon recombination. In the context of a direct bandgap material, the conduction band's energy level nadir is strategically positioned directly above the apex of the valence band on the Energy-Momentum (wave vector 'k') diagram. Upon electron-hole recombination, the resulting energy $E = h\nu$, corresponding to the energy gap Δ (measured in electronvolts), dissipates in the form of luminous energy or photons. Here, 'h' signifies Planck's constant, and 'v' represents the frequency of the emitted light.

3.2.4.2 Direct Band Gap

In the context of semiconductor physics, a band gap is categorized as "direct" when the crystal momentum of both electrons and holes aligns equivalently within both the conduction and valence bands. Under this circumstance, an electron is capable of emitting a photon directly without the necessity of an intermediary state.

This direct band gap behavior is observed in specific materials, an example being amorphous silicon, which exhibits the direct band gap characteristic. Moreover, certain III-V compound materials, notably InAs and GaAs, also manifest the direct band gap phenomenon. In these materials, the seamless transition of electrons and holes facilitates the direct emission of photons, marking a distinctive trait of their optical and electronic behavior.

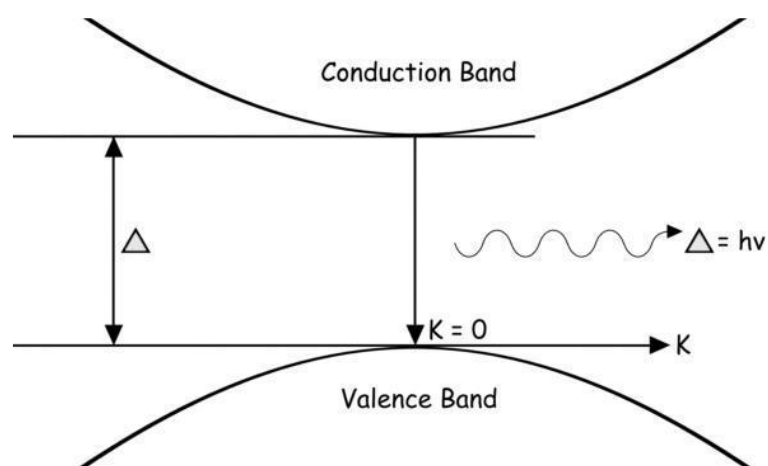


fig 3.6 Direct band gap

3.2.4.3 Indirect Band Gap

Within the context of semiconductors, the concept of an "indirect" band gap pertains to a scenario wherein the emission of a photon is impeded due to the requisite passage of an electron through an intermediary state, thereby necessitating the conveyance of momentum to the crystalline lattice. Materials characterized by an indirect band gap include crystalline silicon and germanium (Ge). Furthermore, select III-V materials, such as aluminum antimonide (AlSb), also exhibit properties indicative of an indirect band gap nature.

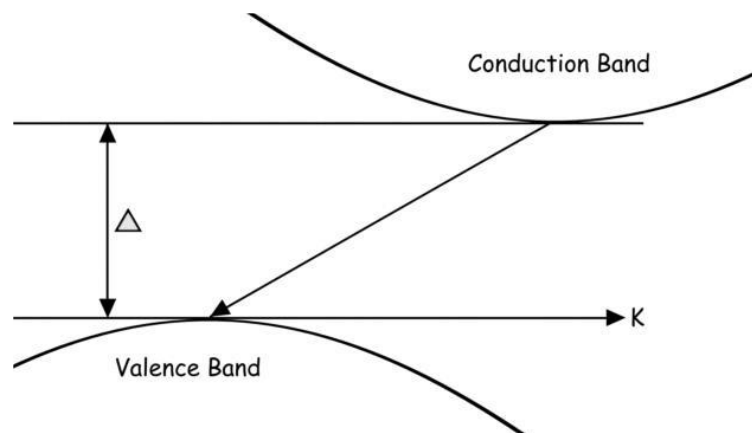


fig 3.7 Indirect band gap

3.2.4.4 White LED (WLED)

White Light Emitting Diodes (White LEDs) represent a significant advancement in the field of lighting technology. Traditionally, LEDs were confined to niche applications such as indicators, displays, and emergency lighting. However, the emergence of white light-emitting LEDs has led to their ubiquitous incorporation across a broad spectrum of lighting applications, encompassing indoor, road, and flood lighting.

It's important to note that a natural emission of white light is not inherent to LEDs. Nevertheless, specific technologies have enabled LEDs to emit white light, thereby expanding their utility.

Currently, the production of white LEDs involves two primary methodologies:

1. Color Mixing: In this approach, red, green, and blue LED chips are integrated within a single package. The combined output of these chips results in white light emission. This method capitalizes on the additive color mixing principle to achieve the desired white light spectrum.

2. Phosphorescence: The second technique relies on phosphorescent materials. A phosphor, encapsulated in the epoxy coating enveloping the LED chip, exhibits fluorescence when subjected to the short-wavelength energy originating from the InGaN (Indium Gallium Nitride) LED device. This fluorescence conversion process leads to the emission of white light.

These advancements in LED technology, particularly the creation of white LEDs through either color mixing or phosphorescence, have revolutionized the lighting landscape, enabling their widespread implementation across diverse lighting scenarios.

- A **Warm White** Integral LED lamp will provide a traditional yellowish colour light, similar to conventional bulbs. This is the most popular choice. (2700-3000K)
- A **Cool White** Integral LED lamp will provide a modern, clean, bright light, that is slightly blue in colour.(4000-5000K)

CHAPTER 4

LIGHTING DESIGN AND STANDARDS

4.1 Introduction to Lighting Design

Lighting design is a crucial aspect of creating functional, aesthetic, and comfortable spaces. Whether it's for residential, commercial, industrial, or outdoor environments, proper lighting design enhances the visual appeal and functionality of the area. To achieve the desired lighting effects and meet specific requirements, lighting designers must consider various parameters and factors. In this extensive discussion, we'll explore these parameters in detail, covering both technical and artistic aspects of lighting design.

Lighting design involves planning and implementing the illumination of a space to fulfill functional needs while considering the aesthetics, mood, and human perception. A well-designed lighting system should balance these elements, resulting in an environment that is visually appealing, energy-efficient, and suited to the intended purpose.

4.2 Lighting Design Parameters

1. Color Temperature (Kelvin)

Color temperature, measured in Kelvin (K), determines the "warmth" or "coolness" of light emitted by a lighting source. Lower color temperatures (around 2700K to 3000K) produce warm, yellowish light reminiscent of incandescent bulbs. Higher color temperatures (around 5000K to 6500K) produce cooler, bluish light similar to daylight.

Color temperature significantly impacts the ambiance and mood of a space. Warm light is generally preferred in spaces like bedrooms and restaurants for a cozy and intimate atmosphere. Cooler light is more suitable for areas like offices and retail spaces, where task performance and focus are essential.

2. Color Rendering Index (CRI)

CRI measures how accurately a light source renders colors compared to natural light. It is expressed on a scale from 0 to 100, with higher values indicating better color rendering. Natural daylight is considered the reference with a CRI of 100.

CRI is crucial in environments where accurate color perception is vital, such as art galleries, retail spaces, and hospitals. For these spaces, lighting designers aim to use light sources with high CRI values to ensure colors appear as true and vibrant as possible.

3. Distribution of Light (Direct/Indirect)

Light distribution refers to how light is spread or directed in a given space. Proper light distribution is essential for even illumination and to avoid harsh shadows or hotspots. Various lighting fixtures, such as floodlights, spotlights, wall sconces, and pendant lights, provide different distribution patterns. The choice of fixtures and their placement depends on the specific requirements of the space and the desired lighting effect.

4. Lighting Uniformity

Uniform lighting helps eliminate dark spots and glaring areas, creating a balanced and comfortable visual environment. Uniformity is achieved by appropriately arranging light sources and selecting appropriate fixtures.

5. Glare and UGR (Unified Glare Rating)

Glare is the uncomfortable or excessive brightness that can impede vision and cause discomfort. It can be either direct glare (light directly entering the eyes) or reflected glare (light bouncing off surfaces).

To minimize glare, lighting designers use strategies like proper fixture selection, shielding, and controlling light angles. In spaces where visual tasks are crucial, glare control is essential to enhance occupant comfort and safety.

UGR is used to quantify glare in indoor environments, and designers aim to keep UGR values as low as possible for a more pleasant experience.

6. Dimming and Control

The ability to adjust lighting levels through dimming and control systems allows for dynamic lighting scenarios, energy savings, and customization based on user preferences.

7. Energy Efficiency

Energy efficiency is a vital consideration in modern lighting design. With a growing focus on sustainability and reducing carbon footprints, designers aim to maximize lighting efficiency while minimizing energy consumption.

Energy-efficient lighting solutions include LED technology, which offers longer lifespans, lower energy consumption, and reduced maintenance costs compared to traditional incandescent or fluorescent bulbs.

8. Safety and Emergency Lighting

Incorporating emergency lighting systems ensures safe evacuation during power outages or emergencies. Exit signs, escape route lighting, and standby power sources are critical components.

9. Flicker and Strobe Effects

Eliminating flicker and strobe effects is crucial as they can cause discomfort, eyestrain, and even health issues. Opting for high-quality light sources and dimming systems can help minimize these effects.

10. Daylight Integration

Maximizing the use of natural daylight through intelligent design reduces reliance on artificial lighting during daylight hours, promoting energy efficiency and providing a more pleasant environment.

11. Architectural Integration

Lighting fixtures should seamlessly integrate into the architecture and complement the overall design aesthetic, enhancing the space's visual appeal.

12. Maintenance and Serviceability

Choosing fixtures that are easy to maintain and replace is essential to ensure the lighting system's longevity and cost-effectiveness.

4.3 Application of Lighting Design

1. Residential Lighting

In residential settings, lighting design aims to create cozy, comfortable, and functional spaces. Warm color temperatures, dimming options, and task-specific lighting are often preferred.

2. Commercial Lighting

In commercial spaces, lighting design combines functionality and aesthetics. Properly lit workspaces, accent lighting for displays, and energy-efficient solutions are typical considerations.

3. Hospitality Lighting

Hospitality settings require a focus on ambiance and mood. Accent lighting, decorative fixtures, and dynamic control systems contribute to creating memorable experiences.

4. Retail Lighting

Retail spaces benefit from strategic lighting to highlight products, create attractive displays, and guide customers through the store.

5. Industrial Lighting

In industrial settings, safety, efficiency, and durability are paramount. High-quality fixtures resistant to dust, moisture, and vibrations are essential.

6. Outdoor Lighting

Outdoor lighting considers safety, security, and aesthetics. Properly designed outdoor lighting enhances the appeal of architecture, landscape, and public spaces.

4.4 Mesopic Vision and Lighting Design

Understanding mesopic vision is crucial for lighting designers because many real-world

Understanding mesopic vision is crucial for lighting designers because many real-world lighting environments, such as street lighting, roadways, and outdoor areas, fall within the mesopic range. Traditional lighting design often focused solely on photopic vision, leading to suboptimal performance and energy inefficiencies in mesopic conditions.

In mesopic lighting environments, the visual system has unique characteristics that influence visual perception and performance. For example, under mesopic conditions, the eyes' sensitivity to blue light increases due to the relatively higher contribution of rods, leading to altered color perception. This phenomenon is known as the Purkinje shift. Additionally, contrast sensitivity and spatial resolution are reduced in mesopic conditions compared to photopic conditions.

4.5 Mesopic Photometry Standards and Recommendations

To address the challenges posed by mesopic lighting environments, various organizations and researchers have developed standards and recommendations for lighting design. These guidelines consider the unique characteristics of mesopic vision to enhance visibility, safety, and overall visual comfort.

4.5.1 CIE 191:2010 ^[2]

The International Commission on Illumination (CIE) published the Technical Report CIE 191:2010, "Recommended System for Mesopic Photometry Based on Visual Performance." This report defines a method for mesopic photometry by combining scotopic and photopic luminous efficiency functions to calculate mesopic luminous efficiency. It also introduces the mesopic luminance level, which is the most significant parameter for mesopic photometry.

4.5.1.1 Recommended System For Performance Based Mesopic Photometry

The recommended system for visual performance based mesopic photometry describes spectral luminous efficiency, $V_{mes}(\lambda)$, in the mesopic region as a linear combination of the photopic spectral luminous efficiency function, $V(\lambda)$, and the scotopic spectral luminous efficiency function, $V'(\lambda)$, and establishes a gradual transition between these two functions throughout the mesopic region. The system is of the form:

$$M(m)V_{mes}(\lambda) = mV(\lambda) + (1 - m)V'(\lambda) \text{ for } 0 \leq m \leq 1$$

$$L_{mes} = \frac{683}{V_{mes}(\lambda_0)} \int V_{mes}(\lambda) L_e(\lambda) d\lambda$$

Where,

$M(x)$ is a normalizing function such that $V_{mes}(\lambda)$ attains a maximum value of 1

$V_{mes}(\lambda_0)$ is the value of $V_{mes}(\lambda)$ at 555 nm

L_{mes} is the mesopic luminance

$L_e(\lambda)$ is spectral radiance in $W \cdot m^{-2} \cdot sr^{-1} \cdot nm^{-1}$

1

if $L_{mes} \geq 5.0 \text{ cd} \cdot m^{-2}$, then $m = 1$

if $L_{mes} \leq 0.005 \text{ cd} \cdot m^{-2}$, then $m = 0$

The coefficient m and the mesopic luminance, L_{mes} , can be calculated using an iterative approach as follows: $m_0 = 0.5$

$$L_{mes,n} = \frac{m_{(n-1)}L_p + (1 - m_{(n-1)})L_s V'(\lambda_0)}{m_{(n-1)} + (1 - m_{(n-1)})V'(\lambda_0)}$$

$$m_n = a + b \log_{10}(L_{mes,n}) \text{ for } 0 \leq m \leq 1$$

Where L_p is the photopic luminance, L_s is the scotopic luminance, and $V'(\lambda_0) = 683/1699$ is the value of scotopic spectral luminous efficiency function at $\lambda_0=555$ nm, a and b are parameters which have the values $a = 0.7670$ and $b = 0.3334$, and n is the iteration step.

The values of m and L_{mes} for this system as a function of photopic luminance and light source S/P-ratio (ratio of scotopic-to-photopic luminous output) are given in Table 4.1.

The system is proposed for evaluation of lighting for visual tasks in the peripheral region of the visual field in the mesopic region; it is recommended that on-axis tasks, where foveal vision is dominant, should be evaluated using the photopic spectral luminous efficiency function, $V(\lambda)$.

A requirement of the recommended system is that it should (within limits) provide a result that is meaningful in relation to human visual psychophysics and provide a correlation with visual performance under a range of different conditions. The degree of correlation with task performance was used as one criterion in determining the recommended system. The other criteria were the practical utility of the system and the requirement that it should maintain additivity, which is an underlying requirement of CIE photometry. The recommended system is an intermediate between the USP-^[13] and MOVE-systems^[14] and (similarly to them) describes mesopic spectral luminous efficiency in terms of a linear combination of the photopic and scotopic spectral luminous efficiency functions that provides a gradual transition between these functions through the mesopic region. The mesopic spectral luminous efficiency functions derived using this system are additive in nature and provide a bridge between the current photopic and scotopic functions, with the further advantage of being relatively easy to implement in a practical measurement system, as well as providing a meaningful correlation with actual task performance. Thus this recommended system represents an effective and practical solution to mesopic photometry, based upon more than a decade of visual psychophysical studies and nearly a century of photometric metrology principles.

Table: 4.1 a) Adaptation Coefficient m and b) L_{mes} of the recommended mesopic system as a function of photopic luminance and S/P-ratio of light source.

		a							
		<i>m</i>	Photopic luminance cd·m ⁻²						
		S/P	0,01	0,03	0,1	0,3	1	3	4,5
LPS –	0,25			0,1542	0,3830	0,5644	0,7538	0,9225	0,9841
	0,35			0,1804	0,3920	0,5688	0,7558	0,9230	0,9842
	0,45	0,0000	0,1992	0,4000	0,5730	0,7576	0,9235	0,9843	0,9843
HPS –	0,55	0,0190	0,2140	0,4073	0,5770	0,7594	0,9240	0,9844	0,9844
	0,65	0,0459	0,2265	0,4139	0,5808	0,7612	0,9245	0,9845	0,9845
	0,75	0,0655	0,2373	0,4201	0,5844	0,7629	0,9249	0,9846	0,9846
	0,85	0,0812	0,2468	0,4258	0,5878	0,7646	0,9254	0,9846	0,9846
	0,95	0,0943	0,2553	0,4311	0,5911	0,7662	0,9258	0,9847	0,9847
	1,05	0,1057	0,2631	0,4361	0,5942	0,7678	0,9263	0,9848	0,9848
MH warm white ~	1,15	0,1157	0,2702	0,4408	0,5972	0,7693	0,9267	0,9849	0,9849
	1,25	0,1247	0,2767	0,4452	0,6001	0,7708	0,9272	0,9850	0,9850
	1,35	0,1329	0,2828	0,4494	0,6029	0,7723	0,9276	0,9851	0,9851
	1,45	0,1404	0,2885	0,4534	0,6056	0,7737	0,9280	0,9852	0,9852
	1,55	0,1473	0,2939	0,4573	0,6082	0,7751	0,9284	0,9853	0,9853
	1,65	0,1538	0,2990	0,4609	0,6107	0,7764	0,9289	0,9853	0,9853
	1,75	0,1598	0,3038	0,4645	0,6131	0,7778	0,9293	0,9854	0,9854
	1,85	0,1654	0,3083	0,4678	0,6155	0,7791	0,9297	0,9855	0,9855
	1,95	0,1708	0,3126	0,4711	0,6178	0,7803	0,9301	0,9856	0,9856
	2,05	0,1758	0,3168	0,4742	0,6200	0,7816	0,9304	0,9857	0,9857
	2,15	0,1806	0,3207	0,4772	0,6221	0,7828	0,9308	0,9857	0,9857
	2,25	0,1852	0,3245	0,4801	0,6242	0,7840	0,9312	0,9858	0,9858
MH day-light –	2,35	0,1895	0,3282	0,4830	0,6263	0,7852	0,9316	0,9859	0,9859
	2,45	0,1937	0,3317	0,4857	0,6283	0,7863	0,9319	0,9860	0,9860
	2,55	0,1977	0,3351	0,4883	0,6302	0,7875	0,9323	0,9860	0,9860
	2,65	0,2015	0,3383	0,4909	0,6321	0,7886	0,9327	0,9861	0,9861
	2,75	0,2052	0,3415	0,4934	0,6339	0,7896	0,9330	0,9862	0,9862

		b							
		<i>L_{mes}</i>	Photopic luminance cd·m ⁻²						
		S/P	0,01	0,03	0,1	0,3	1	3	4,5
LPS ~	0,25		0,0025	0,0145	0,0705	0,2467	0,9130	2,9265	4,4782
	0,35		0,0035	0,0174	0,0750	0,2545	0,9253	2,9367	4,4812
	0,45	0,0045	0,0198	0,0793	0,2620	0,9373	2,9468	4,4842	4,4842
HPS ~	0,55	0,0057	0,0220	0,0834	0,2693	0,9492	2,9568	4,4872	4,4872
	0,65	0,0069	0,0239	0,0873	0,2764	0,9608	2,9668	4,4901	4,4901
	0,75	0,0079	0,0258	0,0911	0,2833	0,9722	2,9763	4,4929	4,4929
	0,85	0,0088	0,0275	0,0947	0,2901	0,9835	2,9859	4,4958	4,4958
	0,95	0,0096	0,0292	0,0983	0,2967	0,9945	2,9953	4,4986	4,4986
	1,05	0,0104	0,0308	0,1017	0,3032	1,0054	3,0046	4,5014	4,5014
MH warm white ~	1,15	0,0111	0,0323	0,1051	0,3096	1,0161	3,0139	4,5041	4,5041
	1,25	0,0118	0,0338	0,1083	0,3158	1,0267	3,0230	4,5068	4,5068
	1,35	0,0125	0,0353	0,1115	0,3220	1,0371	3,0319	4,5095	4,5095
	1,45	0,0132	0,0367	0,1147	0,3280	1,0473	3,0408	4,5122	4,5122
	1,55	0,0138	0,0381	0,1178	0,3339	1,0575	3,0496	4,5148	4,5148
	1,65	0,0145	0,0395	0,1208	0,3398	1,0674	3,0582	4,5174	4,5174
	1,75	0,0151	0,0408	0,1238	0,3455	1,0773	3,0668	4,5200	4,5200
	1,85	0,0157	0,0421	0,1267	0,3512	1,0870	3,0753	4,5225	4,5225
	1,95	0,0163	0,0434	0,1295	0,3568	1,0966	3,0836	4,5250	4,5250
	2,05	0,0169	0,0446	0,1324	0,3623	1,1060	3,0919	4,5275	4,5275
	2,15	0,0174	0,0459	0,1352	0,3677	1,1154	3,1001	4,5299	4,5299
	2,25	0,0180	0,0471	0,1379	0,3731	1,1246	3,1082	4,5323	4,5323
MH day-light ~	2,35	0,0185	0,0483	0,1406	0,3784	1,1338	3,1162	4,5347	4,5347
	2,45	0,0191	0,0495	0,1433	0,3836	1,1428	3,1241	4,5371	4,5371
	2,55	0,0196	0,0506	0,1459	0,3888	1,1517	3,1319	4,5395	4,5395
	2,65	0,0201	0,0518	0,1485	0,3939	1,1605	3,1396	4,5418	4,5418
	2,75	0,0207	0,0529	0,1511	0,3989	1,1693	3,1473	4,5441	4,5441

4.5.1.2 System for mesopic photometry based on visual task performance

The foundations for any system of photometry must lie in empirical visual performance data using human subjects. Photometry has always had its roots in human visual psychophysics. Significantly, however, the current system of photometry is truly representative of the spectral sensitivity of human vision for only a very limited number of visual tasks. The spectral sensitivity of the visual system for mesopic vision is not well represented by either of the spectral luminous efficiency functions, $V(\lambda)$ and $V'(\lambda)$, that currently underlie photometry.

It is worth noting that no single system can ever hope to provide a complete prediction of visual performance for all tasks and lighting conditions. Vision is a hugely complicated process and the spectral luminous efficiency of the eye is influenced by a large number of factors. These factors include size and location of the stimulus in the visual field, ambient light level and spectrum, stimulus contrast and spectrum, and speed of response required by the task being conducted. Changing any of these parameters will change the efficiency of the visual system and the ability to perform the requisite task [15][16].

Instead of trying to describe the detailed performance of the eye under a given set of conditions, the emphasis in this Technical Committee has been on developing a system of photometry for the mesopic region which can be readily implemented in practice, but which may not provide a precise description of visual performance. This places two important constraints on the system:

- It must be additive
- It must tend to $V(\lambda)$ at the upper end of the mesopic region and to $V'(\lambda)$ at the lower end

The simplest form of a system for mesopic photometry that satisfies these constraints is a linear combination of the photopic and scotopic spectral luminous efficiency functions, of the form:

$$V_{mes} = yV(\lambda) + (1 - y)V'(\lambda) \text{ } y \text{ being a function of luminance}$$

The mesopic spectral sensitivity functions, $V_{mes}(\lambda)$, defined by such a system are, by definition, additive in nature (since both $V(\lambda)$ and $V'(\lambda)$ are additive), but it must be remembered that due to the dependence of mesopic spectral sensitivity on the state of adaptation of the eye, additivity applies only within a given adaptation level.

The two recently proposed visual performance based systems for mesopic photometry, namely the USP-system (Rea et al. 2004) and the MOVE-system (Goodman et al., 2007), both take the form presented above, thus bridging the photopic and scotopic domains and preserving the fundamental requirement of additivity. The different experimental conditions underlying these two systems result in differences between the systems, a major difference being the transition point between the mesopic and photopic regions. Also, the different characteristics of the adaptation coefficient (designated X in the USP-system, and x in the MOVE-system), result in different predictions of mesopic values calculated with the two systems. In addition to the USP- and MOVE-systems, an Intermediate system is also considered in this report. The Intermediate system has the form presented above, and like the MOVE-system has a loglinear relationship between ' y ' and mesopic luminance, but has adjusted upper and lower luminance limits for the mesopic region.

4.5.1.2.1 USP-SYSTEM

Two investigations by He et al. (1997, 1998) form the experimental basis of the USP-system. In the first work of He et al. (1997) reaction times were measured monocularly under two light sources (HPS and MH) at eight luminance levels between 0.003 cd/m² and 10 cd/m². A target contrast of $C = 2.3$, was used in the experiments. The spectral power distributions of the test target and the adaptation backgrounds were the same i.e. the only information available to the visual system was the achromatic content of the stimulus. (More specifically, the tasks involved luminance contrast with no colour contrast.) The resultant system was a linear combination of the scotopic $V'(\lambda)$ and the photopic $V_{10}(\lambda)$ functions. The system is based on reaction time data for two subjects. According to He et al. (1997) visual inspection of the two subjects' off-axis

reaction time data showed a separation between the two light sources below 0.3 cd/m^2 , but no clear separation was observed above 1 cd/m^2 . As the midpoint between these luminances in log units is 0.6 cd/m^2 , and the paper described that the rod-cone discontinuity at about this luminance, the 0.6 cd/m^2 luminance value was chosen by He et al. as a convenient point of bifurcation on fitting the data curves. Based on the reaction time data, He et al. concluded that there is no rod contribution above $0.6 \text{ cd}\cdot\text{m}^{-2}$ to the reaction time task investigated. An independent study of Bierman et al. (1998) confirmed the reaction time data of He et al. (1997) by using reaction time differences of the two eyes as the criterion.

In the second work by He et al. (1998) mesopic spectral luminous efficiency functions of one subject were measured using a method of reaction time differences between the two eyes. In this binocular simultaneity method, luminous efficiencies for five quasi-monochromatic stimuli (half bandwidth of 10 nm, peaks at 436 nm, 470 nm, 510 nm, and 630 nm) were measured against a yellow reference field (monochromatic 589 nm) at three light levels (0.3 Td, 3 Td, 10 Td). Thus in this experimental study the spectral power distribution of the reference field was different from that of the test field and each eye was adapted to a different condition (i.e. light level and wavelength). The derived mesopic spectral luminous efficiency functions were fitted with the linear model developed in the earlier work of He et al. (1997). The transition point between mesopic and photopic regions was not reached within the retinal illuminance range studied (0.3 Td, 3 Td, 10 Td). Using a relationship between adaptation coefficient and retinal illuminance, the transition point for the data of the one subject in question was estimated to occur at 21 Td, corresponding to a luminance level of 1.7 cd/m^2 . The latter study of He et al. (1998) resulted in an iterative computational procedure for calculating mesopic light levels. In this procedure, the transition point between mesopic and photopic regions occurs at 21 Td. When the monocular viewing used in the previous study by He et al. (1997) is transferred to correspond to binocular viewing conditions, the transition point of 0.6 cd/m^2 corresponds to a retinal illuminance value of 25 Td as remarked by He et al. (1998).

Table 4.2: The experimental conditions underlying the USP-system (He et al. 1997, He et al. 1998)

Method	Stimuli	Contrast	Luminance	Subject	
RT	MH and HPS	2.3	0.003-10 cd/m ²	2	3
RT	470,510,546,630 nm	2.3	0.3,3,10 Td	1	

Half bandwidth = 10 nm $C = (L_t - L_b)/L_b$

The USP formulation is proposed by Rea et al. (2004) as a unified system of photometry. In the mesopic region the parameter X is used to calculate mesopic luminous efficiency $V_{mes}(\lambda)$ as a linear transition between the scotopic $V'(\lambda)$ and the photopic $V(\lambda)$ functions and is of the form

$$V_{mes}(\lambda) = XV(\lambda) + (1 - X)V'(\lambda) \quad \text{for } 0 \leq X \leq 1$$

where $V_{mes}(\lambda)$ is the mesopic spectral luminous efficiency function under the given conditions, $V(\lambda)$ is the photopic spectral luminous efficiency function, $V'(\lambda)$ is the scotopic spectral luminous efficiency function, and X is a parameter characterizing the relative proportions of the photopic and scotopic luminous efficiency at any luminance level. In the scotopic region the USP-system is equivalent to current scotopic photometry and in the photopic region it is equivalent to current photopic photometry, as also are the other systems described in this report.

In proposing the USP-system Rea et al. (2004) made several simplifications to the approaches of the works of He et al. Firstly, since the pupil size is large and essentially constant below 1 cd/m², it was assumed that a constant pupil diameter of 7 mm could be taken to apply, so that the transition point between the mesopic and photopic regions determined from each of the two studies (He et al. 1997, He et al. 1998) are in substantial agreement. This led to the choice of 0.6 cd/m² as the transition point between the mesopic and photopic regions. Secondly, the relationship between the coefficient X and mesopic luminance was assumed to be linear between 0.001 cd/m² and 0.6 cd/m² in order to develop a closed-form solution for X . And thirdly, in the final form of the USP-system, $V_{10}(\lambda)$ was substituted by $V(\lambda)$, based on the observation that

for most practical conditions photometric quantities based on $V(\lambda)$ and $V_{10}(\lambda)$ do not differ substantially.

Below equations give the closed-form expression for calculating the mesopic luminance L_{mes} and the corresponding coefficient X .

$$L_{mes} = 0.834L_p - 0.335L_s - 0.2 + \sqrt{0.696L_p^2 - 0.333L_p - 0.56L_pL_s + 0.113L_s^2 + 0.537L_s + 0.04}$$

For $0.001 < L_{mes} < 0.6$

$$X = mL_{mes} + \beta \quad \text{for } 0 \leq X \leq 1$$

Where L_p is the photopic luminance, L_s is the scotopic luminance, and m and β are coefficients given by $m = 1/0.599$ and $\beta = -0.001/0.599$ (Rea et al 2004).

The values of X and L_{mes} given by the USP-system as a function of photopic luminance and light source S/P-ratio are presented in Table 4.2. The lamp notations LPS (low pressure sodium), HPS (high pressure sodium) and MH (metal halide) on the left side of the table refer to the typical regions of S/P-ratios of these lamp types.

Table 4.3 a) The values of X given by the USP-system as a function of photopic luminance and S/P-ratio, b) values of L_{mes} given by the USP-system as a function of photopic luminance and S/P-ratio (Rea et al. 2004).

		a							
		x	Photopic luminance $\text{cd}\cdot\text{m}^{-2}$						
		S/P	0,001	0,003	0,01	0,03	0,1	0,3	0,55
LPS ~		0,25		0,0000	0,0026	0,0119	0,0562	0,3306	0,8811
		0,35		0,0001	0,0043	0,0172	0,0749	0,3652	0,8876
		0,45		0,0006	0,0060	0,0223	0,0919	0,3938	0,8934
HPS ~		0,55		0,0011	0,0076	0,0273	0,1074	0,4183	0,8986
		0,65		0,0016	0,0093	0,0322	0,1218	0,4397	0,9032
		0,75		0,0021	0,0110	0,0370	0,1352	0,4588	0,9075
		0,85		0,0026	0,0126	0,0416	0,1477	0,4761	0,9113
		0,95		0,0031	0,0142	0,0462	0,1595	0,4917	0,9149
		1,05	0,0001	0,0036	0,0158	0,0506	0,1707	0,5061	0,9181
MH warm white ~		1,15	0,0002	0,0041	0,0174	0,0549	0,1814	0,5194	0,9211
		1,25	0,0004	0,0046	0,0190	0,0592	0,1915	0,5318	0,9239
		1,35	0,0006	0,0051	0,0206	0,0634	0,2011	0,5433	0,9264
		1,45	0,0007	0,0056	0,0221	0,0675	0,2104	0,5541	0,9288
		1,55	0,0009	0,0060	0,0237	0,0715	0,2192	0,5643	0,9311
		1,65	0,0011	0,0065	0,0252	0,0754	0,2278	0,5739	0,9332
		1,75	0,0012	0,0070	0,0267	0,0793	0,2360	0,5830	0,9352
		1,85	0,0014	0,0075	0,0282	0,0831	0,2439	0,5915	0,9370
		1,95	0,0016	0,0080	0,0297	0,0868	0,2516	0,5997	0,9388
		2,05	0,0017	0,0085	0,0312	0,0905	0,2590	0,6075	0,9404
		2,15	0,0019	0,0090	0,0327	0,0941	0,2661	0,6149	0,9420
		2,25	0,0021	0,0094	0,0342	0,0977	0,2730	0,6220	0,9435
MH day-light ~		2,35	0,0022	0,0099	0,0356	0,1012	0,2798	0,6287	0,9449
		2,45	0,0024	0,1040	0,0371	0,1046	0,2863	0,6352	0,9462
		2,55	0,0026	0,0109	0,0385	0,1080	0,2929	0,6415	0,9475
		2,65	0,0027	0,0114	0,0400	0,1140	0,2989	0,6474	0,9487
		2,75	0,0029	0,0118	0,0414	0,1147	0,3049	0,6532	0,9499

		b							
		L_{mes}	Photopic luminance $\text{cd}\cdot\text{m}^{-2}$						
		S/P	0,001	0,003	0,01	0,03	0,1	0,3	0,55
LPS ~		0,25	0,0002	0,0007	0,0025	0,0082	0,0347	0,1990	0,5288
		0,35	0,0003	0,0010	0,0036	0,0113	0,0459	0,2198	0,5327
		0,45	0,0004	0,0014	0,0046	0,0114	0,0560	0,2369	0,5362
HPS ~		0,55	0,0005	0,0017	0,0056	0,0174	0,0653	0,2516	0,5393
		0,65	0,0006	0,0020	0,0066	0,0203	0,0739	0,2644	0,5420
		0,75	0,0007	0,0023	0,0076	0,0231	0,0820	0,2758	0,5446
		0,85	0,0008	0,0026	0,0085	0,0259	0,0895	0,2862	0,5469
		0,95	0,0009	0,0028	0,0095	0,0286	0,0966	0,2956	0,5490
		1,05	0,0010	0,0031	0,0105	0,0313	0,1033	0,3042	0,5509
MH warm white ~		1,15	0,0011	0,0034	0,0114	0,0339	0,1096	0,3121	0,5527
		1,25	0,0012	0,0037	0,0124	0,0365	0,1157	0,3196	0,5544
		1,35	0,0013	0,0040	0,0133	0,0390	0,1215	0,3265	0,5559
		1,45	0,0014	0,0043	0,0143	0,0414	0,1270	0,3329	0,5574
		1,55	0,0015	0,0046	0,0152	0,0438	0,1323	0,3390	0,5587
		1,65	0,0016	0,0049	0,0161	0,0462	0,1374	0,3448	0,5600
		1,75	0,0017	0,0052	0,0170	0,0485	0,1424	0,3502	0,5612
		1,85	0,0018	0,0055	0,0179	0,0508	0,1471	0,3553	0,5623
		1,95	0,0019	0,0058	0,0188	0,0530	0,1517	0,3602	0,5633
		2,05	0,0020	0,0061	0,0197	0,0552	0,1561	0,3646	0,5643
		2,15	0,0021	0,0064	0,0206	0,0574	0,1604	0,3693	0,5653
		2,25	0,0022	0,0067	0,0215	0,0595	0,1646	0,3736	0,5662
MH day-light ~		2,35	0,0023	0,0069	0,0224	0,0616	0,1686	0,3776	0,5670
		2,45	0,0024	0,0072	0,0232	0,0637	0,1725	0,3815	0,5678
		2,55	0,0025	0,0075	0,0241	0,0657	0,1763	0,3852	0,5686
		2,65	0,0026	0,0078	0,0249	0,0667	0,1800	0,3888	0,5693
		2,75	0,0027	0,0081	0,0258	0,0697	0,1836	0,3923	0,5700

4.5.1.2.2 MOVE – SYSTEM

The MOVE-system proposed by the MOVE consortium (Eloholma et al. 2005, Goodman et al. 2007) is based on an empirical multi-technique approach, where the task of night-time driving was divided into three visual subtasks, which are related to the detection of a visual target, the speed of detection, and the identification of the details of the target. Both chromatic and achromatic targets were included. Thus, unlike the approach taken for the USP- system, the MOVE- system is based on data from tasks that do not inherently obey the laws of additivity. This approach was taken in an attempt to provide a reasonably accurate characterisation of visual effectiveness for a wide range of ‘realistic’ visual tasks, i.e. tasks involving the chromatic as well as the achromatic channels of the human visual system. Like the USP-system, however, a major constraint on the system was that it should be able to be readily implemented in practice, and it was therefore recognised that it could not provide a precise description of visual response for any of the tasks considered.

The detection of a visual target is related to the achromatic threshold (Freiding et al. 2007), i.e. to increments and/or decrements of the visual target’s intensity around the threshold. Achromatic detection thresholds were measured using three experimental setups: modified Goldman perimeter (TKK Helsinki University of Technology, Finland), large homogenous screen (TUD Darmstadt University of Technology, Germany), and screen with computer controlled projector (UP University of Pannonia, Hungary).

The speed of detection is related to reaction times (Walkey et al. 2007). Reaction time data were measured using four different experimental setups: large uniform hemisphere (TKK, Finland), computer controlled CRT display (CU City University, UK), driving simulator (TNO Human Factors, The Netherlands), and large homogenous screen (TUD, Germany).

The identification of the targets is related to achromatic recognition threshold (Várady et al. 2007). These data were measured using a screen with computer-controlled projector (UP, Hungary).

A common set of parameter values were used as the basis of each particular data set generated at each of the different test locations. The joint parameters were: background photopic luminances 0.01 cd/m², 0.1 cd/m², 1 cd/m², and 10 cd/m² (some experiments also used 0.3 cd/m² and 3 cd/m²), target eccentricities 0° and 10°, target size 2° (and 0.29°), and nearly steady presentation $\Delta t \geq 3s$ (or $\Delta t \leq 500$ ms for some of the reaction time experiments). The contrasts were at or near threshold and both quasi-monochromatic (half bandwidth = 10 nm) and broadband light sources were used. For some of the experiments the target and background had the same spectral characteristics (achromatic conditions) whereas the majority used different colours for the target and background (chromatic conditions). Altogether 109 subjects participated in the experiments. Table 4.4 summarises the parameters and experimental conditions underlying the MOVE-system.

Table: 4.4: The experimental conditions underlying the contrast threshold (CT), reaction time (RT) and recognition threshold (RGT) experiments of the MOVE-system [14][16]. The experiments were carried out in different laboratories.

Method	Stimuli	Contrast	Luminance(cd/m ²)	Subject	
CT	380-700 nm steps	At threshold	0.01-10	6	109
	450-700 nm steps	At threshold	0.01-1	10	
	blue,green,red(100 nm bands)	At threshold	0.01-10	19	
RT	466, 503, 522, 594, 638 nm	0.05-3	0.01-10	23	
	various broadband broadb.	Varied	0.01-10	11	
	white,yellow, red, blue	0.14	0.01-10	23	
	380-700 nm, 10 nm steps	Near threshold	0.3-1	7	
RGT	450-700 nm ,10 nm steps	At threshold	0.01-1	10	

It was foreseen in the MOVE work that the spectral response for each visual sub-task might require a distinct description of mesopic spectral sensitivity. Results from each of the three visual sub-tasks were therefore initially modelled separately, with each background level taken in turn. It was subsequently found, however, that an acceptably good fit to all the data sets was obtained with a single model.

The data from the vision experiments of the MOVE project resulted in a linear system for mesopic photometry characterizing the mesopic spectral sensitivity of peripheral vision (Goodman et al. 2007):

$$M(x)V(\lambda) = xV(\lambda) + (1 - x)V'(\lambda) \text{ for } 0 \leq x \leq 1$$

where $M(x)$ is a normalizing function such that the $V_{mes}(\lambda)$ function attains a maximum value of 1, $V_{mes}(\lambda)$ is the mesopic spectral luminous efficiency function under the given conditions, $V(\lambda)$ is the photopic spectral luminous efficiency function, $V'(\lambda)$ is the scotopic spectral luminous efficiency function, and x is a coefficient dependent on the luminance level and spectrum.

The experimental data generated within the MOVE project indicated that mesopic vision extends to approximately 10cd/m², although the differences between mesopic and photopic spectral sensitivity become smaller with increasing luminance. The MOVE-system places the transition between the mesopic and photopic regions at approximately 10 cd/m², and the transition between the mesopic and scotopic at approximately 0.01cd/m², though both the upper- and lower limits are dependent on the S/P-ratio as well.

The coefficient x and mesopic luminance L_{mes} of the MOVE-system are determined iteratively as follows

$$x_{n+1} = a + b \log_{10} \left[\frac{1}{M(x_n)} \left(x_n \frac{L_p}{K_p} + (1 - x_n) \frac{L_s}{K_s} \right) \right] \text{ for } 0 \leq x \leq 1$$

$$L_{mes} = \frac{xL_p + (1 - x)L_s V'(\lambda_0)}{x + (1 - x)V'(\lambda_0)}$$

where a and b are parameters which have the values $a = 1.49$ and $b = 0.282$, L_p is the photopic luminance, L_s is the scotopic luminance, K_p is the photopic maximum luminous efficacy ($K_p = 683 \text{ lm} \cdot \text{W}^{-1}$), K_s is the scotopic maximum luminous efficacy ($K_s = 1699 \text{ lm/W}$), L_{mes} is the mesopic luminance, and $V'(\lambda_0) = 683/1699$ is the value of scotopic spectral sensitivity function at $\lambda_0 = 555 \text{ nm}$, which is the wavelength where photopic spectral sensitivity function attains its maximum $V(\lambda_0) = 1$. The normalizing function $M(x)$ can be approximated as follows:

$$M(x) = \max[xV(\lambda) + (1 - x)V'(\lambda)] \approx 1 - 0.65x + 0.65x^2$$

The values of x and L_{mes} given by the MOVE-system as a function of photopic luminance and light source S/P-ratio are presented in Table 4.5

Table 4.5 a) The values of x given by the MOVE-system as a function of photopic luminance and S/P-ratio, b) values of L_{mes} given by the MOVE-system as a function of photopic luminance and S/P-ratio.

		a							
		x	Photopic luminance cd·m ⁻²						
		S/P	0,01	0,03	0,1	0,3	1	3	10
LPS ~	0,25			0,0000	0,3080	0,4900	0,6660	0,8160	0,9720
	0,35			0,0700	0,3200	0,4950	0,6690	0,8170	0,9720
	0,45			0,1090	0,3300	0,5010	0,6710	0,8180	0,9720
HPS ~	0,55			0,1330	0,3400	0,5050	0,6740	0,8190	0,9720
	0,65			0,1510	0,3480	0,5100	0,6760	0,8200	0,9720
	0,75			0,1660	0,3550	0,5140	0,6780	0,8210	0,9720
	0,85	0,0000		0,1780	0,3620	0,5180	0,6800	0,8220	0,9730
	0,95	0,0120		0,1890	0,3680	0,5220	0,6830	0,8230	0,9730
	1,05	0,0280		0,1980	0,3740	0,5260	0,6850	0,8240	0,9730
MH warm white ~	1,15	0,0410		0,2070	0,3790	0,5290	0,6870	0,8250	0,9730
	1,25	0,0530		0,2150	0,3840	0,5320	0,6880	0,8260	0,9730
	1,35	0,0630		0,2220	0,3890	0,5360	0,6900	0,8270	0,9730
	1,45	0,0720		0,2290	0,3940	0,5390	0,6920	0,8280	0,9730
	1,55	0,0810		0,2350	0,3980	0,5420	0,6940	0,8290	0,9740
	1,65	0,0880		0,2410	0,4020	0,5440	0,6960	0,8300	0,9740
	1,75	0,0960		0,2460	0,4060	0,5470	0,6970	0,8310	0,9740
	1,85	0,1020		0,2510	0,4100	0,5500	0,6990	0,8320	0,9740
	1,95	0,1080		0,2560	0,4130	0,5520	0,7000	0,8320	0,9740
	2,05	0,1140		0,2610	0,4160	0,5550	0,7020	0,8330	0,9740
	2,15	0,1200		0,2650	0,4200	0,5570	0,7040	0,8340	0,9740
	2,25	0,1250		0,2690	0,4230	0,5590	0,7050	0,8350	0,9740
MH day-light ~	2,35	0,1300		0,2730	0,4260	0,5620	0,7060	0,8360	0,9750
	2,45	0,1350		0,2770	0,4290	0,5640	0,7080	0,8360	0,9750
	2,55	0,1390		0,2810	0,4320	0,5660	0,7090	0,8370	0,9750
	2,65	0,1440		0,2840	0,4340	0,5680	0,7110	0,8380	0,9750
	2,75	0,1480		0,2880	0,4370	0,5700	0,7120	0,8390	0,9750

		b							
		L _{mes}	Photopic luminance cd·m ⁻²						
		S/P	0,01	0,03	0,1	0,3	1	3	10
LPS ~	0,25		0,0025	0,0075	0,0640	0,2340	0,8740	2,8100	9,9100
	0,35		0,0035	0,0136	0,0700	0,2430	0,8920	2,8400	9,9300
	0,45		0,0045	0,0173	0,0750	0,2530	0,9100	2,8600	9,9400
HPS ~	0,55		0,0055	0,0202	0,0800	0,2620	0,9270	2,8900	9,9500
	0,65		0,0065	0,0227	0,0850	0,2710	0,9430	2,9100	9,9600
	0,75		0,0075	0,0250	0,0890	0,2790	0,9600	2,9400	9,9700
	0,85		0,0085	0,0271	0,0940	0,2880	0,9760	2,9600	9,9800
	0,95		0,0095	0,0291	0,0980	0,2960	0,9920	2,9900	9,9900
	1,05		0,0105	0,0309	0,1020	0,3040	1,0080	3,0100	10,0100
MH warm white ~	1,15		0,0114	0,0327	0,1060	0,3120	1,0230	3,0400	10,0200
	1,25		0,0122	0,0345	0,1100	0,3200	1,0380	3,0600	10,0300
	1,35		0,0130	0,0361	0,1140	0,3270	1,0530	3,0800	10,0400
	1,45		0,0138	0,0378	0,1170	0,3350	1,0680	3,1000	10,0500
	1,55		0,0145	0,0394	0,1210	0,3420	1,0830	3,1300	10,0600
	1,65		0,0152	0,0409	0,1240	0,3490	1,0970	3,1500	10,0700
	1,75		0,0159	0,0424	0,1280	0,3560	1,1110	3,1700	10,0800
	1,85		0,0166	0,0439	0,1310	0,3630	1,1250	3,1900	10,0900
	1,95		0,0173	0,0454	0,1350	0,3700	1,1390	3,2100	10,1000
	2,05		0,0179	0,0468	0,1380	0,3770	1,1530	3,2300	10,1100
	2,15		0,0186	0,0482	0,1410	0,3840	1,1670	3,2600	10,1200
	2,25		0,0192	0,0496	0,1440	0,3900	1,1800	3,2800	10,1300
MH day-light ~	2,35		0,0198	0,0509	0,1470	0,3970	1,1930	3,3000	10,1400
	2,45		0,0205	0,0523	0,1510	0,4030	1,2060	3,3200	10,1500
	2,55		0,0211	0,0536	0,1540	0,4100	1,2190	3,3400	10,1600
	2,65		0,0216	0,0549	0,1570	0,4160	1,2320	3,3600	10,1700
	2,75		0,0222	0,0562	0,1600	0,4220	1,2450	3,3800	10,1800

4.5.1.2.3 Intermediate-System

Although the USP- and MOVE-systems do show significant differences in the calculated mesopic luminance as a function of photopic luminance, particularly for highly coloured sources at low luminance levels, these differences become smaller at all levels for the majority of 'white light' sources used in typical lighting applications, such as roadway lighting at night. In practical terms, therefore, the results obtained using either of the two systems are similar. The principal difference between the systems lies in the form of the transition from the mesopic to photopic regimes. The USP-system has a transition from mesopic (mixed scotopic and photopic) functions to the single, photopic spectral luminous efficiency function at 0.6 cd/m^2 . The MOVE-system includes a contribution from the scotopic spectral luminous efficiency function, albeit an ever-diminishing one, until about 10 cd/m^2 . The upper luminance limit of the mesopic region has been regarded to be too high for the MOVE-system (Rea and Bullough 2007) and too low for the USP-system (Eloholma and Halonen 2006).

In some respects the USP- and MOVE-systems can be considered as representing two extremes. In the one case (USP), only reaction times were measured and chromatic effects were removed from consideration, with the result that this may limit the applicability to achromatic tasks only; in the other case (MOVE) a broad range of tasks is considered, but this introduces a greater degree of variability (or uncertainty) into the results, since the transition from the scotopic to the photopic condition is complicated by non-linear interactions between the chromatic and achromatic channels which may be different for each individual task. In the USP-system a small number (3) of observers were used to minimize

'noise' and in the MOVE-system a large number (119) of observers were used to minimize effects of inter-observer variability. It is also worth noting that although the MOVE experiments included achromatic as well as chromatic tasks, the chromatic tasks dominated. Real-life situations, such as driving on a road at night, involve both achromatic and chromatic tasks, and the achromatic tasks may be slightly under-weighted in the MOVE analysis.

An Intermediate system between the USP- and MOVE-systems was therefore also considered. This system was intended to ensure reasonably wide applicability while also giving increased weight to achromatic tasks as compared with the MOVE-system. Although being an Intermediate system, it is not an average of the USP- and MOVE-systems. There is a significant degree of freedom in the choice of the precise form of the transition and the following points have been considered in deciding this:

- It is advantageous, in terms of practical implementation of a new system of photometry, for there to be a definite upper and lower limit above and below which no change to the current system of photometry is necessary. This makes it clear, for example, whether a particular lighting specification standard needs to be changed to refer to the new system and avoids complicating unnecessarily general lighting applications where peripheral vision plays a less significant role. (It has been shown that $V(\lambda)$ applies at all levels for tasks involving foveal vision only.)
- Based on the argument that the different experimental conditions underlying the USP-system and the MOVE-system explain the difference between the luminance level for the photopic mesopic transition in the two systems, the transition point for the Intermediate-system would be expected to lie between the USP-system value of 0.6 cd/m^2 and the MOVE-system value of 10 cd/m^2 . Two different upper limits for the Intermediate-system, 3 cd/m^2 and 5 cd/m^2 , have therefore been considered in the report.
- A log-linear relationship between the mesopic luminance and the adaptation coefficient 'y' value was selected, since this provides a better match to the data gathered within the MOVE project than a linear-linear relationship of the form used in the USP-system, and therefore provides a better approximation to actual visual performance for a wider range of tasks.

The Intermediate system with upper and lower limits of 3 cd/m^2 and 0.01 cd/m^2 , respectively, is denoted as the MES1-system and takes the form:

$$M(m_1)V_{mes}(\lambda) = m_1V(\lambda) + (1 - m_1)V'(\lambda)$$

where $M(m_1)$ is a normalizing function such that the mesopic spectral luminous efficiency function, $V_{mes}(\lambda)$, attains a maximum value of 1.

If $L_{mes} \geq 3.0 \text{ cd/m}^2$, then $m_1 = 1$

If $L_{mes} \leq 0.01 \text{ cd/m}^2$, then $m_1 = 0$

If $0.01 \text{ cd.m}^{-2} < L_{mes} < 3.0 \text{ cd/m}^2$ then $m_1 = 0.404 \log L_{mes} + 0.807$

where L_{mes} is the mesopic luminance.

The coefficient m_1 and the mesopic luminance L_{mes} obtained using the MES1-system can be iteratively calculated as follows: $m_{1,0} = 0.5$

$$L_{mes,n} = \frac{m_{1,(n-1)}L_p + (1 - m_{1,(n-1)})L_s V'(\lambda_0)}{m_{1,(n-1)} + (1 - m_{1,(n-1)})V'(\lambda_0)}$$

$$m_{1,n} = a + b \log_{10}(L_{mes,n}) \text{ for } 0 \leq m_{1,n} \leq 1$$

Where L_p is the photopic luminance, L_s is the scotopic luminance, $V'(\lambda_0) = 683/1699$ is the value of scotopic spectral sensitivity function at $\lambda_0 = 555 \text{ nm}$, a and b are parameters which have the values $a = 0.807$ and $b = 0.404$, and n is an iteration step

The values of m_1 and L_{mes} given by the MES1-system as a function of photopic luminance

and light source S/P-ratio are presented in Table 4.6.

Table 4.6 a) The values of m_1 given by the MES1-system as a function of photopic luminance and S/P-ratio, b) values of L_{mes} given by the MES1-system as a function of photopic luminance and S/P-ratio.

		a							
		m_1	Photopic luminance $\text{cd}\cdot\text{m}^{-2}$						
		S/P	0,01	0,03	0,1	0,3	1	2	3
LPS ~	0,25	0	0	0,3311	0,5611	0,7941	0,9244	1	
	0,35	0	0,0283	0,3450	0,5667	0,7960	0,9250	1	
	0,45	0	0,0894	0,3569	0,5719	0,7978	0,9256	1	
HPS ~	0,55	0	0,1199	0,3673	0,5768	0,7996	0,9261	1	
	0,65	0	0,1417	0,3766	0,5814	0,8013	0,9267	1	
	0,75	0	0,1591	0,3849	0,5858	0,8030	0,9273	1	
	0,85	0	0,1736	0,3926	0,5899	0,8046	0,9278	1	
	0,95	0	0,1861	0,3997	0,5939	0,8062	0,9284	1	
	1,05	0,0074	0,1971	0,4062	0,5976	0,8078	0,9289	1	
MH warm white ~	1,15	0,0223	0,2070	0,4123	0,6012	0,8093	0,9294	1	
	1,25	0,0352	0,2160	0,4181	0,6047	0,8107	0,9299	1	
	1,35	0,0486	0,2243	0,4235	0,6080	0,8121	0,9304	1	
	1,45	0,0589	0,2319	0,4286	0,6111	0,8135	0,9309	1	
	1,55	0,0663	0,2390	0,4334	0,6142	0,8149	0,9314	1	
	1,65	0,0749	0,2456	0,4381	0,6172	0,8162	0,9318	1	
	1,75	0,0828	0,2518	0,4425	0,6200	0,8175	0,9323	1	
	1,85	0,0902	0,2577	0,4467	0,6228	0,8188	0,9328	1	
	1,95	0,0971	0,2632	0,4507	0,6254	0,8200	0,9332	1	
	2,05	0,1036	0,2685	0,4546	0,6280	0,8212	0,9337	1	
	2,15	0,1098	0,2735	0,4583	0,6305	0,8224	0,9341	1	
	2,25	0,1156	0,2783	0,4619	0,6330	0,8236	0,9345	1	
MH day-light ~	2,35	0,1211	0,2829	0,4653	0,6353	0,8247	0,9349	1	
	2,45	0,1263	0,2873	0,4687	0,6376	0,8258	0,9354	1	
	2,55	0,1314	0,2915	0,4719	0,6399	0,8269	0,9358	1	
	2,65	0,1362	0,2956	0,4750	0,6421	0,8280	0,9362	1	
	2,75	0,1408	0,2995	0,4781	0,6442	0,8291	0,9366	1	
	2,85	0,1452	0,3033	0,4810	0,6463	0,8301	0,9370	1	
	2,95	0,1494	0,3069	0,4838	0,6483	0,8311	0,9373	1	

		b							
		L_{mes}	Photopic luminance $\text{cd}\cdot\text{m}^{-2}$						
		S/P	0,01	0,03	0,1	0,3	1	2	3
LPS ~	0,25	0,0025	0,0075	0,0864	0,2462	0,9292	1,9522	3	
	0,35	0,0035	0,0118	0,0719	0,2541	0,9393	1,9590	3	
	0,45	0,0045	0,0167	0,0769	0,2618	0,9492	1,9656	3	
HPS ~	0,55	0,0055	0,0199	0,0816	0,2692	0,9588	1,9720	3	
	0,65	0,0065	0,0226	0,0860	0,2764	0,9683	1,9784	3	
	0,75	0,0075	0,0249	0,0902	0,2834	0,9776	1,9847	3	
	0,85	0,0085	0,0270	0,0942	0,2902	0,9867	1,9909	3	
	0,95	0,0095	0,0290	0,0981	0,2968	0,9956	1,9970	3	
	1,05	0,0105	0,0309	0,1019	0,3032	1,0044	2,0030	3	
MH warm white ~	1,15	0,0114	0,0327	0,1055	0,3095	1,0130	2,0089	3	
	1,25	0,0123	0,0344	0,1090	0,3156	1,0215	2,0147	3	
	1,35	0,0131	0,0361	0,1124	0,3216	1,0298	2,0204	3	
	1,45	0,0139	0,0377	0,1157	0,3275	1,0380	2,0261	3	
	1,55	0,0147	0,0393	0,1189	0,3333	1,0460	2,0316	3	
	1,65	0,0154	0,0408	0,1221	0,3389	1,0540	2,0371	3	
	1,75	0,0161	0,0422	0,1252	0,3445	1,0618	2,0425	3	
	1,85	0,0168	0,0437	0,1283	0,3499	1,0694	2,0479	3	
	1,95	0,0175	0,0451	0,1312	0,3553	1,0770	2,0531	3	
	2,05	0,0182	0,0465	0,1342	0,3606	1,0845	2,0583	3	
	2,15	0,0188	0,0478	0,1370	0,3658	1,0918	2,0634	3	
	2,25	0,0194	0,0491	0,1399	0,3709	1,0991	2,0685	3	
MH day-light ~	2,35	0,0201	0,0504	0,1427	0,3759	1,1063	2,0735	3	
	2,45	0,0207	0,0517	0,1454	0,3809	1,1133	2,0784	3	
	2,55	0,0213	0,0530	0,1481	0,3858	1,1203	2,0832	3	
	2,65	0,0219	0,0542	0,1508	0,3906	1,1272	2,0880	3	
	2,75	0,0224	0,0554	0,1534	0,3954	1,1340	2,0928	3	
	2,85	0,0230	0,0566	0,1560	0,4001	1,1407	2,0974	3	
	2,95	0,0236	0,0578	0,1585	0,4047	1,1473	2,1021	3	

The Intermediate system with upper and lower limits of 5 cd/m² and 0.005 cd/m², respectively, is denoted as the MES2-system and takes the form:

$$M(m_2)V_{mes}(\lambda) = m_2V(\lambda) + (1 - m_2)V'(\lambda)$$

Where $M(m_2)$ is a normalizing function such that the mesopic spectral luminous efficiency function, $V_{mes}(\lambda)$, attains a maximum value of 1.

If $L_{mes} \geq 5.0$ cd/m², then $m_2 = 1$

If $L_{mes} \leq 0.005$ cd/m², then $m_2 = 0$

If $0.005 \text{ cd.m}^{-2} < L_{mes} < 5.0 \text{ cd/m}^2$, then $m_2 = 0.3334 \log L_{mes} + 0.767$

Where L_{mes} is the mesopic luminance .

The coefficient m_2 and the mesopic luminance L_{mes} obtained using the MES2-system can be iteratively calculated as follows: $m_{2,0} = 0.5$

$$L_{mes,n} = \frac{m_{2,(n-1)}L_p + (1 - m_{2,(n-1)})L_sV'(\lambda_0)}{m_{2,(n-1)} + (1 - m_{2,(n-1)})V'(\lambda_0)}$$

$$m_{2,n} = a + b \log_{10}(L_{mes,n}) \quad \text{for } 0 \leq m_{2,n} \leq 1$$

Where L_p is the photopic luminance, L_s is the scotopic luminance, and $V'(\lambda_0) = 683/1699$ is the value of scotopic spectral sensitivity function at $\lambda_0 = 555$ nm, a and b are parameters which have the values $a = 0.7670$ and $b = 0.3334$, and n is an iteration step.

The values of m_2 and L_{mes} given by the MES2-system as a function of photopic luminance and light source S/P-ratio are presented in Table 4.6.

Table 4.7 a) The values of m_2 given by the MES2-system as a function of photopic luminance and S/P-ratio, b) values of L_{mes} given by the MES2-system as a function of photopic luminance and S/P-ratio. (At photopic luminances of 5 cd/m² the coefficient m_2 has a value of 1 and the mesopic luminance is therefore 5 cd/m², thus the photopic luminance 4.5 cd/m² is more informative and is given in the table 4.7.

		a							
		m_2	Photopic luminance $\text{cd}\cdot\text{m}^{-2}$						
		S/P	0,01	0,03	0,1	0,3	1	3	4,5
LPS ~	0,25			0,1542	0,3830	0,5644	0,7538	0,9225	0,9841
	0,35			0,1804	0,3920	0,5688	0,7558	0,9230	0,9842
	0,45		0,0000	0,1992	0,4000	0,5730	0,7576	0,9235	0,9843
HPS ~	0,55		0,0190	0,2140	0,4073	0,5770	0,7594	0,9240	0,9844
	0,65		0,0459	0,2265	0,4139	0,5808	0,7612	0,9245	0,9845
	0,75		0,0655	0,2373	0,4201	0,5844	0,7629	0,9249	0,9846
	0,85		0,0812	0,2468	0,4258	0,5878	0,7646	0,9254	0,9846
	0,95		0,0943	0,2553	0,4311	0,5911	0,7662	0,9258	0,9847
	1,05		0,1057	0,2631	0,4361	0,5942	0,7678	0,9263	0,9848
MH warm white ~	1,15		0,1157	0,2702	0,4408	0,5972	0,7693	0,9267	0,9849
	1,25		0,1247	0,2767	0,4452	0,6001	0,7708	0,9272	0,9850
	1,35		0,1329	0,2828	0,4494	0,6029	0,7723	0,9276	0,9851
	1,45		0,1404	0,2885	0,4534	0,6056	0,7737	0,9280	0,9852
	1,55		0,1473	0,2939	0,4573	0,6082	0,7751	0,9284	0,9853
	1,65		0,1538	0,2990	0,4609	0,6107	0,7764	0,9289	0,9853
	1,75		0,1598	0,3038	0,4645	0,6131	0,7778	0,9293	0,9854
	1,85		0,1654	0,3083	0,4678	0,6155	0,7791	0,9297	0,9855
	1,95		0,1708	0,3126	0,4711	0,6178	0,7803	0,9301	0,9856
	2,05		0,1758	0,3168	0,4742	0,6200	0,7816	0,9304	0,9857
	2,15		0,1806	0,3207	0,4772	0,6221	0,7828	0,9308	0,9857
	2,25		0,1852	0,3245	0,4801	0,6242	0,7840	0,9312	0,9858
MH day-light ~	2,35		0,1895	0,3282	0,4830	0,6263	0,7852	0,9316	0,9859
	2,45		0,1937	0,3317	0,4857	0,6283	0,7863	0,9319	0,9860
	2,55		0,1977	0,3351	0,4883	0,6302	0,7875	0,9323	0,9860
	2,65		0,2015	0,3383	0,4909	0,6321	0,7886	0,9327	0,9861
	2,75		0,2052	0,3415	0,4934	0,6339	0,7896	0,9330	0,9862

		b							
		L_{mes}	Photopic luminance $\text{cd}\cdot\text{m}^{-2}$						
		S/P	0,01	0,03	0,1	0,3	1	3	4,5
LPS ~	0,25		0,0025	0,0145	0,0705	0,2467	0,9130	2,9265	4,4782
	0,35		0,0035	0,0174	0,0750	0,2545	0,9253	2,9367	4,4812
	0,45		0,0045	0,0198	0,0793	0,2620	0,9373	2,9468	4,4842
HPS ~	0,55		0,0057	0,0220	0,0834	0,2693	0,9492	2,9568	4,4872
	0,65		0,0069	0,0239	0,0873	0,2764	0,9608	2,9668	4,4901
	0,75		0,0079	0,0258	0,0911	0,2833	0,9722	2,9763	4,4929
	0,85		0,0088	0,0275	0,0947	0,2901	0,9835	2,9859	4,4958
	0,95		0,0096	0,0292	0,0983	0,2967	0,9945	2,9953	4,4986
	1,05		0,0104	0,0308	0,1017	0,3032	1,0054	3,0046	4,5014
MH warm white ~	1,15		0,0111	0,0323	0,1051	0,3096	1,0161	3,0139	4,5041
	1,25		0,0118	0,0338	0,1083	0,3158	1,0267	3,0230	4,5068
	1,35		0,0125	0,0353	0,1115	0,3220	1,0371	3,0319	4,5095
	1,45		0,0132	0,0367	0,1147	0,3280	1,0473	3,0408	4,5122
	1,55		0,0138	0,0381	0,1178	0,3339	1,0575	3,0496	4,5148
	1,65		0,0145	0,0395	0,1208	0,3398	1,0674	3,0582	4,5174
	1,75		0,0151	0,0408	0,1238	0,3455	1,0773	3,0668	4,5200
	1,85		0,0157	0,0421	0,1267	0,3512	1,0870	3,0753	4,5225
	1,95		0,0163	0,0434	0,1295	0,3568	1,0966	3,0836	4,5250
	2,05		0,0169	0,0446	0,1324	0,3623	1,1060	3,0919	4,5275
	2,15		0,0174	0,0459	0,1352	0,3677	1,1154	3,1001	4,5299
	2,25		0,0180	0,0471	0,1379	0,3731	1,1246	3,1082	4,5323
MH day-light ~	2,35		0,0185	0,0483	0,1406	0,3784	1,1338	3,1162	4,5347
	2,45		0,0191	0,0495	0,1433	0,3836	1,1428	3,1241	4,5371
	2,55		0,0196	0,0506	0,1459	0,3888	1,1517	3,1319	4,5395
	2,65		0,0201	0,0518	0,1485	0,3939	1,1605	3,1396	4,5418
	2,75		0,0207	0,0529	0,1511	0,3989	1,1693	3,1473	4,5441

CHAPTER-5

LIGHTING DESIGN IN PHOTOPIC REGION

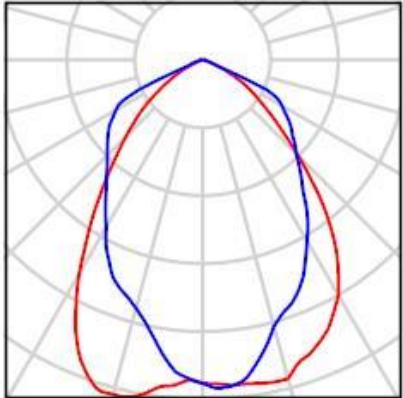
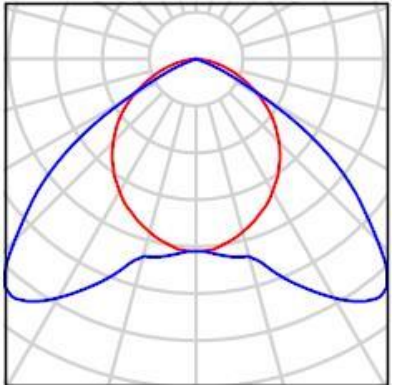
In this chapter, the lighting calculations and analysis for the simulated area lighting design of the 20x10 meter space using metal halide(MH),high pressure sodium vapour (HPSV) and cool white led lamps in DIALux are presented. The goal of this section is to evaluate the average illuminance using the lamps separately.

5.1 Design using high pressure sodium vapour light (HPSV)

5.1.1 Luminaire Details:

The details of the lamps and luminaires used for the design have been given in Table 5.1.

Table-5.1: Luminaires with Specification

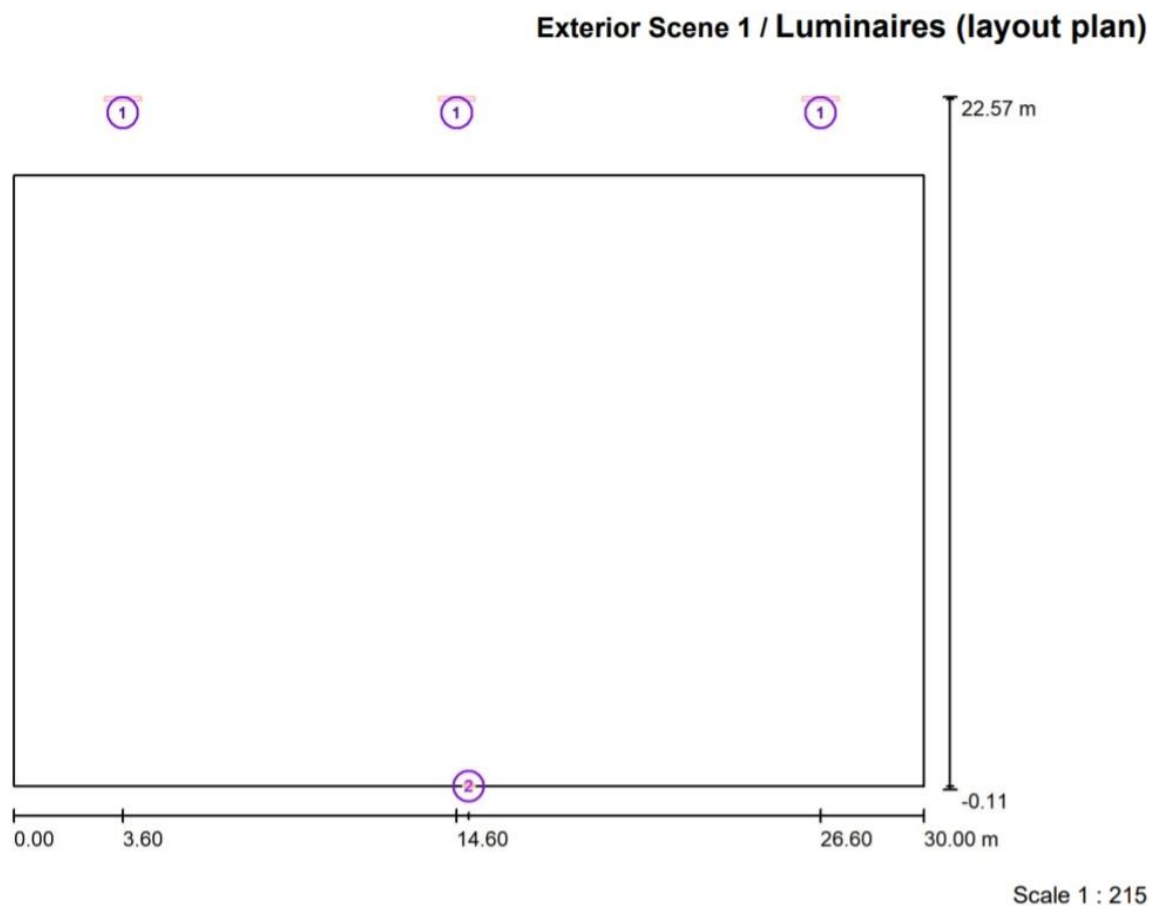
Name of Luminaire	Details of Fixture	Light Distribution Curve
PHILIPS SWF 101/150W [SYMMETRIC], CLOSED	Luminous flux (Luminaire): 9856 lm Luminous flux (Lamps): 14000 lm Luminaire Wattage: 170.0 W Luminaire classification according to CIE: 100 CIE flux code: 62 91 99 100 70 Fitting: 1 x SON T 150W (Correction Factor 1.000).	
TCS 306 / 136 M1	Luminous flux (Luminaire): 2261 lm Luminous flux (Lamps): 3250 lm Luminaire Wattage: 45.2 W Luminaire classification according to CIE: 100 CIE flux code: 49 87 98 100 70 Fitting: 1 x TL'D'36W/865 (Correction Factor 1.000).	

5.1.2 Design Considerations:

- Area of the space: 30*20m.

- Luminaire used: 3 x PHILIPS SWF 101/150W [SYMMETRIC], and 3 x TCS 306 / 136 M1(surrounding light source).
- Pole height : 9m.
- Light loss factor: 0.80,
- ULR (Upward Light Ratio): 19.0%

In **Fig. 5.1**, the layout of the designed area and the positions of the luminaire are shown.Here two different type of lamp are used one is fluorescent lamp (used as surrounding light source) denoted as 1 and other is high pressure sodium vapour lamp which is denoted as 2.



Luminaire Parts List

No.	Pieces	Designation
1	3	TCS 306 / 136 M1
2	3	PHILIPS SWF 101/150W [SYMMETRIC], CLOSED,

Fig:5.1 Luminaires layout plan

Luminous intensity table of the lamp high pressure sodium vapour is shown in **fig 5.2**.

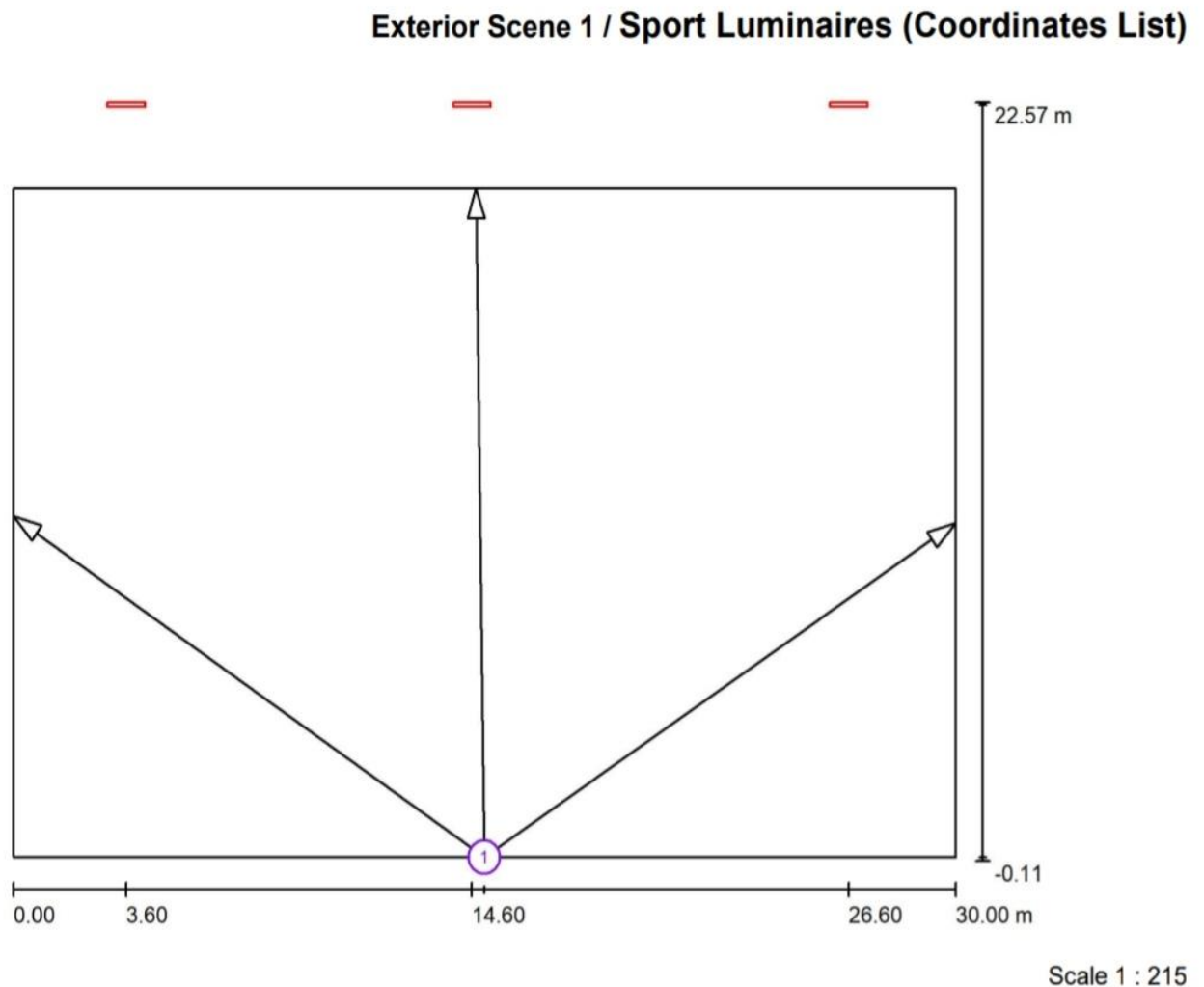
PHILIPS SWF 101/150W [SYMMETRIC], CLOSED, / Luminous intensity table

Luminaire: PHILIPS SWF 101/150W [SYMMETRIC], CLOSED,
Lamps: 1 x SON T 150W

Gamma	C 0°	C 30°	C 60°	C 90°	C 120°	C 150°	C 180°	C 210°	C 240°	C 270°	C 300°	C 330°	C 360°
0.0°	381	381	381	381	381	381	381	381	381	381	381	381	381
5.0°	385	395	390	386	388	389	385	377	374	369	379	383	385
10.0°	387	394	371	364	379	406	400	375	342	332	349	377	387
15.0°	389	383	347	325	351	407	408	356	311	303	318	355	389
20.0°	369	361	322	306	322	374	396	324	288	286	296	323	369
25.0°	350	328	301	281	299	334	354	293	268	261	282	299	350
30.0°	320	292	272	246	267	287	291	256	245	227	255	270	320
35.0°	275	256	233	214	232	241	226	223	213	199	217	242	275
40.0°	219	212	194	181	191	189	170	185	180	176	181	207	219
45.0°	159	171	162	156	159	143	128	151	155	159	157	168	159
50.0°	113	135	138	138	129	112	95	128	137	146	146	132	113
55.0°	80	99	129	124	110	88	63	105	123	134	138	100	80
60.0°	56	78	110	108	93	67	38	79	109	118	113	80	56
65.0°	31	57	80	84	80	40	16	44	92	82	90	59	31
70.0°	13	25	14	13	18	11	6.00	14	12	15	14	24	13
75.0°	4.00	5.00	7.00	8.00	6.00	5.00	3.00	4.00	6.00	8.00	7.00	5.00	4.00
80.0°	2.00	3.00	3.00	4.00	3.00	2.00	2.00	2.00	3.00	4.00	3.00	3.00	2.00
85.0°	2.00	2.00	2.00	2.00	2.00	2.00	2.00	2.00	2.00	2.00	2.00	2.00	2.00
90.0°	0.00	0.00	0.00	0.00	0.00	0.00	0.00	0.00	0.00	0.00	0.00	0.00	0.00

Fig 5.2: Luminous intensity table

In **Fig. 5.3**, the positions of the luminaires (HPSV) are shown. In addition to the luminaire positions, the figure also shows aiming point, angle and alignment of the luminaires (HPSV).



List of the Sport Luminaires

Luminaire	Index	Position [m]			Aiming Point [m]			Angle [°]	Alignment	Pole
		X	Y	Z	X	Y	Z			
PHILIPS SWF 101/150W [SYMMETRIC], CLOSED,	1	15.000	0.000	9.000	14.735	20.000	0.000	24.2	(C 0, G 0)	/
PHILIPS SWF 101/150W [SYMMETRIC], CLOSED,	1	15.000	0.000	9.000	30.000	10.000	0.000	26.5	(C 0, G 0)	/
PHILIPS SWF 101/150W [SYMMETRIC], CLOSED,	1	15.000	0.000	9.000	0.000	10.201	0.000	26.4	(C 0, G 0)	/

Fig 5.3: Coordinates list of luminaires.

Fig 5.4 shows the isolux line of the calculated area.

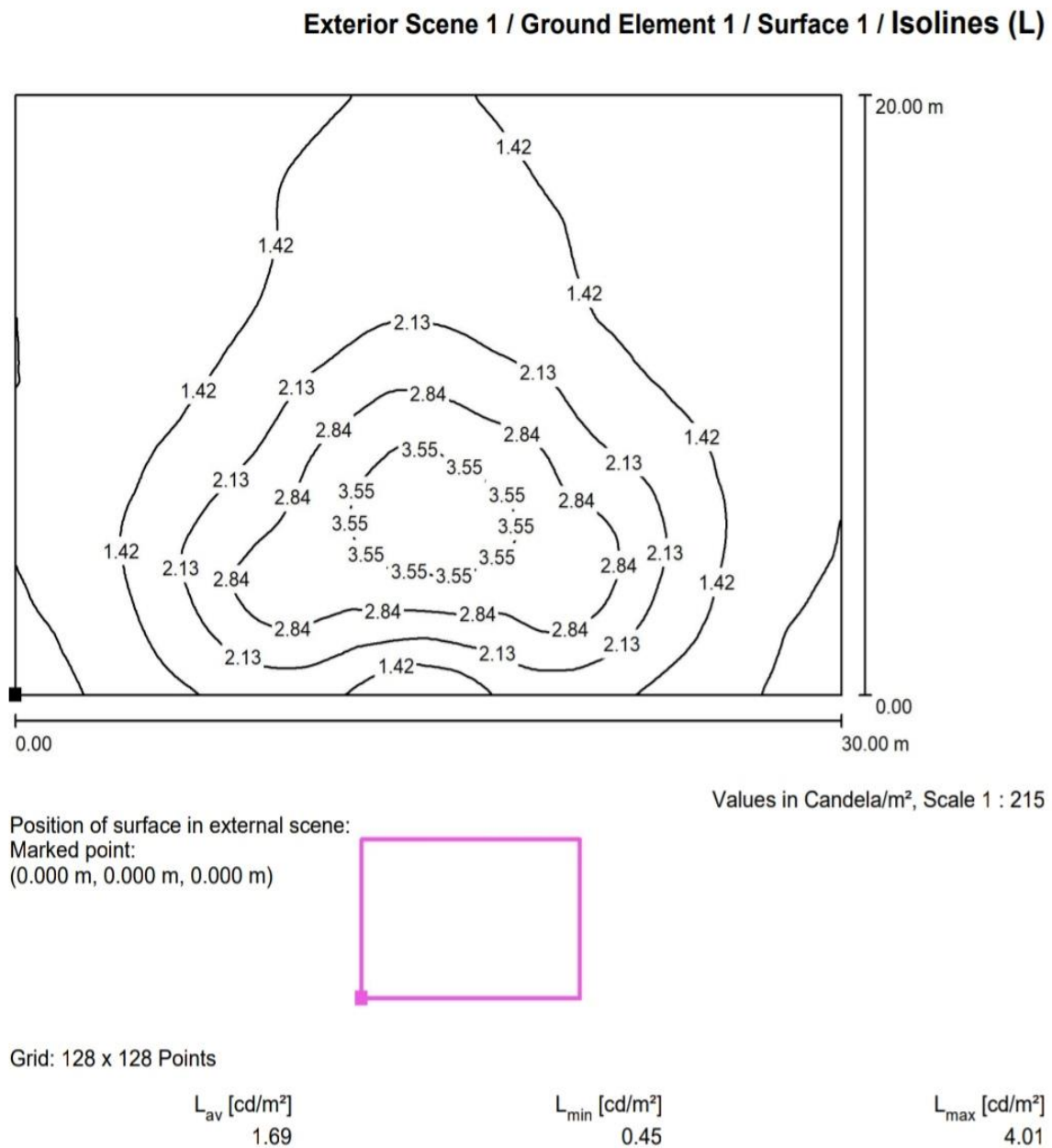


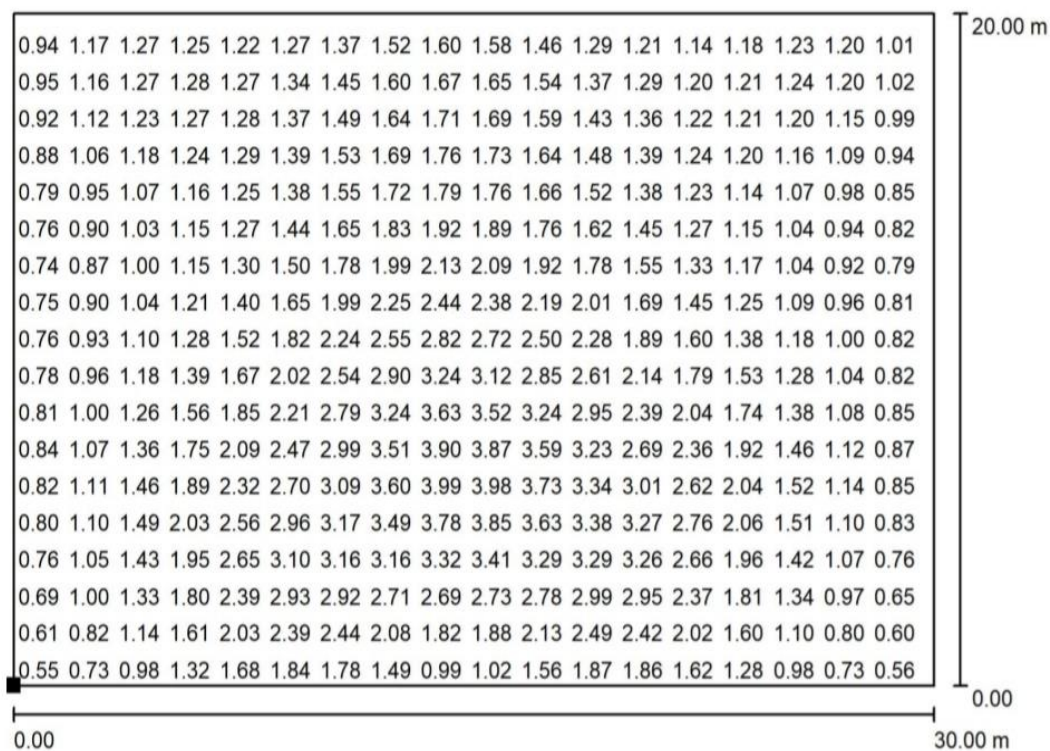
Fig 5.4: Isolines diagram

Fig 5.5 shows the value chart for the calculated area. It also shows the average, maximum and minimum luminance value of the design area.

The values obtained throughout the area are as follows:

- Average luminance (L_{avg}) = 1.69 cd/m².
- Overall Uniformity (U_0) = 0.265.

Exterior Scene 1 / Ground Element 1 / Surface 1 / Value Chart (L)



Values in Candela/m², Scale 1 : 215

Not all calculated values could be displayed.

Position of surface in external scene:

Marked point:

(0.000 m, 0.000 m, 0.000 m)



Grid: 128 x 128 Points

L_{av} [cd/m²]
1.69

L_{min} [cd/m²]
0.45

L_{max} [cd/m²]
4.01

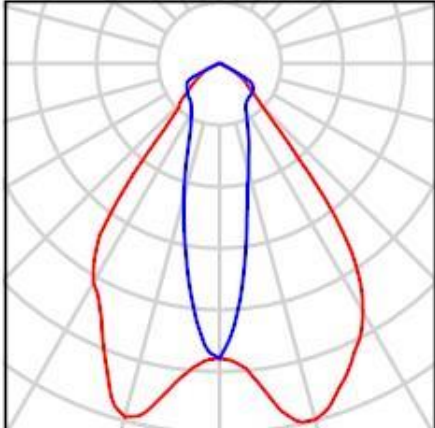
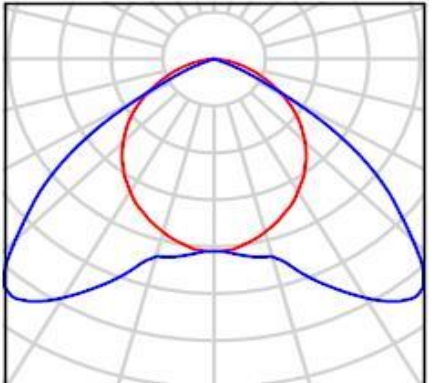
Fig5.5: Value chart

5.2 Design using Metal Halide lamp (MH)

5.2.1 Luminaire Details:

The details of the lamps and luminaires used for the design have been given in Tables 5.2

Table-5.2: Luminaires with Specification

Name of Luminaire	Details of Fixture	Light Distribution Curve
PHILIPS MWF 101/150W [SYMMETRIC], CLOSED	Luminous flux (Luminaire): 8627 lm Luminous flux (Lamps): 12100 lm Luminaire Wattage: 170.0 W Luminaire classification according to CIE: 100 CIE flux code: 71 93 99 100 71 Fitting: 1 x MHN TD 150W (Correction Factor 1.000).	
TCS 306 / 136 M1	Luminous flux (Luminaire): 2261 lm Luminous flux (Lamps): 3250 lm Luminaire Wattage: 45.2 W Luminaire classification according to CIE: 100 CIE flux code: 49 87 98 100 70 Fitting: 1 x TL'D'36W/865 (Correction Factor 1.000).	

5.2.2 Design Considerations:

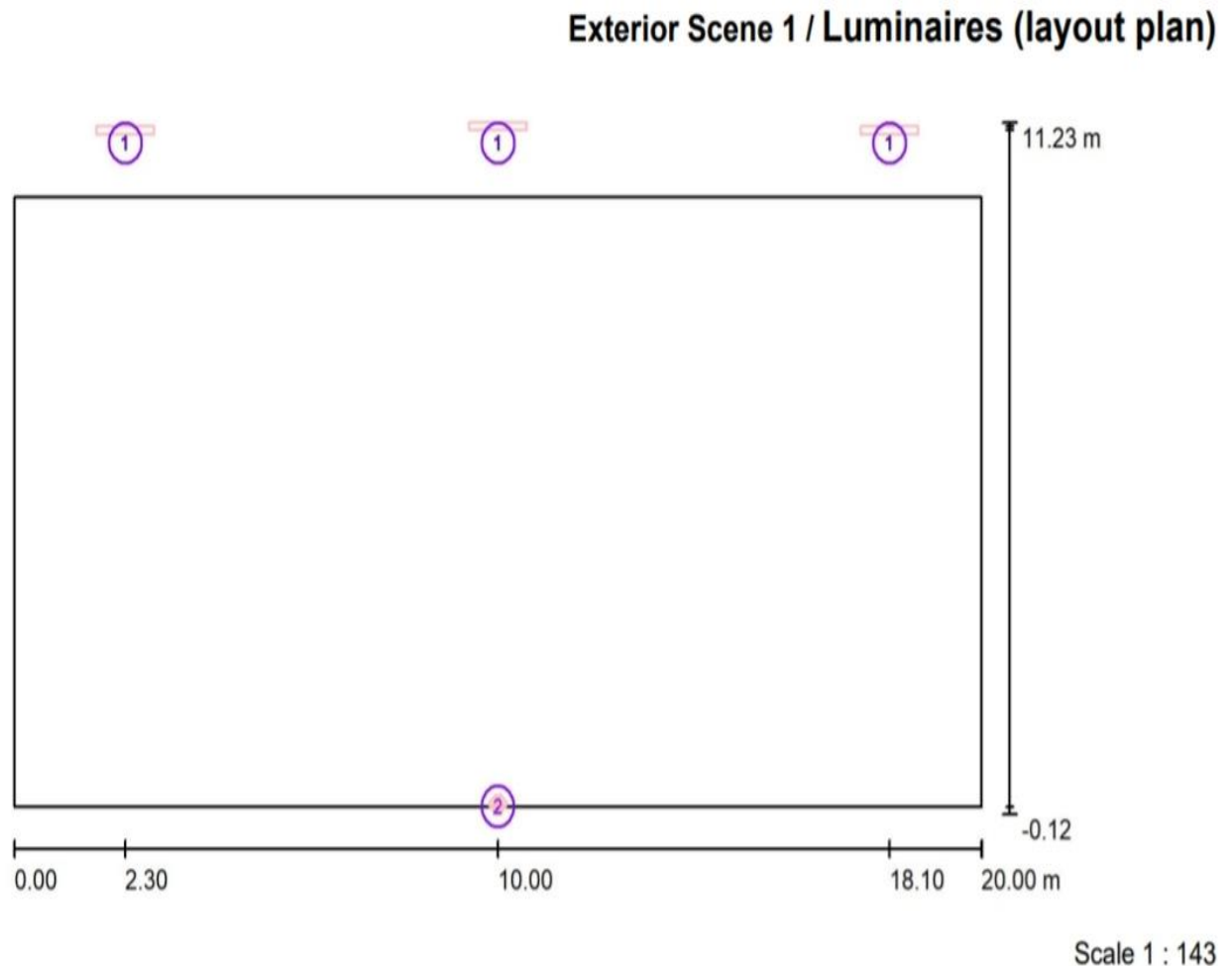
- Area of the space: 20*10m.
- Luminaire used: 2 x PHILIPS MWF 101/150W [SYMMETRIC], CLOSED and 3 x TCS 306 / 136 M1(surrounding light source).
- Pole height : 9m.
- Light loss factor: 0.80
- ULR (Upward Light Ratio): 4.0%

Luminous intensity table of the lamp Metal Halide is shown in **fig 5.6**.

PHILIPS MWF 101/150W [SYMMETRIC], CLOSED, / Luminous intensity table													
Luminaire: PHILIPS MWF 101/150W [SYMMETRIC], CLOSED, Lamps: 1 x MHN TD 150W													
Gamma	C 0°	C 30°	C 60°	C 90°	C 120°	C 150°	C 180°	C 210°	C 240°	C 270°	C 300°	C 330°	C 360°
0.0°	718	718	718	718	718	718	718	718	718	718	718	718	718
5.0°	746	689	611	576	616	695	743	722	664	632	640	703	746
10.0°	858	658	454	382	465	665	827	735	544	472	524	688	858
15.0°	898	557	318	271	346	627	891	724	421	337	402	640	898
20.0°	845	407	237	210	246	465	799	580	289	226	292	532	845
25.0°	776	297	192	160	186	325	682	416	199	165	202	418	776
30.0°	698	234	158	127	145	244	615	290	150	137	154	322	698
35.0°	562	187	133	114	117	177	508	200	123	121	130	242	562
40.0°	290	157	116	109	102	128	209	138	110	113	114	174	290
45.0°	146	131	107	108	96	117	138	112	104	109	105	128	146
50.0°	97	103	104	105	92	97	95	103	98	102	101	100	97
55.0°	75	90	94	99	86	86	70	95	88	97	93	87	75
60.0°	45	79	86	85	78	59	49	81	80	91	85	79	45
65.0°	24	55	16	17	53	32	34	39	69	32	72	55	24
70.0°	8.00	9.00	6.00	10	7.00	6.00	6.00	6.00	10	9.00	11	9.00	8.00
75.0°	3.00	4.00	4.00	7.00	5.00	4.00	3.00	3.00	5.00	6.00	5.00	4.00	3.00
80.0°	2.00	2.00	3.00	4.00	3.00	2.00	2.00	2.00	3.00	3.00	3.00	2.00	2.00
85.0°	2.00	2.00	2.00	2.00	2.00	2.00	2.00	2.00	2.00	2.00	2.00	2.00	2.00
90.0°	0.00	0.00	0.00	0.00	0.00	0.00	0.00	0.00	0.00	0.00	0.00	0.00	0.00

Fig 5.6: Luminous intensity table

In **Fig. 5.7**, the layout of the designed area and the positions of the luminaire are shown. Here two different type of lamp are used one is fluorescent lamp (used as surrounding light source) denoted as 1 and other is Metal Halide(MH) which is denoted as 2.

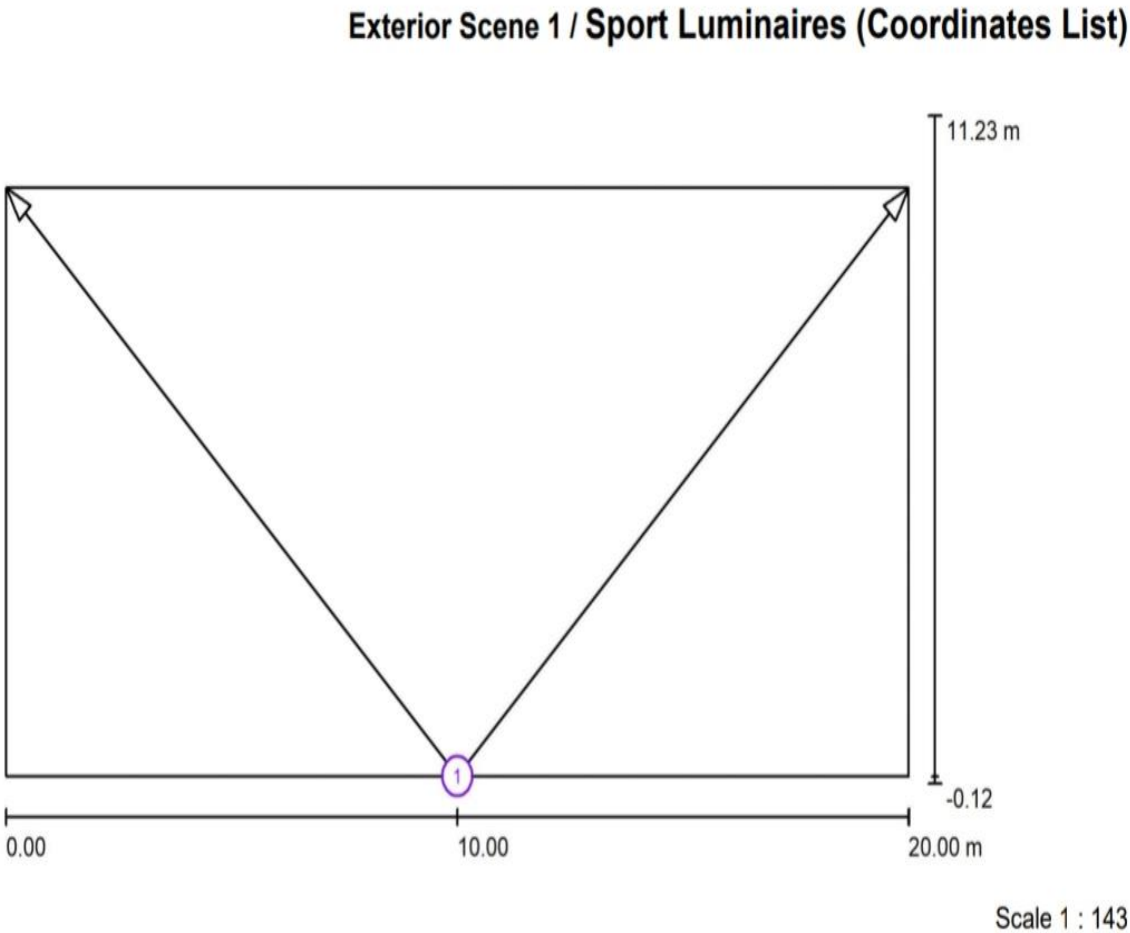


Luminaire Parts List

No.	Pieces	Designation
1	3	TCS 306 / 136 M1
2	2	PHILIPS MWF 101/150W [SYMMETRIC], CLOSED,

Fig 5.7: Luminaires layout plan

In Fig. 5.8 the positions of the luminaires (MH) are shown. In addition to the luminaire positions, the figure also shows aiming point, angle and alignment of the luminaires (MH).



List of the Sport Luminaires

Luminaire	Index	Position [m]			Aiming Point [m]			Angle [°]	Alignment	Pole
		X	Y	Z	X	Y	Z			
PHILIPS MWF 101/150W [SYMMETRIC], CLOSED,	1	10.000	0.000	9.000	0.000	10.000	0.000	32.5	(C 90, G IMax)	/
PHILIPS MWF 101/150W [SYMMETRIC], CLOSED,	1	10.000	0.000	9.000	20.000	10.000	0.000	32.5	(C 90, G IMax)	/

Fig 5.8: Luminaires coordinate list

Fig 5.9 shows the isolux line of the calculated area.

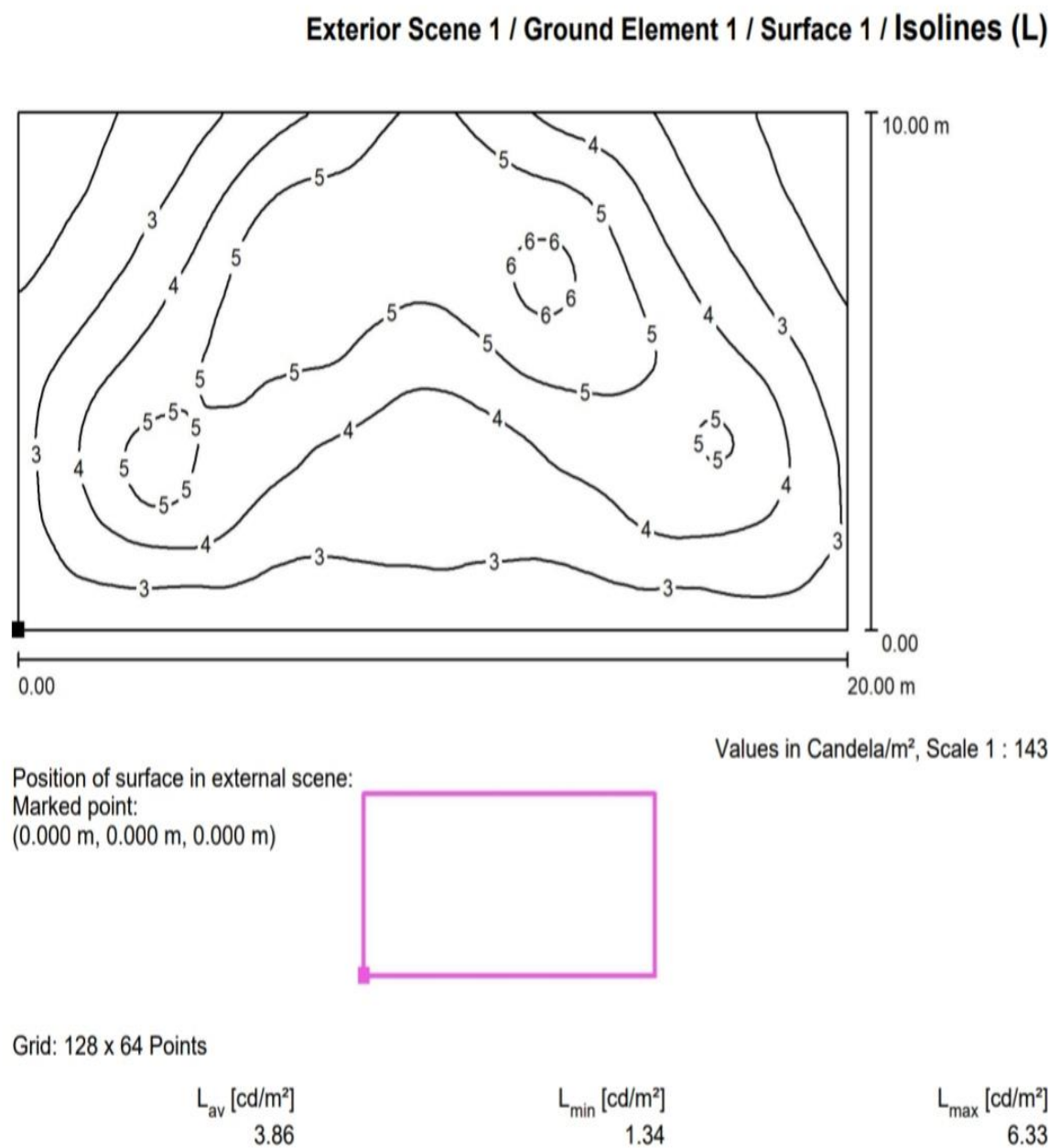


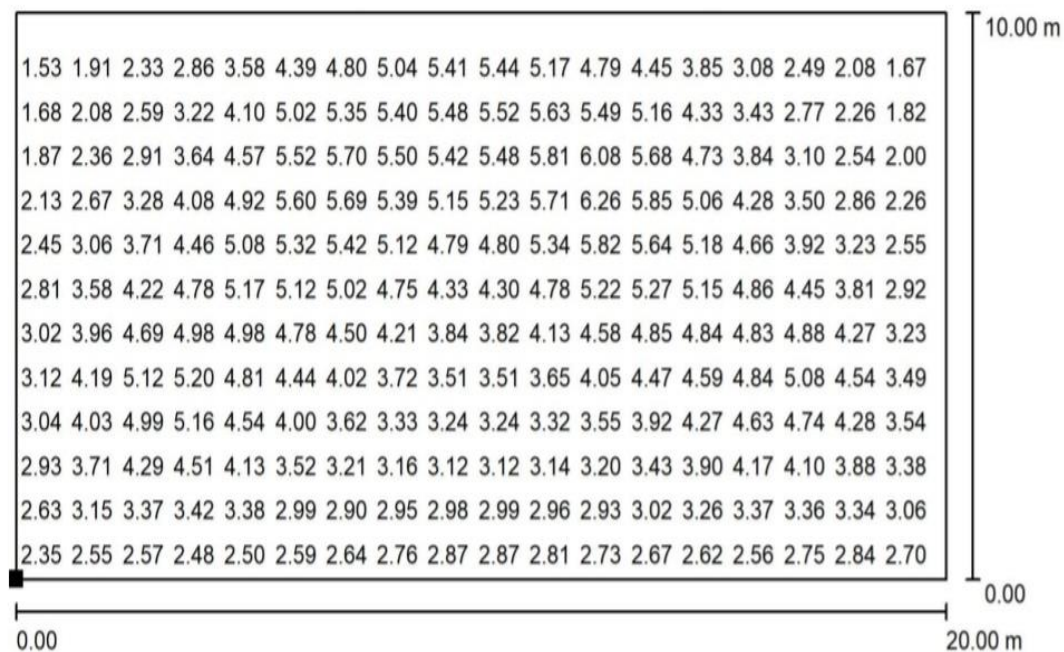
Fig 5.9: Isoline diagram

Fig 5.10 shows the value chart for the calculated area. It also shows the average, maximum and minimum luminance value of the design area.

The values obtained throughout the area are as follows:

- Average luminance (L_{avg}) = 3.86 cd/m^2 .
- Overall Uniformity (U_0) = 0.347.

Exterior Scene 1 / Ground Element 1 / Surface 1 / Value Chart (L)



Values in Candela/m², Scale 1 : 143

Not all calculated values could be displayed.

Position of surface in external scene:

Marked point:

(0.000 m, 0.000 m, 0.000 m)



Grid: 128 x 64 Points

L_{av} [cd/m^2]
3.86

L_{min} [cd/m^2]
1.34

L_{max} [cd/m^2]
6.33

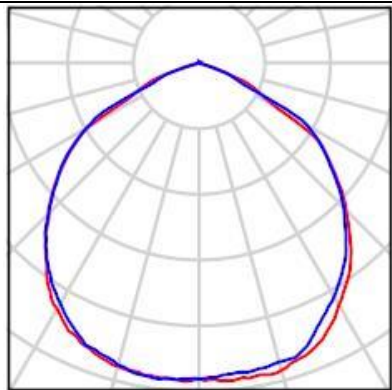
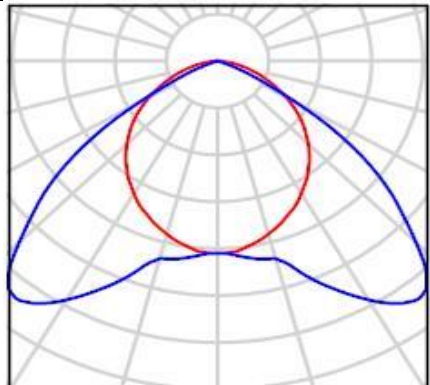
Fig 5.10: value chart

5.2 Design using Cool White LED

5.3.1 Luminaire Details:

The details of the lamps and luminaires used for the design have been given in Tables 5.3

Table-5.2: Luminaires with Specification

Name of Luminaire	Details of Fixture	Light Distribution Curve
Orbit Industries, Inc.	Luminous flux (Luminaire): 14498 lm Luminous flux (Lamps): 14499 lm Luminaire Wattage: 158.6 W Luminaire classification according to CIE: 100 CIE flux code: 54 89 100 100 100 Fitting: 1 x LFL4-160W (Correction Factor 1.000).	
TCS 306 / 136 M1	Luminous flux (Luminaire): 2261 lm Luminous flux (Lamps): 3250 lm Luminaire Wattage: 45.2 W Luminaire classification according to CIE: 100 CIE flux code: 49 87 98 100 70 Fitting: 1 x TL'D'36W/865 (Correction Factor 1.000).	

5.3.2 Design Considerations:

- Area of the space: 20*10m.
- Luminaire used: 2 x PHILIPS MWF 101/150W [SYMMETRIC], CLOSED and 3 x TCS 306 / 136 M1(surrounding light source).
- Pole height : 9m.
- Light loss factor: 0.80
- ULR (Upward Light Ratio): 7.0%

Luminous intensity table of the lamp CWLED is shown in **fig 5.11**.

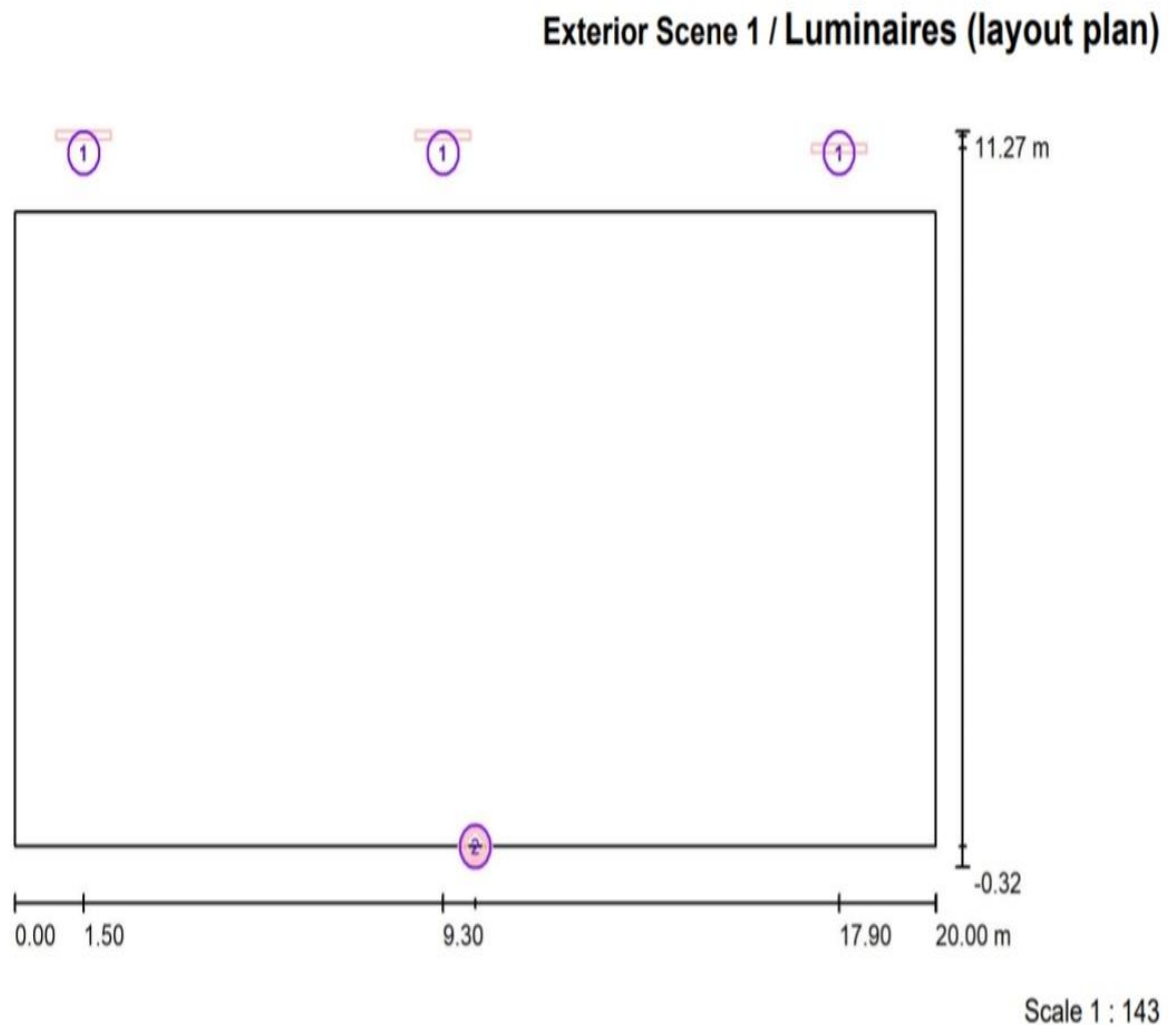
Orbit Industries, Inc. / Luminous intensity table

Luminaire: Orbit Industries, Inc.
Lamps: 1 x LFL4-160W

Gamma	C 0°	C 30°	C 60°	C 90°	C 120°	C 150°	C 180°	C 210°	C 240°	C 270°	C 300°	C 330°	C 360°
0.0°	385	385	385	385	385	385	385	385	385	385	385	385	385
5.0°	388	384	381	381	381	379	386	383	386	386	384	384	388
10.0°	388	384	382	381	379	378	387	384	385	386	386	381	388
15.0°	387	382	382	377	378	379	382	383	384	381	384	384	387
20.0°	379	377	374	372	372	374	375	379	377	371	379	381	379
25.0°	364	369	360	349	358	363	364	368	364	358	367	370	364
30.0°	340	350	339	329	339	348	346	353	348	338	349	354	340
35.0°	317	323	317	306	316	325	322	335	327	315	331	327	317
40.0°	287	293	289	278	292	302	291	309	302	291	304	297	287
45.0°	253	257	257	249	262	269	259	276	273	259	272	263	253
50.0°	219	224	223	216	229	233	229	242	239	226	238	229	219
55.0°	187	185	187	185	192	196	194	204	205	197	200	192	187
60.0°	110	146	150	152	156	158	155	166	168	158	160	149	110
65.0°	76	85	86	55	93	95	83	106	123	86	116	90	76
70.0°	26	35	30	34	40	52	55	64	57	46	47	46	26
75.0°	1.88	7.17	2.92	1.66	5.09	13	16	19	7.21	1.64	4.82	11	1.88
80.0°	0.53	0.49	0.54	0.70	0.82	1.10	1.10	1.15	0.83	0.74	0.66	0.58	0.53
85.0°	0.12	0.12	0.14	0.18	0.23	0.33	0.36	0.40	0.32	0.27	0.21	0.14	0.12
90.0°	0.03	0.04	0.03	0.04	0.05	0.05	0.04	0.06	0.05	0.03	0.03	0.03	0.03

Fig 5.11: luminous intensity table.

In Fig. 5.12, the layout of the designed area and the positions of the luminaire are shown. Here two different type of lamp are used one is fluorescent lamp (used as surrounding light source) denoted as 1 and other is CWLED which is denoted as 2.

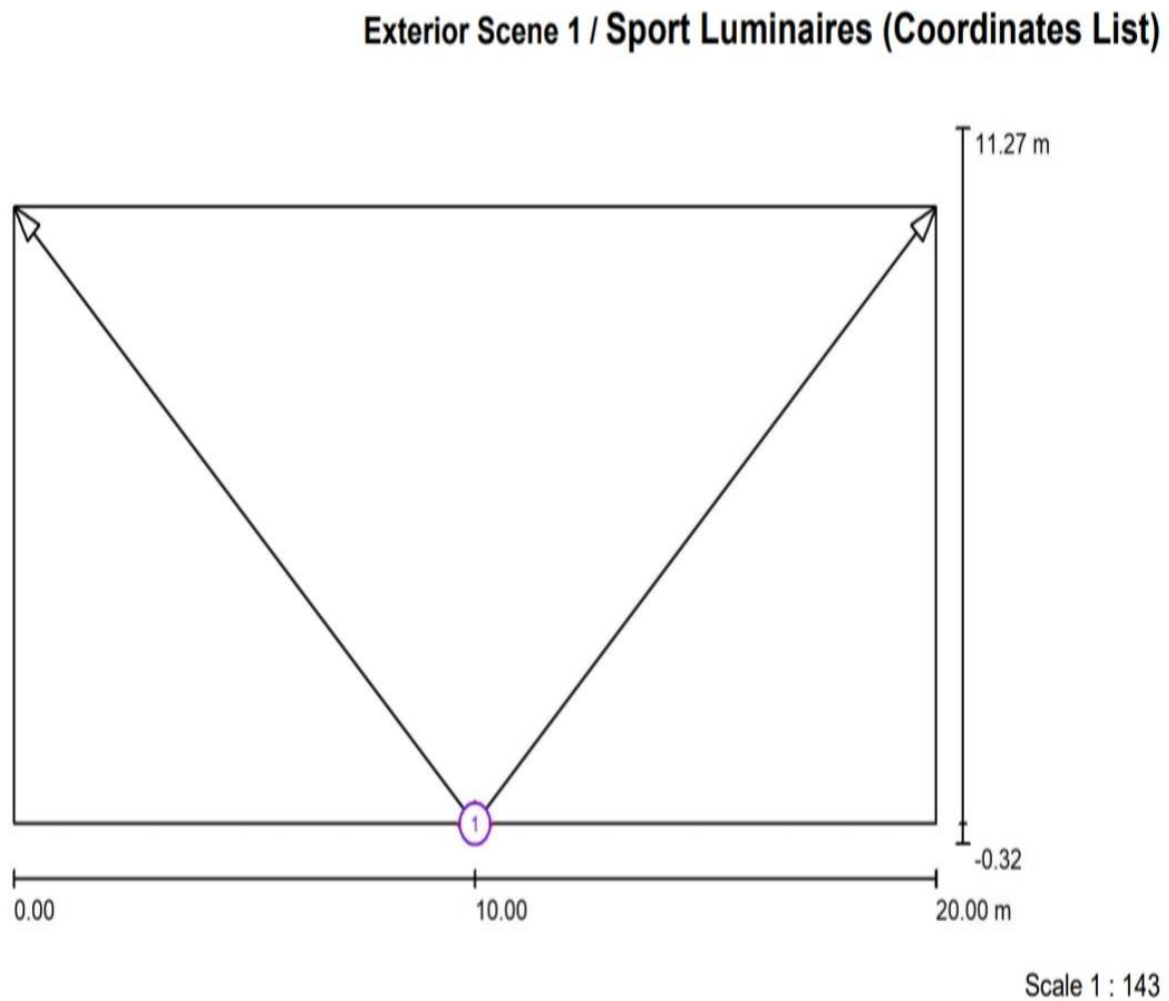


Luminaire Parts List

No.	Pieces	Designation
1	3	TCS 306 / 136 M1
2	2	Orbit Industries, Inc.

Fig 5.12: Luminaires layout plan

In **Fig. 5.13** the positions of the luminaires (CWLED) are shown. In addition to the luminaire positions, the figure also shows aiming point, angle and alignment of the luminaires (CWLED).



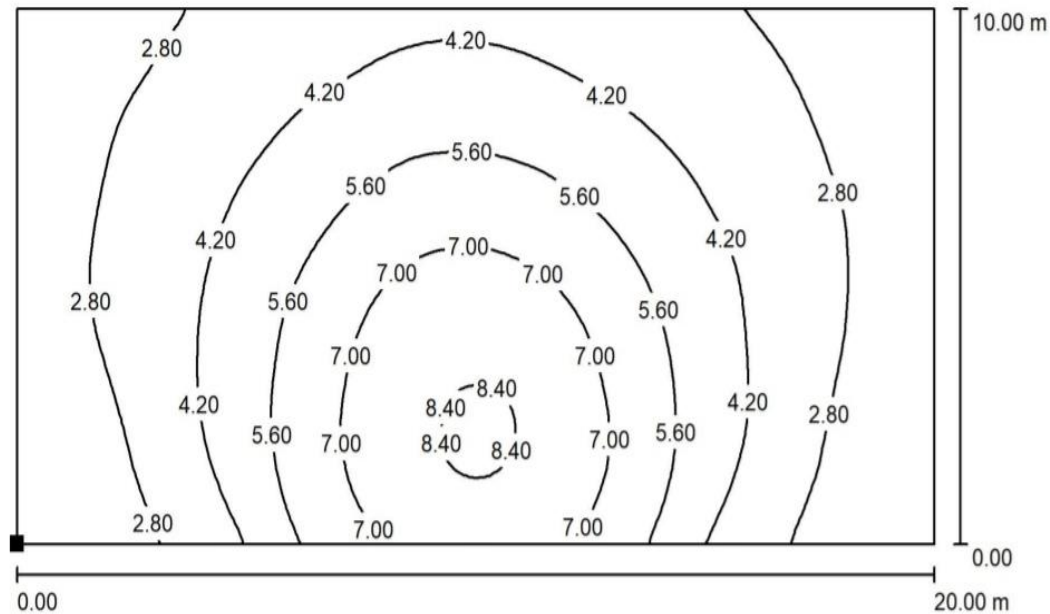
List of the Sport Luminaires

Luminaire	Index	Position [m]			Aiming Point [m]			Angle [°]	Alignment	Pole
		X	Y	Z	X	Y	Z			
Orbit Industries, Inc.	1	10.000	0.000	9.000	0.000	10.000	0.000	32.5	(C 90, G IMax)	/
Orbit Industries, Inc.	1	10.000	0.000	9.000	20.000	10.000	0.000	32.5	(C 90, G IMax)	/

Fig 5.13: Luminaires coordinates list

Fig 5.14 shows the isolux line of the calculated area

Exterior Scene 1 / Ground Element 1 / Surface 1 / Isolines (L)



Values in Candela/m², Scale 1 : 143

Position of surface in external scene:

Marked point:

(0.000 m, 0.000 m, 0.000 m)



Grid: 128 x 64 Points

L_{av} [cd/m²]
4.44

L_{min} [cd/m²]
1.58

L_{max} [cd/m²]
8.58

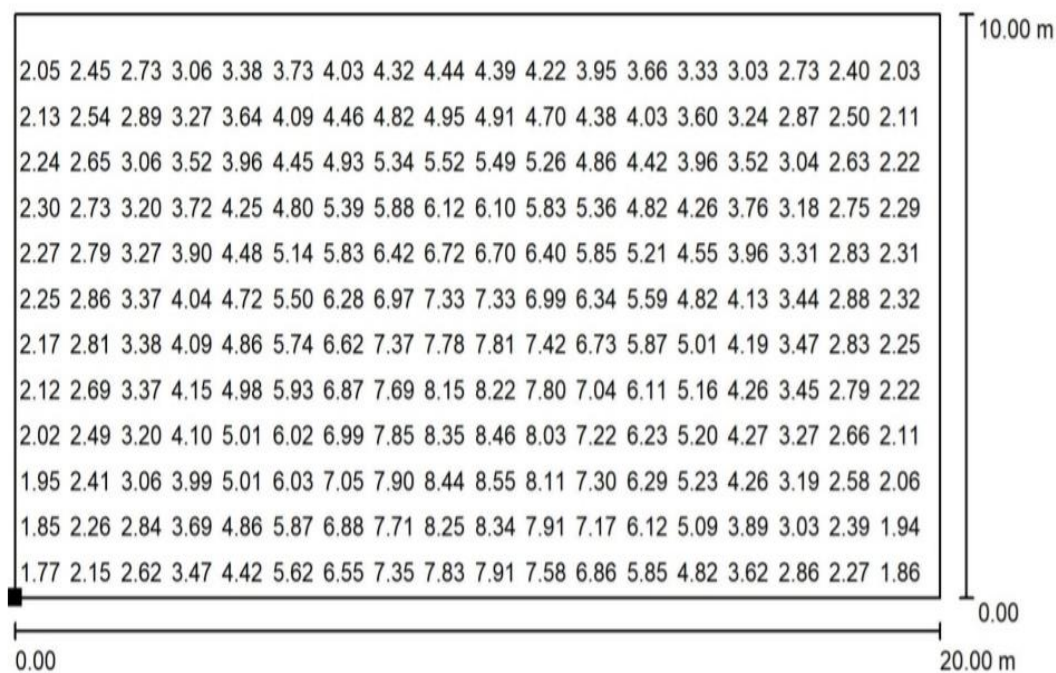
Fig 5.14: Isoline diagram

Fig 5.15 shows the value chart for the calculated area. It also shows the average, maximum and minimum luminance value of the design area.

The values obtained throughout the area are as follows:

- Average luminance (L_{avg}) = 4.44 cd/m^2 .
- Overall Uniformity (U_0) = 0.357.

Exterior Scene 1 / Ground Element 1 / Surface 1 / Value Chart (L)



Values in Candela/m², Scale 1 : 143

Not all calculated values could be displayed.

Position of surface in external scene:

Marked point:

(0.000 m, 0.000 m, 0.000 m)



Grid: 128 x 64 Points

L_{av} [cd/m^2]
4.44

L_{min} [cd/m^2]
1.58

L_{max} [cd/m^2]
8.58

Fig 5.15: Value chart

Table 5.3: Design Summary for All the luminaires

Main Light source	Quantity of Luminaire	Average photopic luminance (L_p)	Overall Uniformity (U_o)
HPSV	3	1.69	0.265
MH	2	3.86	0.347
CWLED	2	4.44	0.357

CHAPTER 6

Lighting design in mesopic region

6.1 Method for converting photopic data to the corresponding mesopic data

For the lighting design in mesopic region the first step needed is to transform the photopic luminous flux provided by the manufacturer of the luminaire into its equivalent mesopic luminous flux. For this purpose different steps are followed:

Step 1: After calculating the photopic luminance(L_p) (which is done in the pervious chapter), corresponding Mesopic luminance(L_m) is calculated using CIE 191:2010 and S/P ratio of the light source. Using Scotopic/Photopic meter the S/P ratio of the light source HPSV, MH and CWLED were determined. Then Mesopic luminance values are interpolated from the known photopic luminance values and s/p ratios using CIE191-2010 as shown in table 6.1.

		Photopic luminance / cd·m ⁻²						
	S/P	0,01	0,03	0,1	0,3	1	3	4,5
LPS ~	0,25	0,002 5	0,014 5	0,070 5	0,246 7	0,913 0	2,926 5	4,478 2
	0,35	0,003 5	0,017 4	0,075 0	0,254 5	0,925 3	2,936 7	4,481 2
	0,45	0,004 5	0,019 8	0,079 3	0,262 0	0,937 3	2,946 8	4,484 2
HPS ~	0,55	0,005 7	0,022 0	0,083 4	0,269 3	0,949 2	2,956 8	4,487 2
	0,65	0,006 9	0,023 9	0,087 3	0,276 4	0,960 8	2,966 6	4,490 1
	0,75	0,007 9	0,025 8	0,091 1	0,283 3	0,972 2	2,976 3	4,492 9
	0,85	0,008 8	0,027 5	0,094 7	0,290 1	0,983 5	2,985 9	4,495 8
	0,95	0,009 6	0,029 2	0,098 3	0,296 7	0,994 5	2,995 3	4,498 6
MH warm white ~	1,05	0,010 4	0,030 8	0,101 7	0,303 2	1,005 4	3,004 6	4,501 4
	1,15	0,011 1	0,032 3	0,105 1	0,309 6	1,016 1	3,013 9	4,504 1
	1,25	0,011 8	0,033 8	0,108 3	0,315 8	1,026 7	3,023 0	4,506 8
	1,35	0,012 5	0,035 3	0,111 5	0,322 0	1,037 1	3,031 9	4,509 5
	1,45	0,013 2	0,036 7	0,114 7	0,328 0	1,047 3	3,040 8	4,512 2
	1,55	0,013 8	0,038 1	0,117 8	0,333 9	1,057 5	3,049 6	4,514 8
	1,65	0,014 5	0,039 5	0,120 8	0,339 8	1,067 4	3,058 2	4,517 4
	1,75	0,015 1	0,040 8	0,123 8	0,345 5	1,077 3	3,066 8	4,520 0
	1,85	0,015 7	0,042 1	0,126 7	0,351 2	1,087 0	3,075 3	4,522 5
	1,95	0,016 3	0,043 4	0,129 5	0,356 8	1,096 6	3,083 6	4,525 0
MH day-light ~	2,05	0,016 9	0,044 6	0,132 4	0,362 3	1,106 0	3,091 9	4,527 5
	2,15	0,017 4	0,045 9	0,135 2	0,367 7	1,115 4	3,100 1	4,529 9
	2,25	0,018 0	0,047 1	0,137 9	0,373 1	1,124 6	3,108 2	4,532 3
	2,35	0,018 5	0,048 3	0,140 6	0,378 4	1,133 8	3,116 2	4,534 7
	2,45	0,019 1	0,049 5	0,143 3	0,383 6	1,142 8	3,124 1	4,537 1
	2,55	0,019 6	0,050 6	0,145 9	0,388 8	1,151 7	3,131 9	4,539 5
	2,65	0,020 1	0,051 8	0,148 5	0,393 9	1,160 5	3,139 6	4,541 8
	2,75	0,020 7	0,052 9	0,151 1	0,398 9	1,169 3	3,147 3	4,544 1

Table 6.1: Values of L_M of the recommended Mesopic system as a function of photopic luminance and s/p ratio ^[1].

Step 2: Once the mesopic luminous (L_m) was determined, the Mesopic vs. Photopic ratio (M/P) was calculated.

Step 3: After the determination of M/P ratio for each of the sources included in my thesis work, the photopic luminance values provided by the manufacturers through their photometric files is corrected. For this editing purpose the LDT Editor of the DIAL company is used. With this application, the original photopic luminance value is modified with the corresponding mesopic values, obtained by multiplying the source luminance values by the M/P ratio adequate in each case.

Step 4: Then the edited photometric files of the three selected luminaires were entered in the Dialux light simulation software and the average luminance is calculated. In this case the design parameters are identical as the previous chapter (chapter 5) design.

To summarize the results, the flow diagram of the proposed method is detailed in **Fig 6.1**

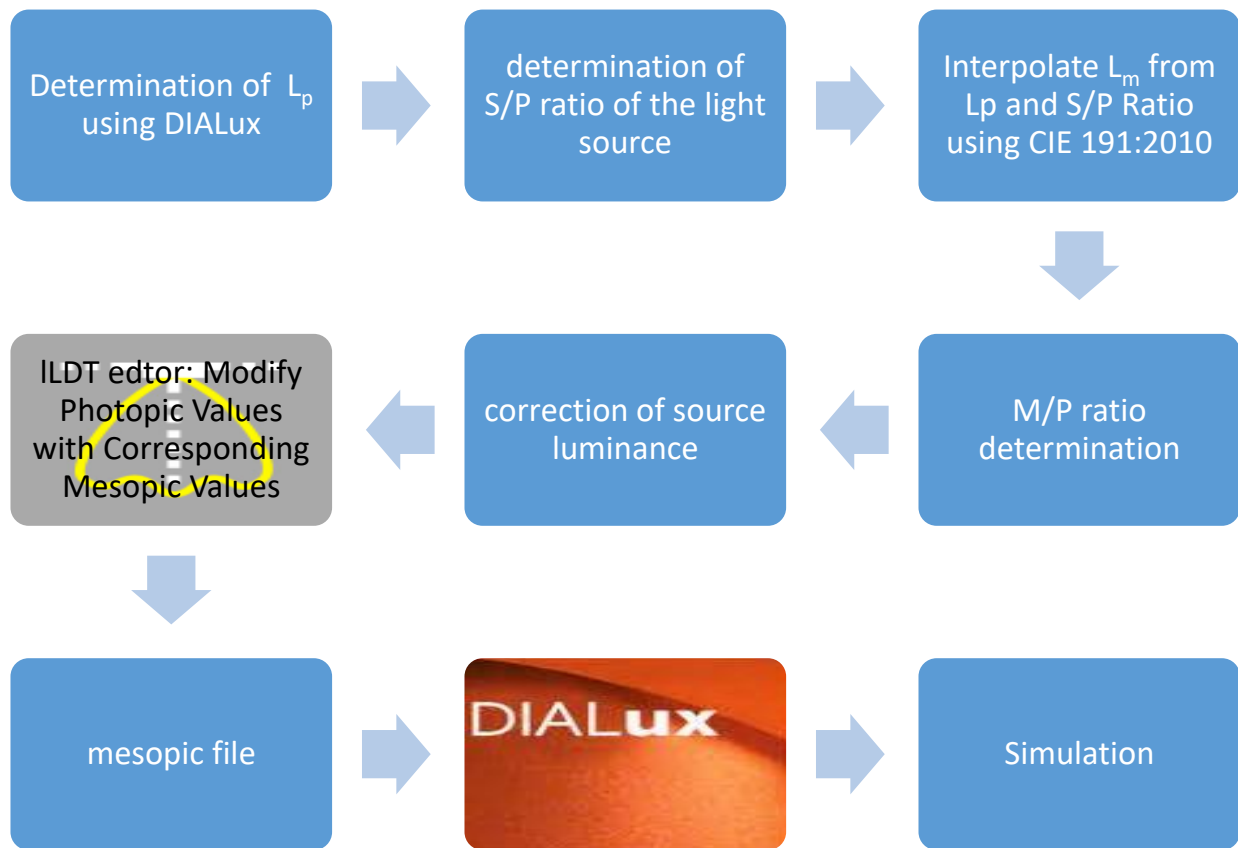


Fig 6.1. Conceptual flow diagram of the proposed study methodology.

All the measured s/p ratio, calculated mesopic luminance value using CIE 191:2010 and m/p ratio are shown table 6.2.

$$\text{M/P ratio} = L_m / L_p.$$

Main Light source	Average photopic luminance (L_p)	Measured S/P ratio	Calculated mesopic luminance (L_m) using CIE 191:2010	Calculated M/P ratio
HPSV	1.69	0.48	1.634	0.9669
MH	3.86	1.32	3.88	1.0052
CWLED	4.44	2.02	4.47	1.0068

Table 6.2: measured and calculated value.

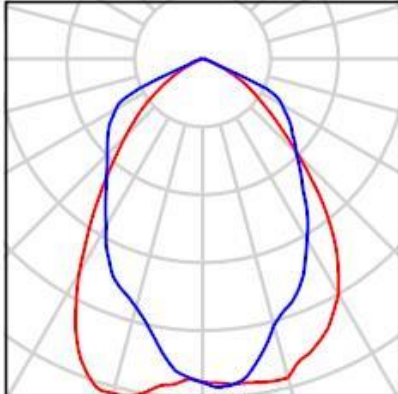
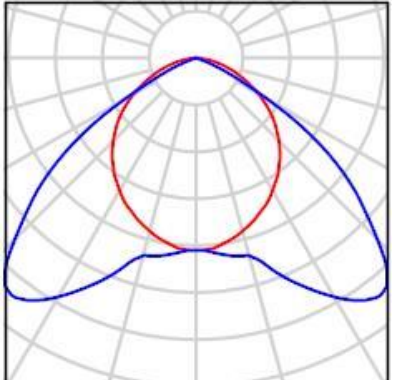
6.2 DIALUX design using modified photometric file

6.2.1 Design using high pressure sodium vapour light (HPSV)

6.2.1.1 Luminaire Details:

The details of the lamps and luminaires used for the design are given in Tables 6.3.

Table-6.3: Luminaires with Specification

Name of Luminaire	Details of Fixture	Light Distribution Curve
PHILIPS SWF 101/150W [SYMMETRIC], CLOSED	Luminous flux (Luminaire): 9530 lm Luminous flux (Lamps): 14000 lm Luminaire Wattage: 170.0 W Luminaire classification according to CIE: 100 CIE flux code: 62 91 99 100 68 Fitting: 1 x SON T 150W (Correction Factor 1.000).	
TCS 306 / 136 M1	Luminous flux (Luminaire): 2261 lm Luminous flux (Lamps): 3250 lm Luminaire Wattage: 45.2 W Luminaire classification according to CIE: 100 CIE flux code: 49 87 98 100 70 Fitting: 1 x TL'D'36W/865 (Correction Factor 1.000).	

6.2.1.2 Design Considerations:

- Area of the space: 30*20m.
- Luminaire used: 3 x PHILIPS SWF 101/150W [SYMMETRIC], and 3 x TCS 306 / 136 M1(surrounding light source).
- Pole height : 9m.
- Light loss factor: 0.80,
- ULR (Upward Light Ratio): 19.0%

In fig 6.2 modified luminous intensity table is shown.

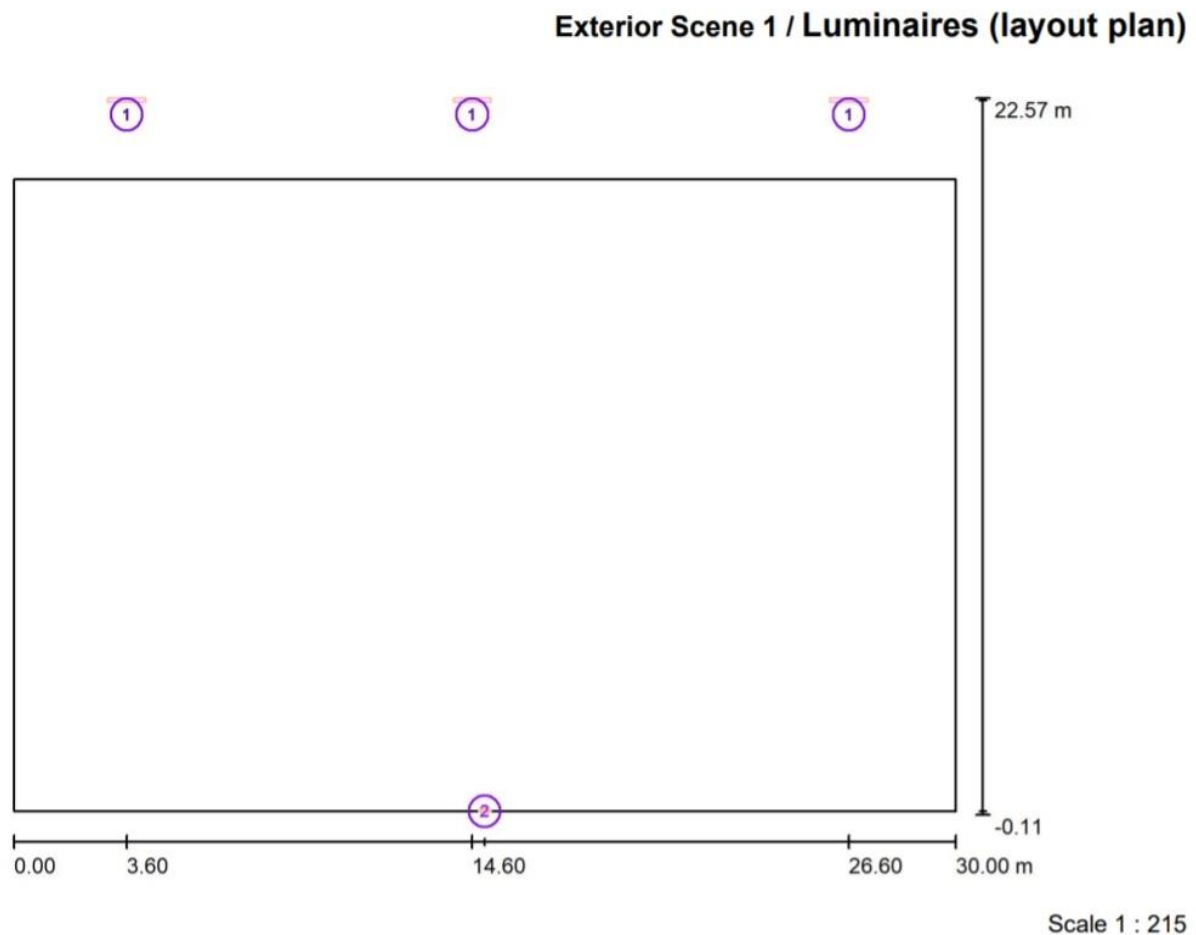
PHILIPS SWF 101/150W [SYMMETRIC], CLOSED, / Luminous intensity table

Luminaire: PHILIPS SWF 101/150W [SYMMETRIC], CLOSED,
Lamps: 1 x SONT 150W

Gamma	C 0°	C 30°	C 60°	C 90°	C 120°	C 150°	C 180°	C 210°	C 240°	C 270°	C 300°	C 330°	C 360°
0.0°	381	381	381	381	381	381	381	381	381	381	381	381	381
5.0°	385	395	390	386	388	389	385	377	374	369	379	383	385
10.0°	387	394	371	364	379	406	400	375	342	332	349	377	387
15.0°	389	383	347	325	351	407	408	356	311	303	318	355	389
20.0°	369	361	322	306	322	374	396	324	288	286	296	323	369
25.0°	350	328	301	281	299	334	354	293	268	261	282	299	350
30.0°	320	292	272	246	267	287	291	256	245	227	255	270	320
35.0°	275	256	233	214	232	241	226	223	213	199	217	242	275
40.0°	219	212	194	181	191	189	170	185	180	176	181	207	219
45.0°	159	171	162	156	159	143	128	151	155	159	157	168	159
50.0°	113	135	138	138	129	112	95	128	137	146	146	132	113
55.0°	80	99	129	124	110	88	63	105	123	134	138	100	80
60.0°	56	78	110	108	93	67	38	79	109	118	113	80	56
65.0°	31	57	80	84	80	40	16	44	92	82	90	59	31
70.0°	13	25	14	13	18	11	6.00	14	12	15	14	24	13
75.0°	4.00	5.00	7.00	8.00	6.00	5.00	3.00	4.00	6.00	8.00	7.00	5.00	4.00
80.0°	2.00	3.00	3.00	4.00	3.00	2.00	2.00	2.00	3.00	4.00	3.00	3.00	2.00
85.0°	2.00	2.00	2.00	2.00	2.00	2.00	2.00	2.00	2.00	2.00	2.00	2.00	2.00
90.0°	0.00	0.00	0.00	0.00	0.00	0.00	0.00	0.00	0.00	0.00	0.00	0.00	0.00

Fig 6.2: modified luminous intensity table

In **Fig. 6.3**, the layout of the designed area and the positions of the luminaire are shown. Here two different type of lamp are used one is fluorescent lamp (used as surrounding light source) denoted as 1 and other is high pressure sodium vapour lamp which is denoted as 2.

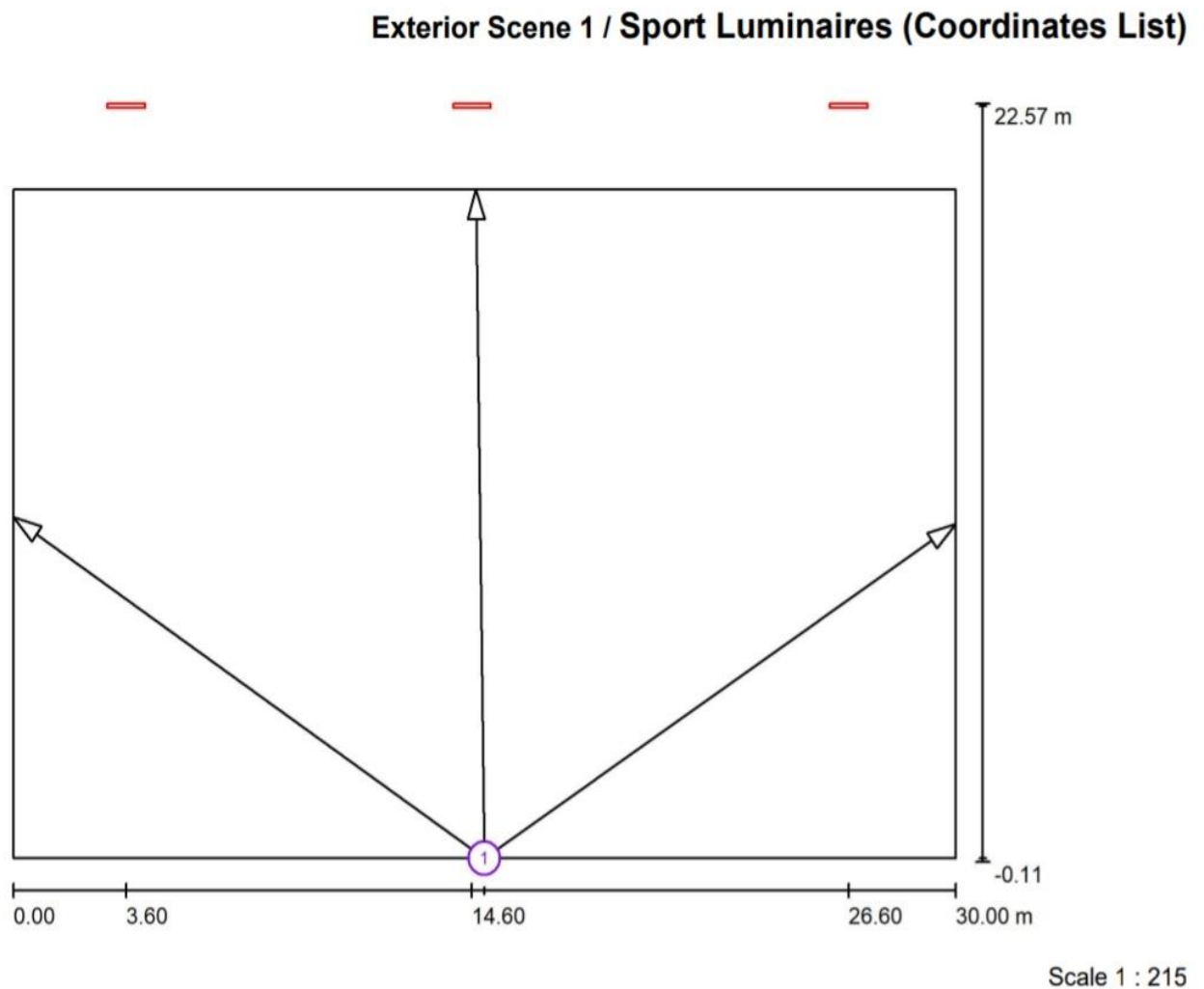


Luminaire Parts List

No.	Pieces	Designation
1	3	TCS 306 / 136 M1
2	3	PHILIPS SWF 101/150W [SYMMETRIC], CLOSED,

Fig:6.3 Luminaires layout plan

In **Fig. 6.4**, the positions of the luminaires (HPSV) are shown. In addition to the luminaire positions, the figure also shows aiming point, angle and alignment of the luminaires (HPSV).



List of the Sport Luminaires

Luminaire	Index	Position [m]			Aiming Point [m]			Angle [°]	Alignment	Pole
		X	Y	Z	X	Y	Z			
PHILIPS SWF 101/150W [SYMMETRIC], CLOSED,	1	15.000	0.000	9.000	14.735	20.000	0.000	24.2	(C 0, G 0)	/
PHILIPS SWF 101/150W [SYMMETRIC], CLOSED,	1	15.000	0.000	9.000	30.000	10.000	0.000	26.5	(C 0, G 0)	/
PHILIPS SWF 101/150W [SYMMETRIC], CLOSED,	1	15.000	0.000	9.000	0.000	10.201	0.000	26.4	(C 0, G 0)	/

Fig 6.4: Coordinates list of luminaires.

Fig 6.5 shows the isolux line of the calculated area.

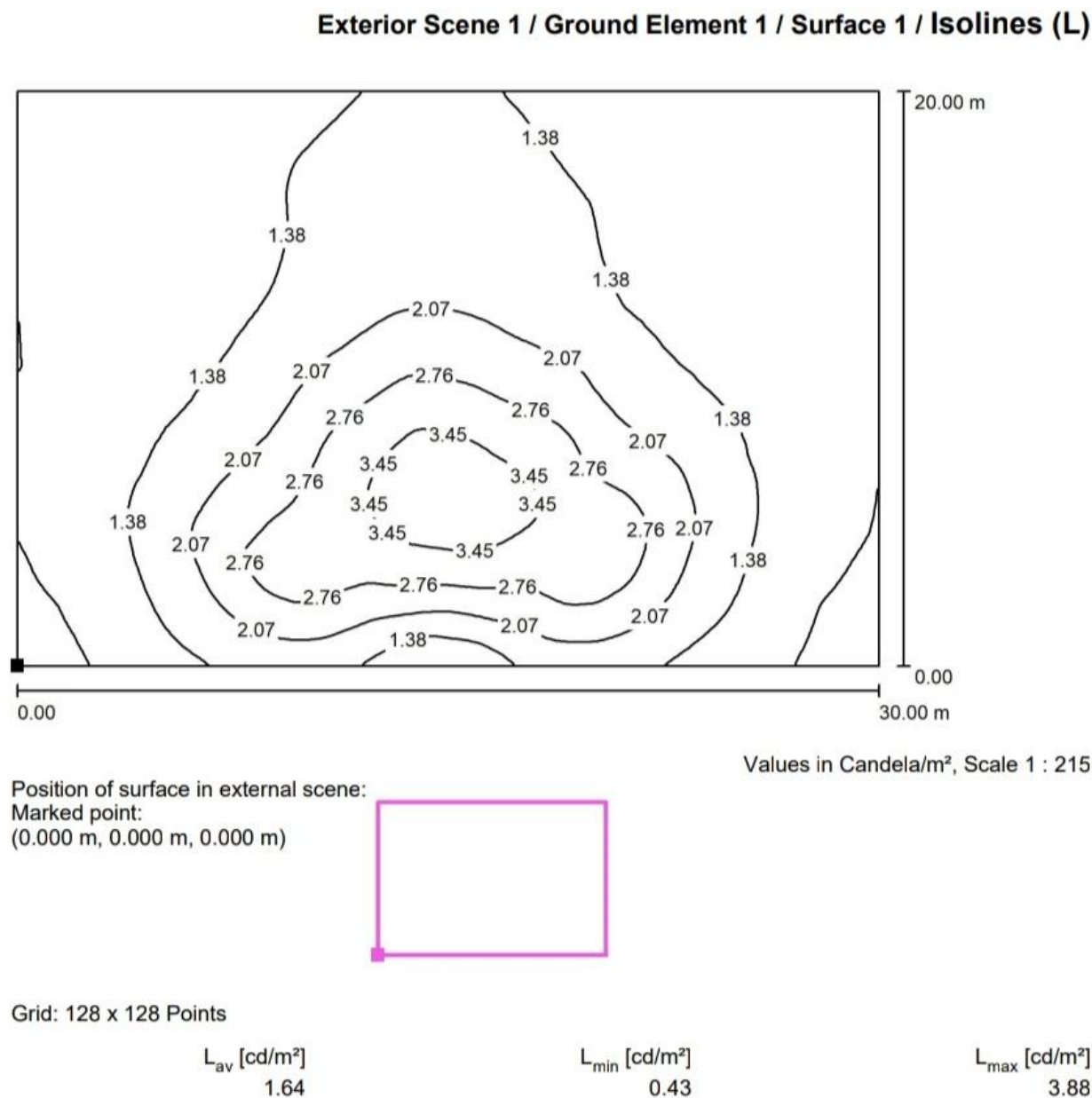


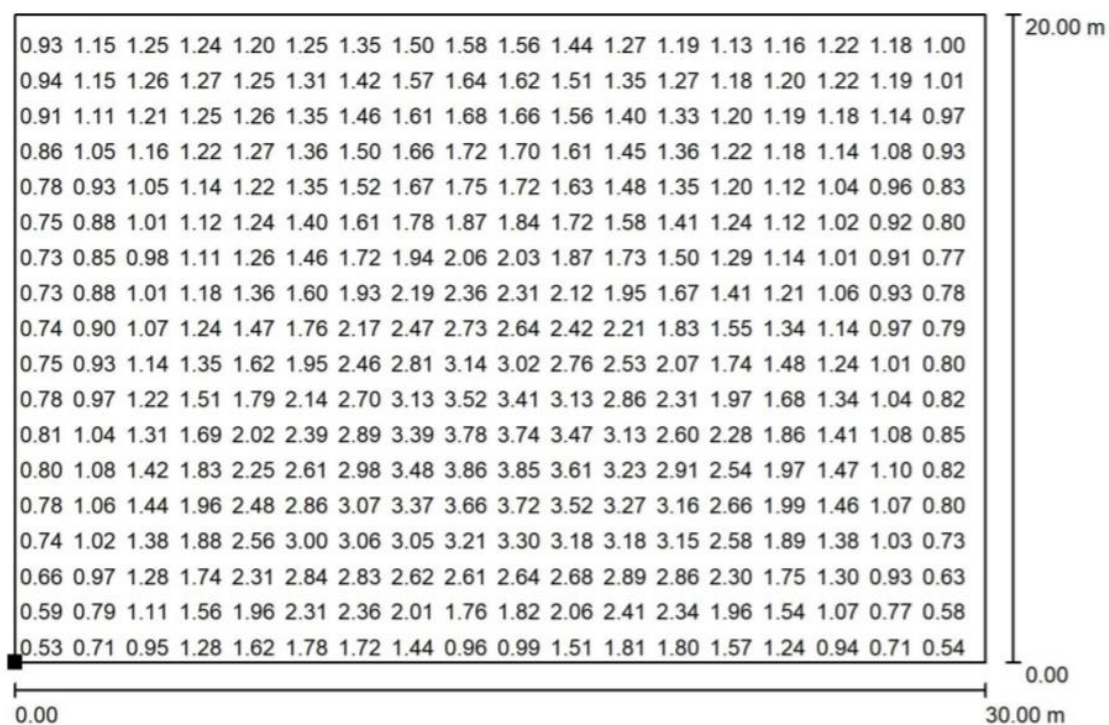
Fig 6.5: Isolines diagram

Fig 6.6 shows the value chart for the calculated area. It also shows the average, maximum and minimum luminance value of the design area.

The values obtained throughout the area are as follows:

- Average luminance (L_{avg}) = 1.64 cd/m².
- Overall Uniformity (U_0) = 0.264.

Exterior Scene 1 / Ground Element 1 / Surface 1 / Value Chart (L)



Values in Candela/m², Scale 1 : 215

Not all calculated values could be displayed.

Position of surface in external scene:

Marked point:

(0.000 m, 0.000 m, 0.000 m)



Grid: 128 x 128 Points

L_{av} [cd/m²]
1.64

L_{min} [cd/m²]
0.43

L_{max} [cd/m²]
3.88

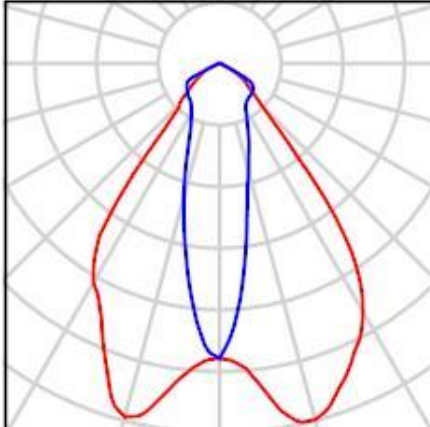
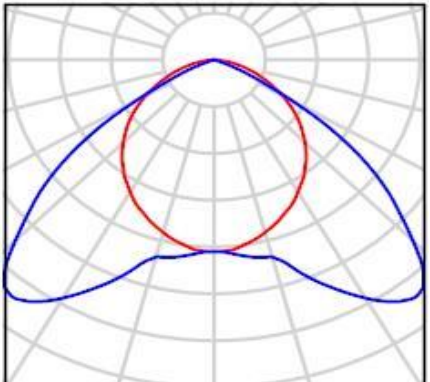
Fig 6.6: Value chart

6.2.2 Using Metal Halide lamp (MH)

6.2.2.1 Luminaire Details:

The details of the lamps and luminaires used for the design have been given in Tables 6.4

Table-6.4: Luminaires with Specification

Name of Luminaire	Details of Fixture	Light Distribution Curve
PHILIPS MWF 101/150W [SYMMETRIC], CLOSED	Luminous flux (Luminaire): 8671 lm Luminous flux (Lamps): 12100 lm Luminaire Wattage: 170.0 W Luminaire classification according to CIE: 100 CIE flux code: 71 93 99 100 72 Fitting: 1 x MHN TD 150W (Correction Factor 1.000).	
TCS 306 / 136 M1	Luminous flux (Luminaire): 2261 lm Luminous flux (Lamps): 3250 lm Luminaire Wattage: 45.2 W Luminaire classification according to CIE: 100 CIE flux code: 49 87 98 100 70 Fitting: 1 x TL'D'36W/865 (Correction Factor 1.000).	

6.2.2.2 Design Considerations:

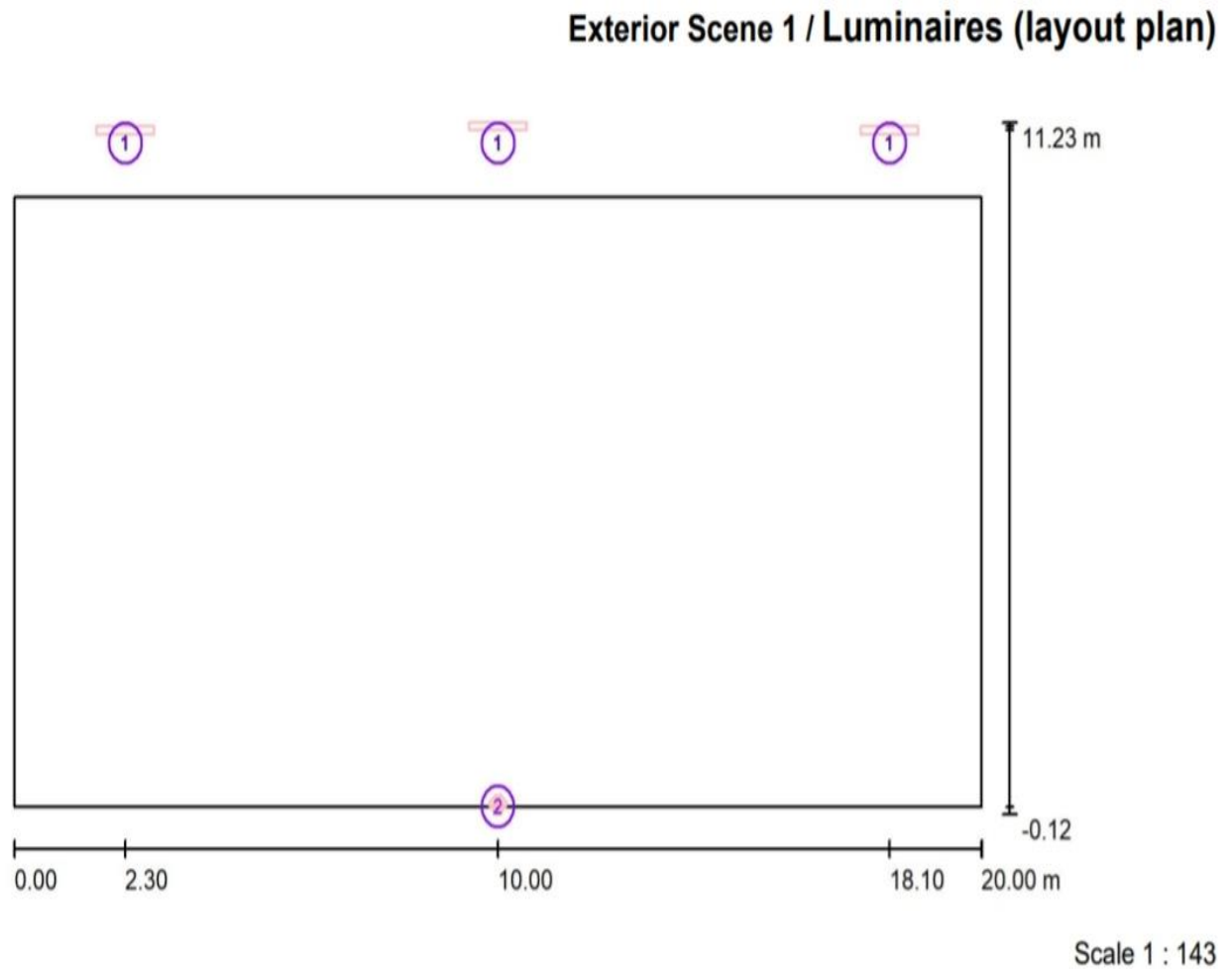
- Area of the space: 20*10m.
- Luminaire used: 2 x PHILIPS MWF 101/150W [SYMMETRIC], CLOSED and 3 x TCS 306 / 136 M1(surrounding light source).
- Pole height : 9m.
- Light loss factor: 0.80
- ULR (Upward Light Ratio): 4.0%

Modified luminous intensity table of the lamp Metal Halide is shown in **fig 6.7**.

PHILIPS MWF 101/150W [SYMMETRIC], CLOSED, / Luminous intensity table													
Luminaire: PHILIPS MWF 101/150W [SYMMETRIC], CLOSED, Lamps: 1 x MHN TD 150W													
Gamma	C 0°	C 30°	C 60°	C 90°	C 120°	C 150°	C 180°	C 210°	C 240°	C 270°	C 300°	C 330°	C 360°
0.0°	722	722	722	722	722	722	722	722	722	722	722	722	722
5.0°	750	693	614	579	619	699	747	726	667	635	643	707	750
10.0°	862	661	456	384	467	668	831	739	547	474	527	692	862
15.0°	903	560	320	272	348	630	896	728	423	339	404	643	903
20.0°	849	409	238	211	247	467	803	583	291	227	294	535	849
25.0°	780	299	193	161	187	327	686	418	200	166	203	420	780
30.0°	702	235	159	128	146	245	618	292	151	138	155	324	702
35.0°	565	188	134	115	118	178	511	201	124	122	131	243	565
40.0°	292	158	117	110	103	129	210	139	111	114	115	175	292
45.0°	147	132	108	109	96	118	139	113	105	110	106	129	147
50.0°	98	104	105	106	92	98	95	104	99	103	102	101	98
55.0°	75	90	94	100	86	86	70	95	88	98	93	87	75
60.0°	45	79	86	85	78	59	49	81	80	91	85	79	45
65.0°	24	55	16	17	53	32	34	39	69	32	72	55	24
70.0°	8.04	9.05	6.03	10	7.04	6.03	6.03	6.03	10	9.05	11	9.05	8.04
75.0°	3.02	4.02	4.02	7.04	5.03	4.02	3.02	3.02	5.03	6.03	5.03	4.02	3.02
80.0°	2.01	2.01	3.02	4.02	3.02	2.01	2.01	2.01	3.02	3.02	3.02	2.01	2.01
85.0°	2.01	2.01	2.01	2.01	2.01	2.01	2.01	2.01	2.01	2.01	2.01	2.01	2.01
90.0°	0.00	0.00	0.00	0.00	0.00	0.00	0.00	0.00	0.00	0.00	0.00	0.00	0.00

Fig 6.7: Modified luminous intensity table.

In **Fig. 6.8**, the positions of the luminaire are shown. Here two different type of lamp are used one is fluorescent lamp (used as surrounding light source) denoted as 1 and other is Metal Halide(MH) which is denoted as 2.

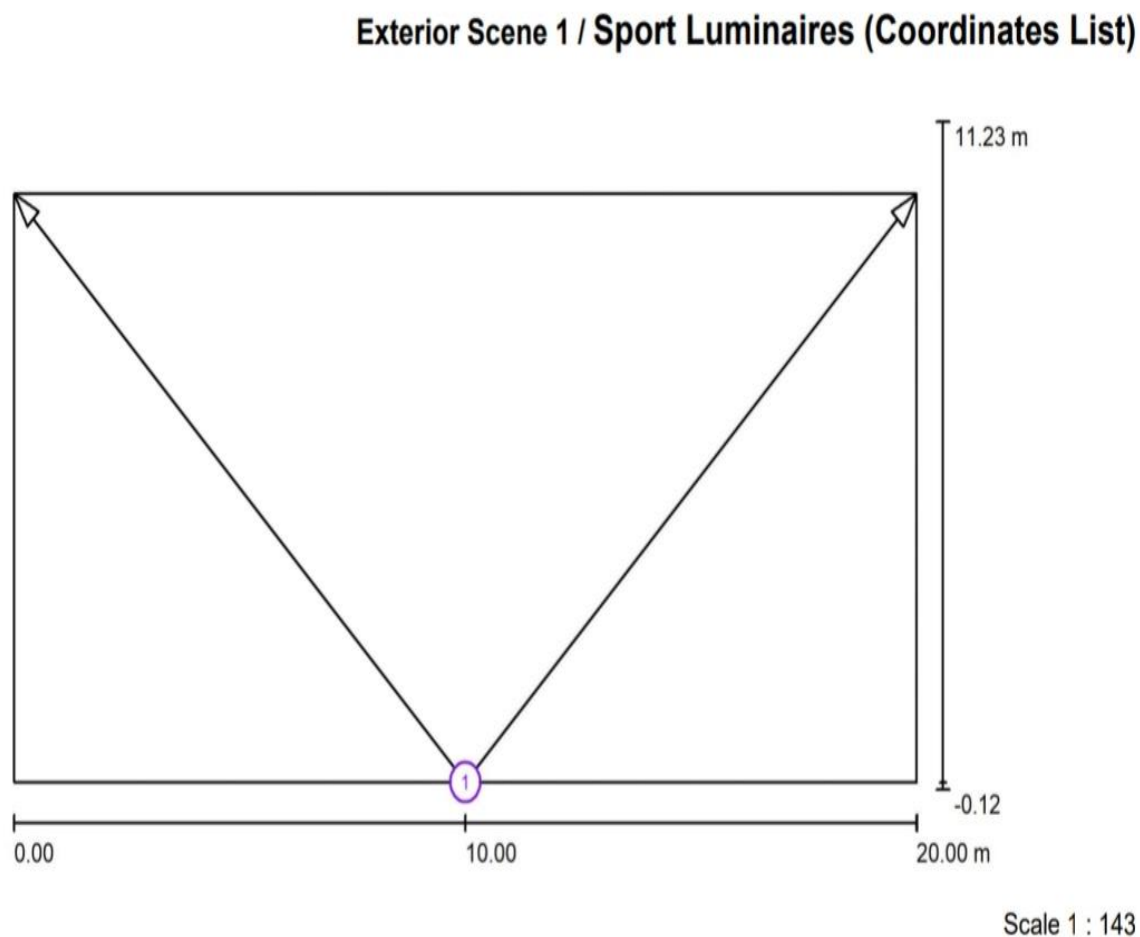


Luminaire Parts List

No.	Pieces	Designation
1	3	TCS 306 / 136 M1
2	2	PHILIPS MWF 101/150W [SYMMETRIC], CLOSED,

Fig 6.8: Luminaires layout plan

In Fig. 6.9 the positions of the luminaires (MH) are shown. In addition to the luminaire positions, the figure also shows aiming point, angle and alignment of the luminaires (MH).



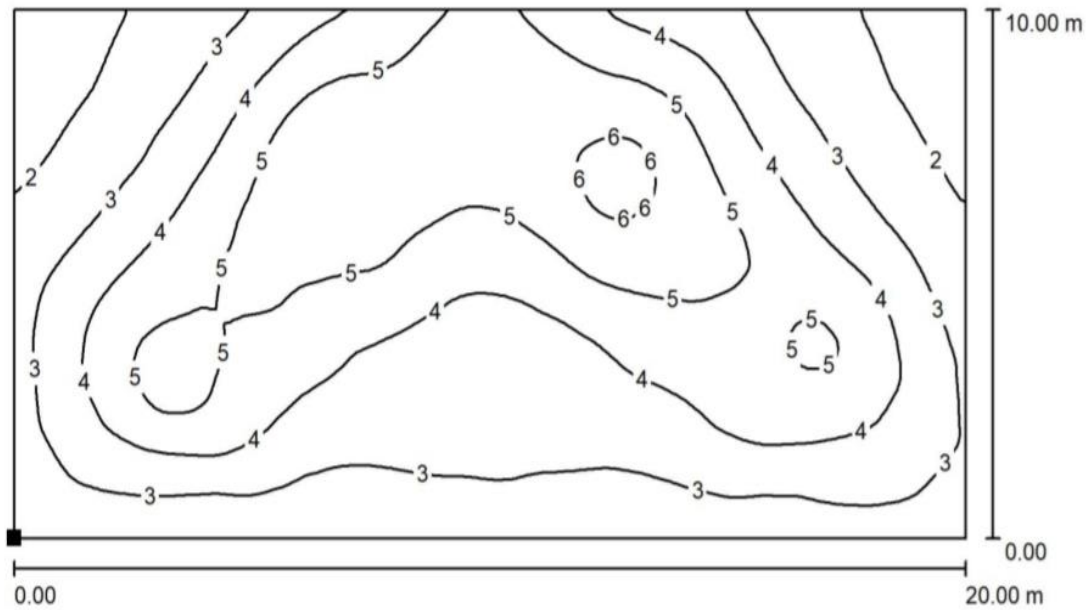
List of the Sport Luminaires

Luminaire	Index	Position [m]			Aiming Point [m]			Angle [°]	Alignment	Pole
		X	Y	Z	X	Y	Z			
PHILIPS MWF 101/150W [SYMMETRIC], CLOSED,	1	10.000	0.000	9.000	0.000	10.000	0.000	32.5	(C 90, G IMax)	/
PHILIPS MWF 101/150W [SYMMETRIC], CLOSED,	1	10.000	0.000	9.000	20.000	10.000	0.000	32.5	(C 90, G IMax)	/

Fig 6.9: Luminaires coordinate list

Fig 6.10 shows the isolux line of the calculated area.

Exterior Scene 1 / Ground Element 1 / Surface 1 / Isolines (L)



Values in Candela/m², Scale 1 : 143

Position of surface in external scene:
Marked point:
(0.000 m, 0.000 m, 0.000 m)



Grid: 128 x 128 Points

L_{av} [cd/m²]
3.88

L_{min} [cd/m²]
1.34

L_{max} [cd/m²]
6.36

Fig 5.10: Isoline diagram

Fig 6.11 shows the value chart for the calculated area. It also shows the average, maximum and minimum luminance value of the design area.

The values obtained throughout the area are as follows:

- Average luminance (L_{avg}) = 3.88 cd/m².
- Overall Uniformity (U_0) = 0.346.

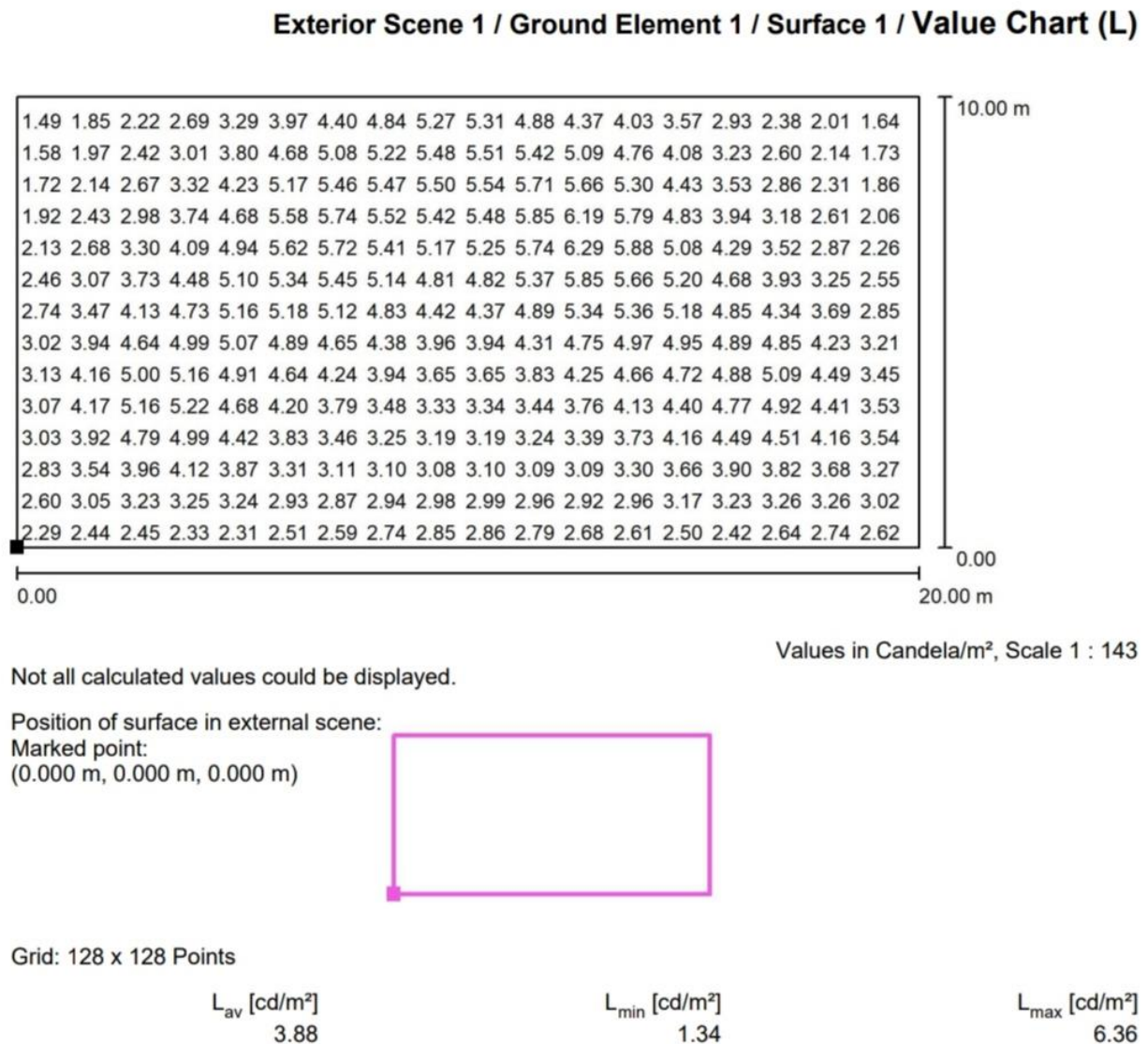


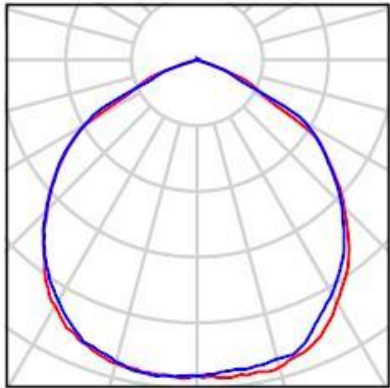
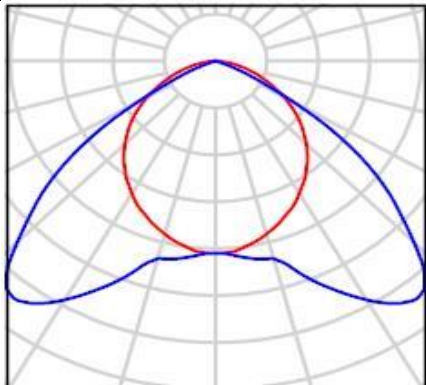
Fig 5.11: value chart

6.2.3 Design using Cool White LED

6.2.3.1 Luminaire Details:

The details of the lamps and luminaires used for the design have been given in Tables 6.5

Table-6.5: Luminaires with Specification

Name of Luminaire	Details of Fixture	Light Distribution Curve
Orbit Industries, Inc.	Luminous flux (Luminaire): 14597 lm Luminous flux (Lamps): 14499 lm Luminaire Wattage: 158.6 W Luminaire classification according to CIE: 100 CIE flux code: 54 89 100 100 101 Fitting: 1 x LFL4-160W (Correction Factor 1.000).	
TCS 306 / 136 M1	Luminous flux (Luminaire): 2261 lm Luminous flux (Lamps): 3250 lm Luminaire Wattage: 45.2 W Luminaire classification according to CIE: 100 CIE flux code: 49 87 98 100 70 Fitting: 1 x TL'D'36W/865 (Correction Factor 1.000).	

6.2.3.2 Design Considerations:

- Area of the space: 20*10m.
- Luminaire used: 2 x Orbit Industries, Inc and 3 x TCS 306 / 136 M1(surrounding light source).
- Pole height : 9m.
- Light loss factor: 0.80
- ULR (Upward Light Ratio): 7.0%

Modified luminous intensity table of the lamp CWLED is shown in fig 6.12.

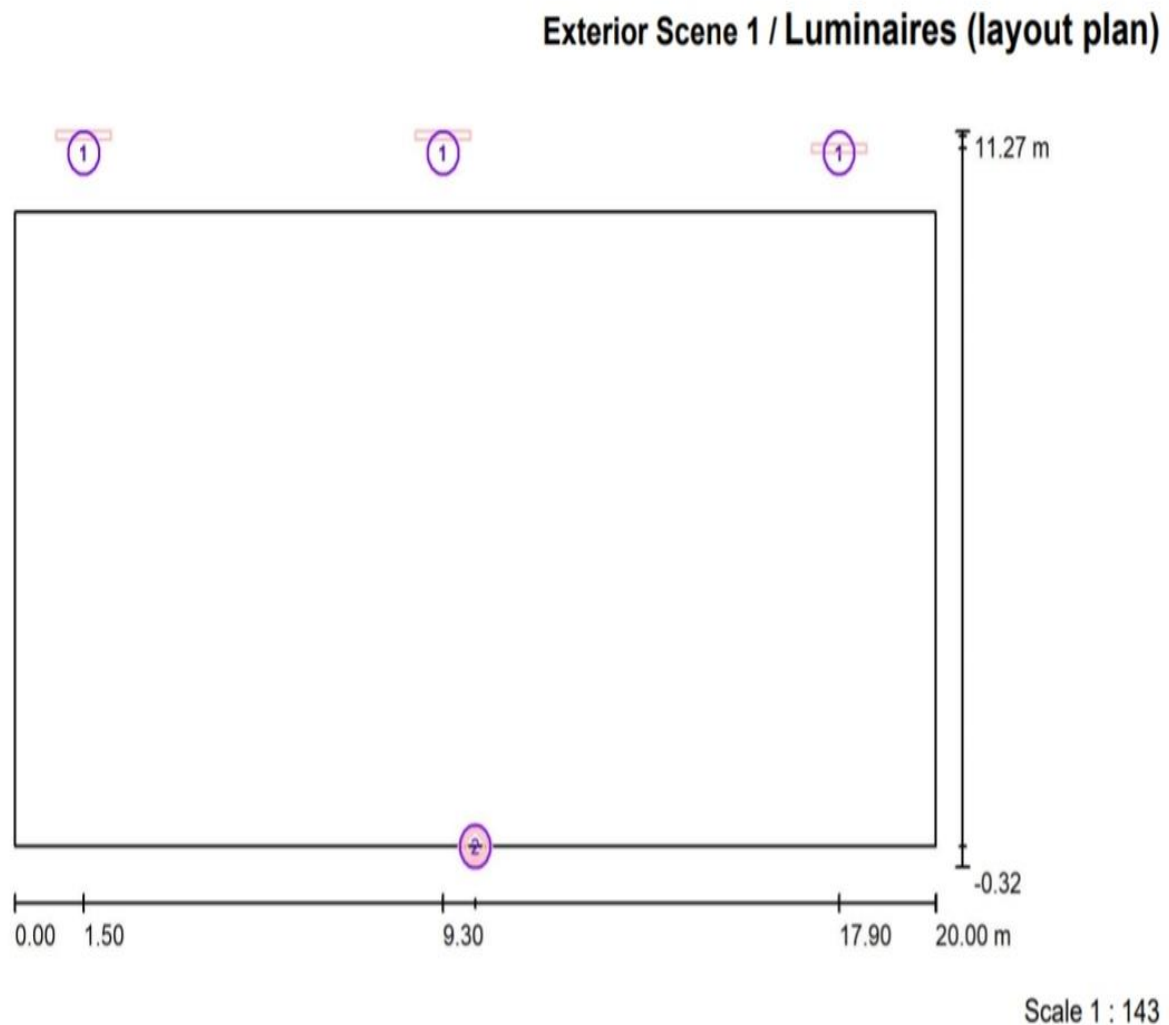
Orbit Industries, Inc. / Luminous intensity table

Luminaire: Orbit Industries, Inc.
Lamps: 1 x LFL4-160W

Gamma	C 0°	C 30°	C 60°	C 90°	C 120°	C 150°	C 180°	C 210°	C 240°	C 270°	C 300°	C 330°	C 360°
0.0°	387	387	387	387	387	387	387	387	387	387	387	387	387
5.0°	391	387	384	383	384	382	388	385	389	389	387	387	391
10.0°	390	386	385	383	381	381	389	386	388	389	388	383	390
15.0°	390	384	385	380	381	382	385	386	387	383	386	387	390
20.0°	382	380	377	374	374	377	378	381	379	374	382	384	382
25.0°	367	371	363	351	361	366	366	370	366	361	369	373	367
30.0°	343	352	342	331	342	350	348	355	350	340	352	356	343
35.0°	320	325	319	308	318	328	325	338	329	318	333	329	320
40.0°	288	295	291	280	294	304	293	311	304	293	306	299	288
45.0°	255	259	259	251	264	271	261	278	275	261	273	265	255
50.0°	221	225	225	218	231	235	231	244	241	228	240	231	221
55.0°	188	186	188	187	193	198	196	206	206	198	202	193	188
60.0°	111	147	151	153	157	159	156	167	169	159	161	151	111
65.0°	77	85	86	56	94	96	84	107	124	87	117	91	77
70.0°	26	35	30	34	40	52	56	65	58	46	47	46	26
75.0°	1.89	7.22	2.94	1.67	5.12	14	16	19	7.26	1.65	4.86	11	1.89
80.0°	0.53	0.49	0.54	0.70	0.83	1.11	1.11	1.16	0.84	0.75	0.66	0.58	0.53
85.0°	0.12	0.12	0.14	0.19	0.23	0.33	0.36	0.40	0.32	0.27	0.21	0.14	0.12
90.0°	0.03	0.04	0.03	0.04	0.05	0.05	0.04	0.06	0.05	0.03	0.03	0.03	0.03

Fig 6.12: luminous intensity table.

In Fig. 6.13, the positions of the luminaire are shown. Here two different type of lamp are used one is fluorescent lamp (used as surrounding light source) denoted as 1 and other is CWLED which is denoted as 2.

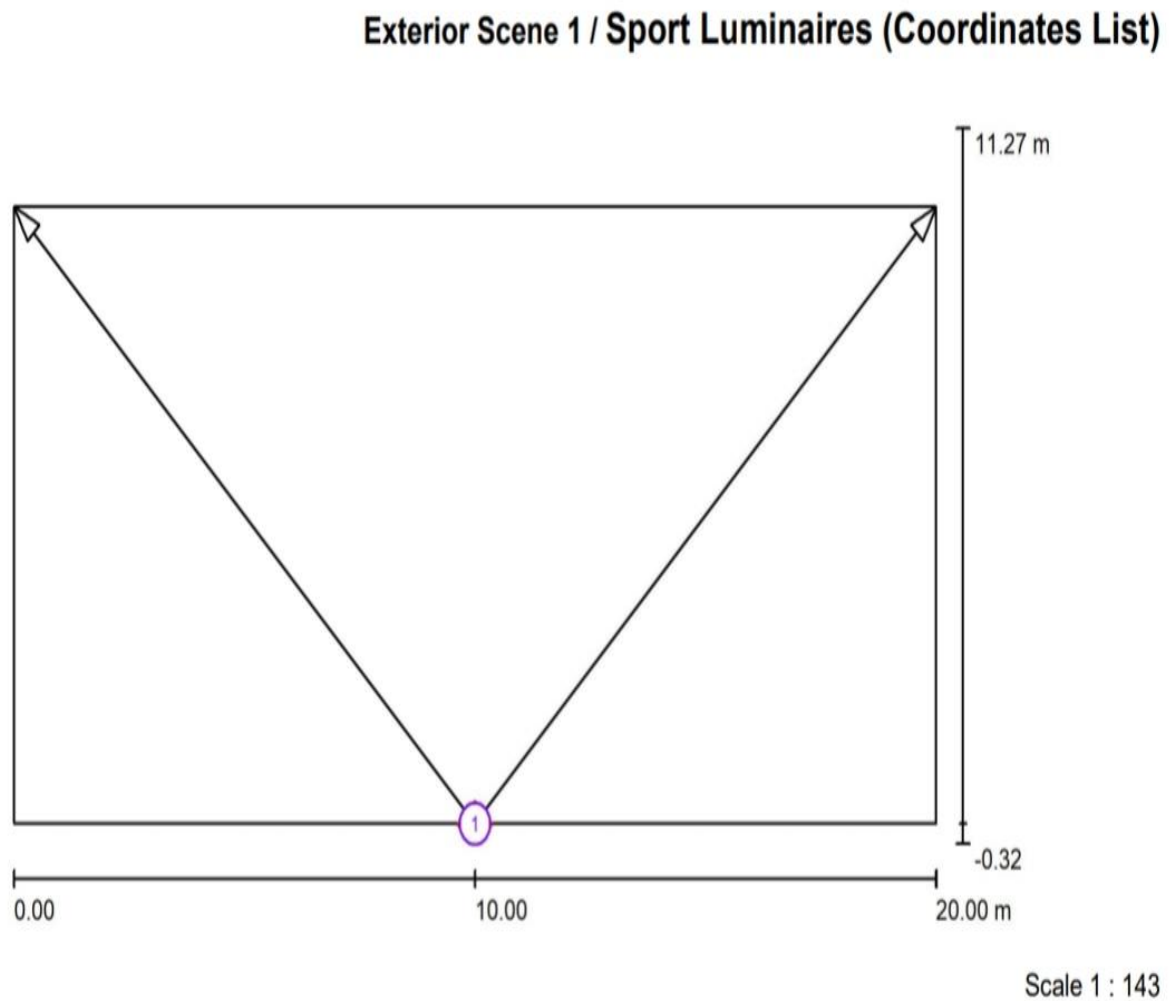


Luminaire Parts List

No.	Pieces	Designation
1	3	TCS 306 / 136 M1
2	2	Orbit Industries, Inc.

Fig 6.13: Luminaires layout plan

In **Fig. 6.14** the positions of the luminaires (CWLED) are shown. In addition to the luminaire positions, the figure also shows aiming point, angle and alignment of the luminaires (CWLED).



List of the Sport Luminaires

Luminaire	Index	Position [m]			Aiming Point [m]			Angle [°]	Alignment	Pole
		X	Y	Z	X	Y	Z			
Orbit Industries, Inc.	1	10.000	0.000	9.000	0.000	10.000	0.000	32.5	(C 90, G IMax)	/
Orbit Industries, Inc.	1	10.000	0.000	9.000	20.000	10.000	0.000	32.5	(C 90, G IMax)	/

Fig 6.14: Luminaires coordinates list

Fig 6.15 shows the isolux line of the calculated area

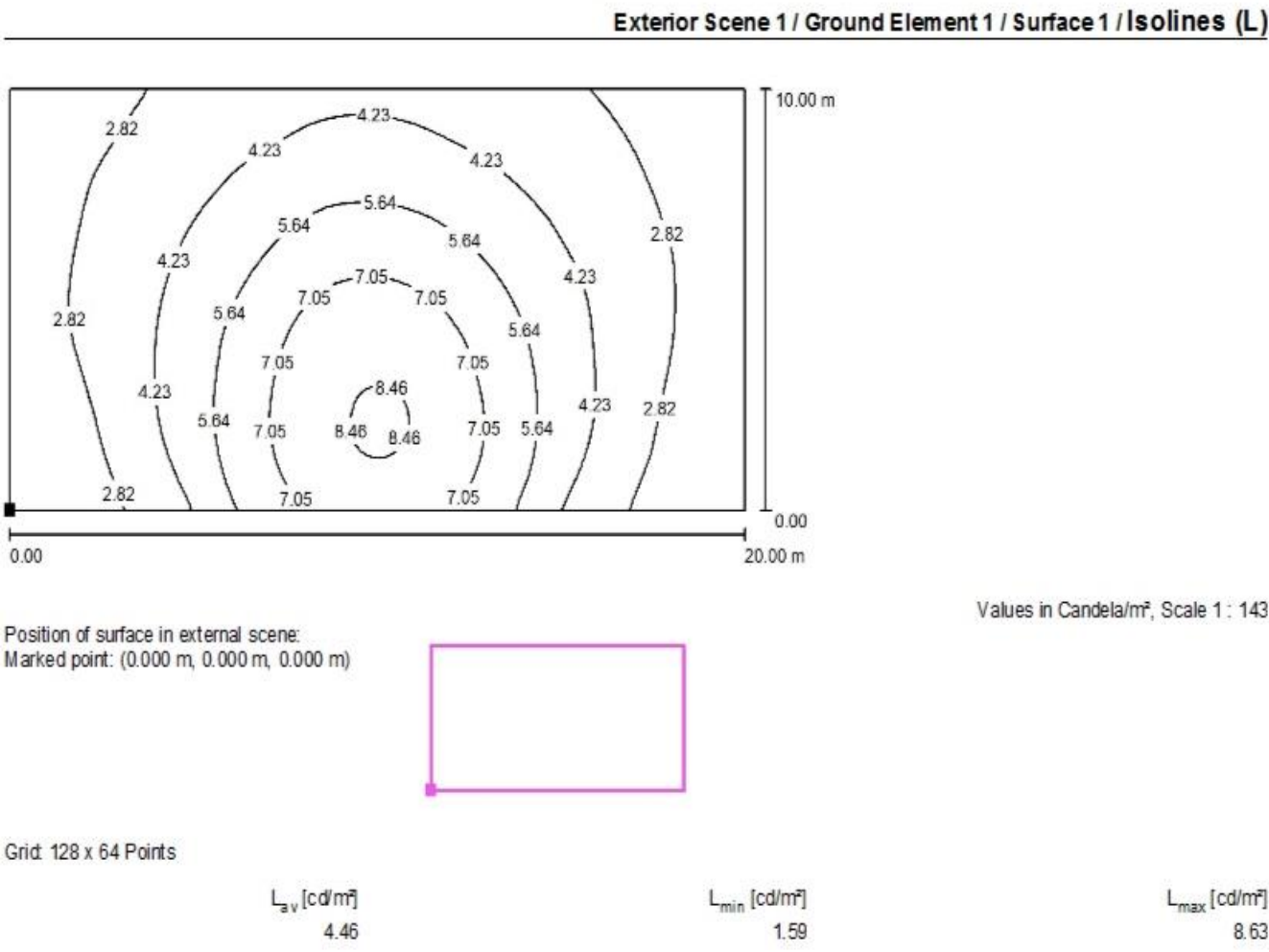


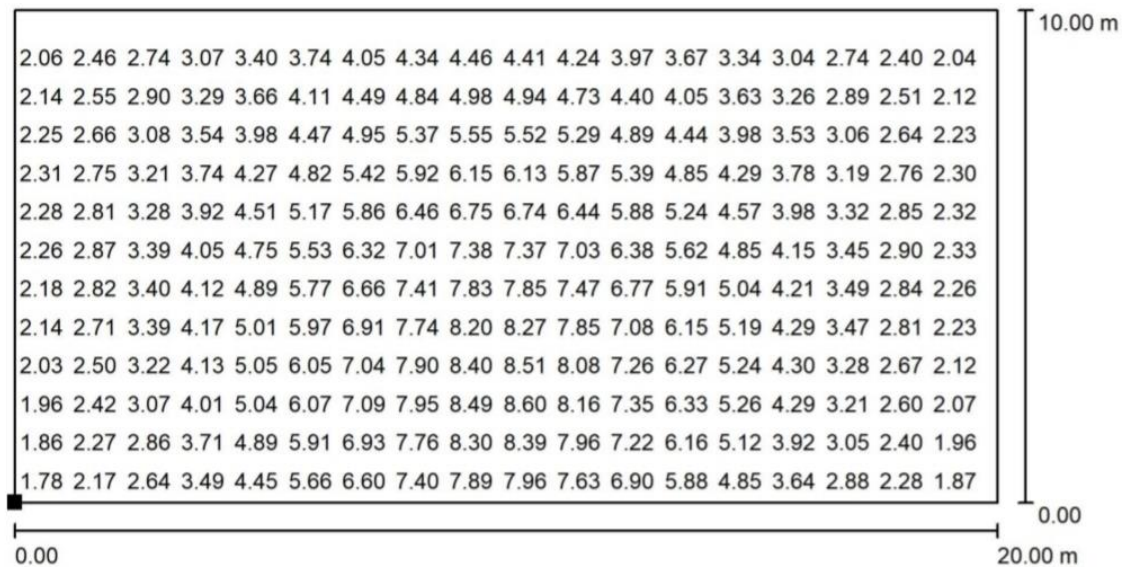
Fig 6.15: Isoline diagram

Fig 6.16 shows the value chart for the calculated area. It also shows the average , maximum and minimum luminance value of the design area.

The values obtained throughout the area are as follows:

- Average luminance (L_{avg}) = 4.46 cd/m^2 .
- Overall Uniformity (U_0) = 0.357.

Exterior Scene 1 / Ground Element 1 / Surface 1 / Value Chart (L)



Values in Candela/m², Scale 1 : 143

Not all calculated values could be displayed.

Position of surface in external scene:

Marked point:

(0.000 m, 0.000 m, 0.000 m)



Grid: 128 x 64 Points

L_{av} [cd/m^2]
4.46

L_{min} [cd/m^2]
1.59

L_{max} [cd/m^2]
8.63

Fig 6.16: Value chart

Table 6.6: Design Summary for All the luminaires

Main Light source	Quantity of Luminaire	Average mesopic luminance (L_m)	Overall Uniformity (U_o)
HPSV	3	1.64	0.264
MH	2	3.88	0.346
CWLED	2	4.46	0.357

CHAPTER 7

RESULT ANALYSIS

In this study photopic luminance is simulated for an area using different type of lamps. Corresponding mesopic luminance values are calculated from CIE 191:2010 Table. And also mesopic luminance for the said area of measurement is simulated by the method described in previous Chapter. The results are compared in different forms as comparison of simulated photopic luminance (L_p), Calculated mesopic luminance (L_m) & Simulated mesopic luminance (L_{ms}) for different lamps.

7.1 Comparison of Simulated photopic luminance (L_p), Calculated mesopic luminance (L_m) & Simulated mesopic luminance (L_{ms}) for different lamps

L_p , L_m , L_{ms} values are compared for 3 different set of lamps.

- A. High Pressure Sodium Vapour (HPSV) lamp.
- B. Metal Halide (MH).
- C. Cool White LED (CWLED).

7.1.1 For High Pressure Sodium Vapour (HPSV) lamp

Photopic luminance (L_p), Calculated mesopic luminance (L_m) & Simulated mesopic luminance (L_{ms}) values for HPSV lamp are shown in table 7.1

Main source	Simulated photopic luminance(L_p)	Calculated mesopic luminance (L_m)	Simulated mesopic luminance (L_{ms})
HPSV	1.69	1.634	1.64

Table 7.1 Average luminance values of HPSV

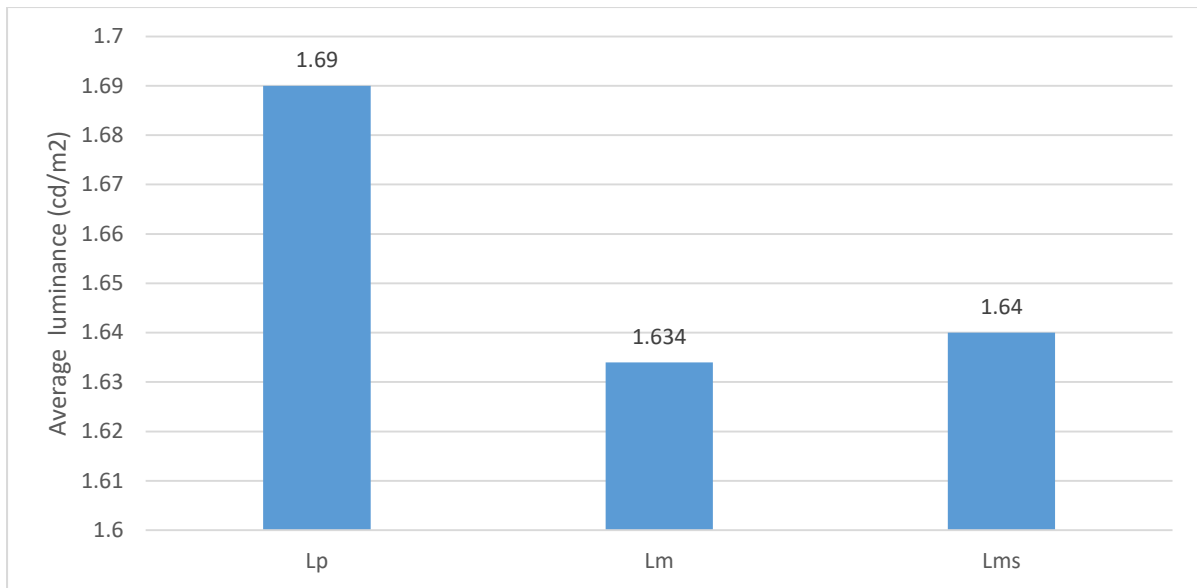


Fig 7.1 Comparison of L_p , L_m , L_{ms} of HPSV

Fig 7.1 shows that lamps which have lower S/P ratio, such as HPSV, have lower L_m value than L_p values in the mesopic zone. So in case of HPSV lamps effective luminance of the field will decrease in mesopic vision as compared to that of photopic luminance. There is slight difference between the calculated mesopic value (L_m) and the simulated mesopic value (L_{ms}).

Comparison of photopic and mesopic region uniformity

Photopic region uniformity ($U_{0,p}$) and Mesopic region uniformity ($U_{0,m}$) are shown in table 7.2

Main source	Photopic region uniformity	Mesopic region uniformity
HPSV	0.265	0.264

Table 7.2 photopic and mesopic region uniformity

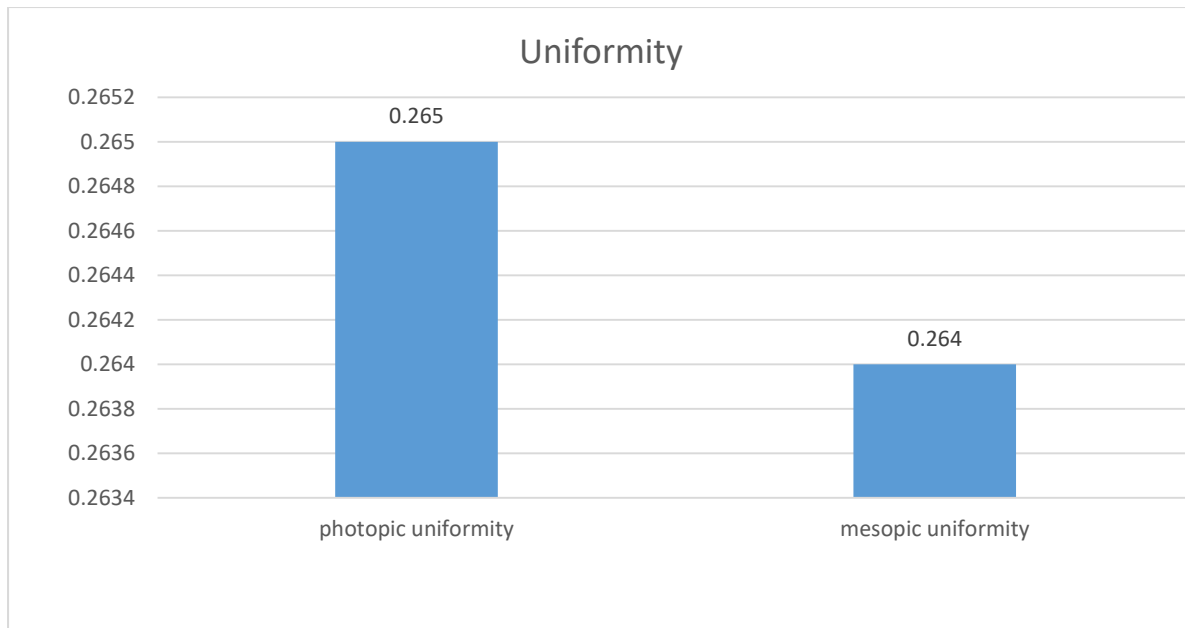


Fig 7.2 Comparison of photopic and mesopic uniformity.

Fig 7.2 shows the comparison between simulated photopic region uniformity and simulated mesopic region uniformity.

7.1.2 For Metal Halide (MH) lamp

Simulated photopic luminance (L_p), Calculated mesopic luminance (L_m) & Simulated mesopic luminance (L_{ms}) values for MH lamp are shown in table 7.3

Main source	Simulated photopic luminance(L_p)	Calculated mesopic luminance (L_m)	Simulated mesopic luminance (L_{ms})
MH	3.86	3.88	3.88

Table 7.3 Average luminance values of MH

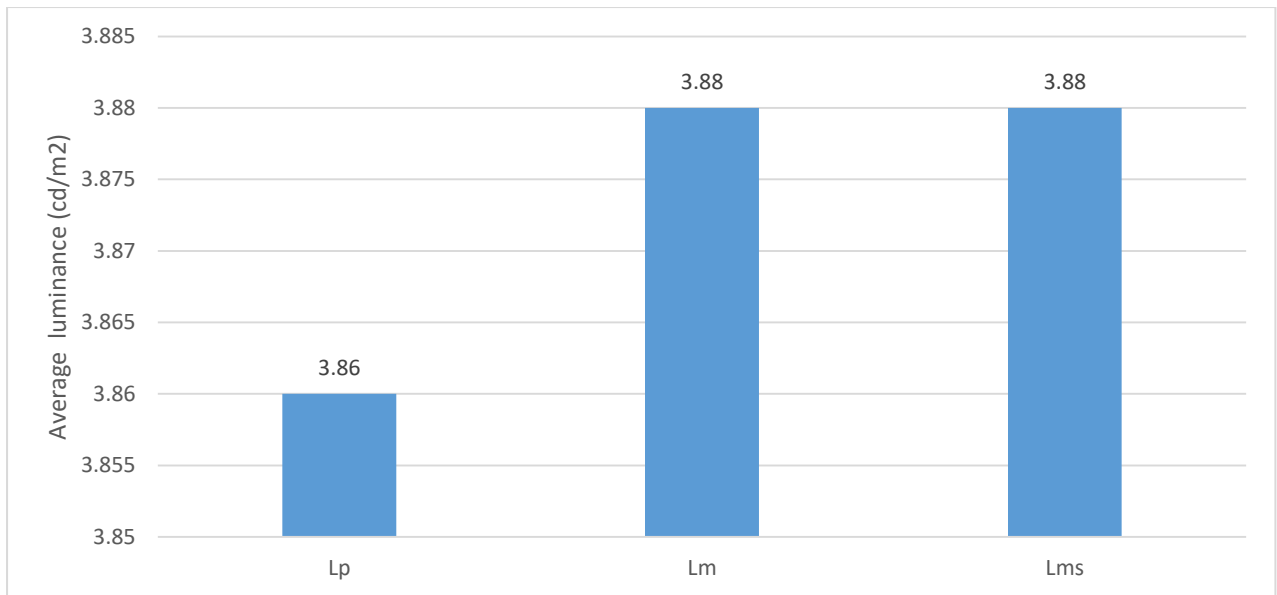


Fig 7.3 Comparison of L_p , L_m , L_{ms} of MH

Mesopic luminance values for Metal Halide are higher than photopic luminance, as seen in Fig. 7.3. Effective brightness is higher than the actual measured photopic luminance because MH lamps are a more white source than HPSV. Due to the S/P ratio of 1.32 of MH lamps, the effective brightness of the field will therefore be greater in mesopic vision than in photopic vision. — There is no difference between the calculated mesopic value (L_m) and the simulated mesopic value (L_{ms}).

Comparison of photopic and mesopic region uniformity

Photopic region uniformity ($U_{0,p}$) and Mesopic region uniformity ($U_{0,m}$) are shown in table 7.2

Main source	Photopic region uniformity	Mesopic region uniformity
MH	0.347	0.346

Table 7.4 photopic and mesopic region uniformity

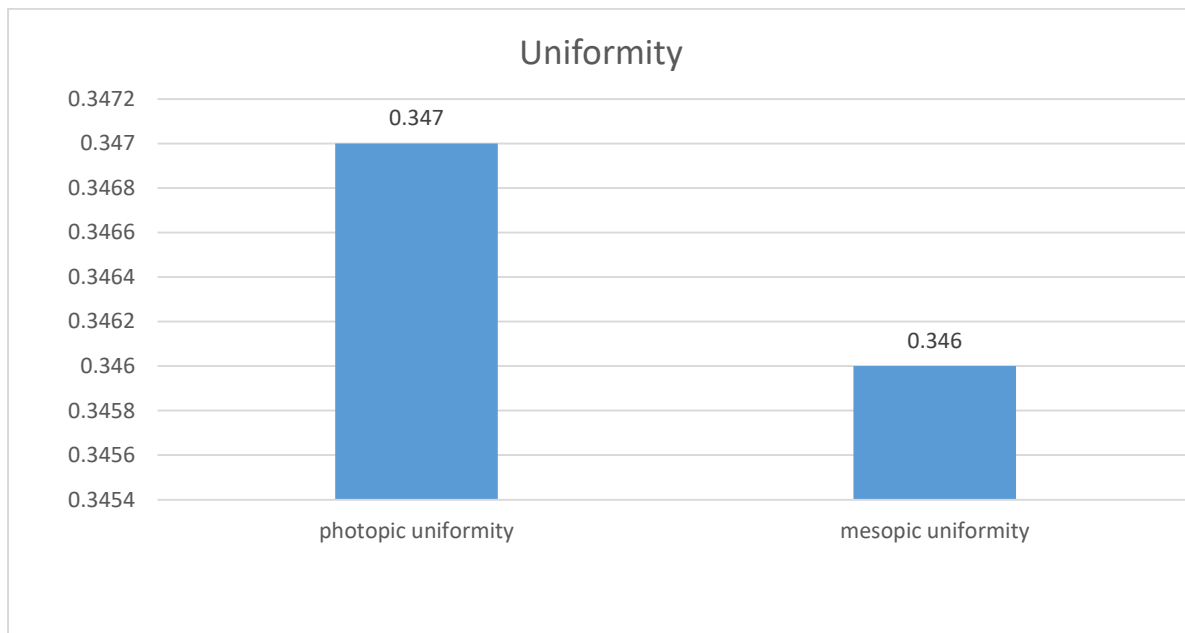


Fig 7.4 Comparison of photopic and mesopic uniformity.

Fig 7.4 shows the comparison between simulated photopic region uniformity and simulated mesopic region uniformity.

7.1.3 For Cool White LED (CWLED)

Simulated photopic luminance (L_p), Calculated mesopic luminance (L_m) & Simulated mesopic luminance (L_{ms}) values for MH lamp are shown in table 7.5

Main source	Simulated photopic luminance(L_p)	Calculated mesopic luminance (L_m)	Simulated mesopic luminance (L_{ms})
CWLED	4.44	4.47	4.46

Table 7.5 Average luminance values of CWLED

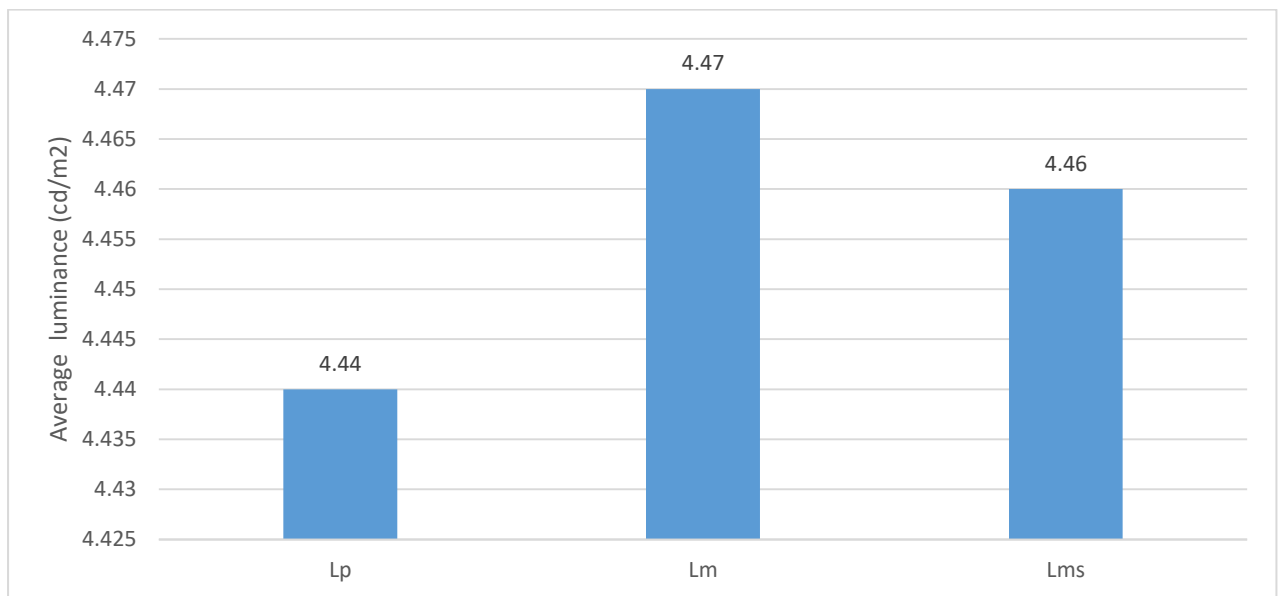


Fig 7.5 Comparison of L_p , L_m , L_{ms} of CWLED

Higher S/P ratio lamps, like CWLED, displayed L_m values that were noticeably greater than L_p values. According to Fig. 7.5, mesopic luminance for Cool White LEDs is higher than photopic luminance. In the case of CWLED sources, effective brightness is higher than the actual measured photopic luminance because of the existence of additional bluish content in its spectrum. Due to its S/P ratio of 2.02, mesopic vision will have a field of view that is more effective than photopic vision. In the mesopic area, those lamps would provide the best energy-efficient performance. There is slight difference between the calculated mesopic value(L_m) and the simulated mesopic value(L_{ms}).

Comparison of photopic and mesopic region uniformity

Photopic region uniformity ($U_{0,p}$) and Mesopic region uniformity ($U_{0,m}$) are shown in table 7.6

Main source	Photopic region uniformity	Mesopic region uniformity
CWLED	0.357	0.357

Table 7.6 photopic and mesopic region uniformity

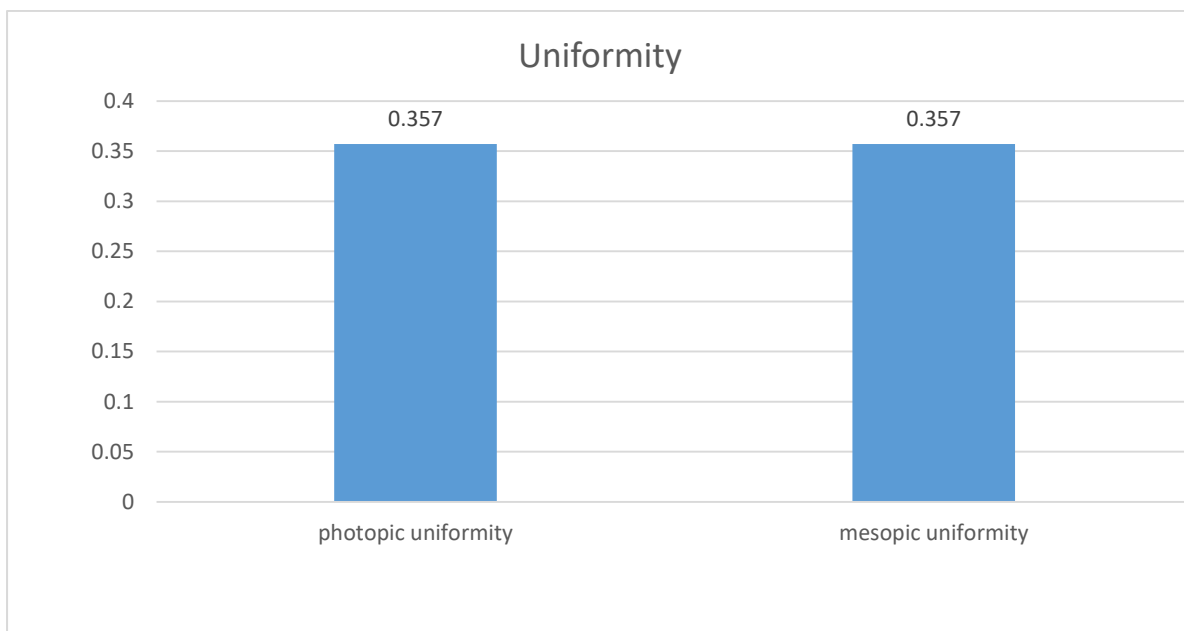


Fig 7.6 Comparison of photopic and mesopic uniformity.

Fig 7.6 shows the comparison between simulated photopic region uniformity and simulated mesopic region uniformity.

7.2 Comparison of average luminances for different lamps

Simulated photopic luminance (L_p), Calculated mesopic luminance (L_m) & Simulated mesopic luminance (L_{ms}) values for HPSV, MH, CWLED lamp are shown in table 7.7

Main source	Simulated photopic luminance(L_p)	Calculated mesopic luminance (L_m)	Simulated mesopic luminance (L_{ms})
HPSV	1.69	1.634	1.64
MH	3.86	3.88	3.88
CWLED	4.44	4.47	4.46

Table 7.7 Average luminance values of HPSV, MH, CWLED

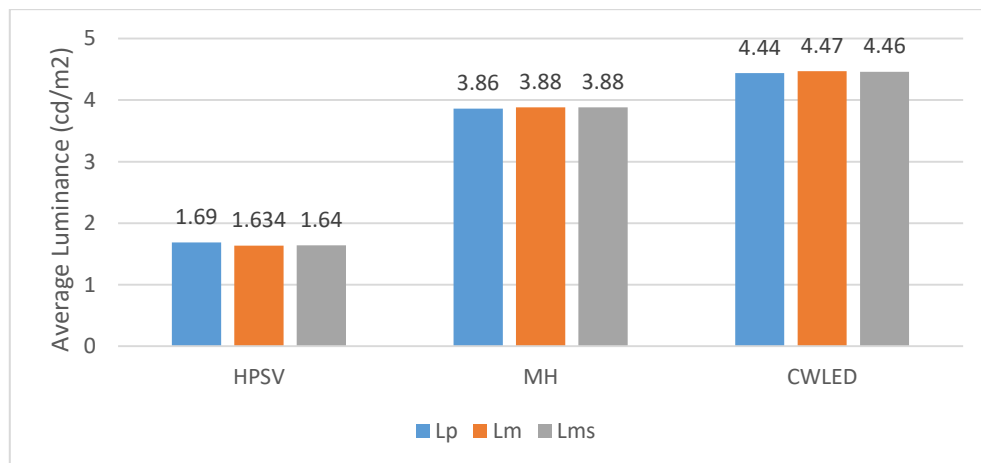


Fig 7.7 Comparison of L_p , L_m , L_{ms} for different lamps

As seen in Fig. 7.7, HPSV lamps, which have a lower S/P ratio, have lower mesopic luminance values than photopic luminance. The environment is less bright because to the decreased mesopic luminance value. For that reason, larger wattage lamps are needed for the outdoor lighting system. However, light sources with a higher S/P ratio, such as MH and CWLED, have mesopic luminances that are greater than photopic luminances. These are more energy-efficient in comparison.

7.3 Validation of the proposed Model

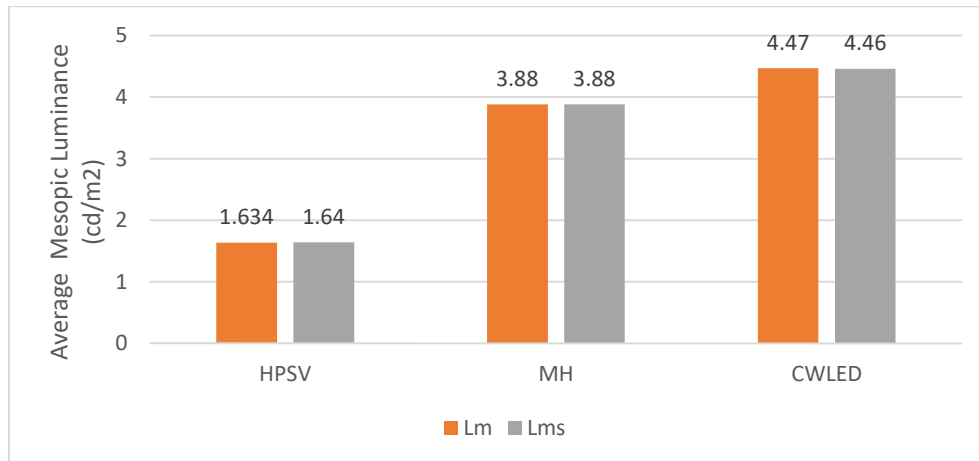


Fig 7.8 Comparison of L_m , L_{ms} for different lamps

The calculated mesopic value using CIE 191: 2010, denoted as L_m and represented in orange, closely aligns with the simulated mesopic value using DIALux, denoted as L_{ms} in grey which is shown in fig 7.8 for different lamps (HPSV,MH,CWLED) . So the proposed method in this thesis follows and satisfies the condition provided in CIE 191 2010.

CHAPTER 8

CONCLUSIONS & FUTURE SCOPE

Conclusions & Future scope

The main goal of the proposed system is to use of mesopic values in DIALux, a lighting design software primarily designed for photopic calculations. This approach aimed to address specific scenarios where mesopic vision plays a crucial role in lighting design, such as outdoor street lighting. While DIALux is traditionally optimized for photopic conditions, our adaptation to mesopic values allowed for a more comprehensive analysis in select lighting applications.

In this thesis work, we compared the simulated mesopic luminance values generated by Dialux with the values obtained through interpolation from known photopic luminance values and S/P (Scotopic/Photopic) ratios using the CIE 191-2010 method. we found that the mesopic luminance values generated by Dialux and those obtained through interpolation using CIE 191-2010 are generally in close agreement for a wide range of lighting scenarios and also we see that there is slight or no change in uniformity in both the simulated case(photopic and mesopic).

Lamps with lower S/P ratios, like High-Pressure Sodium Vapor (HPSV) lamps, exhibit lower L_m (mesopic luminance) values compared to their L_p (photopic luminance) values within the mesopic zone. Consequently, in such environments, the human eye perceives reduced brightness. To attain the same level of brightness, it becomes necessary to use lamps with higher wattage, leading to increased energy consumption. As a result, employing these low S/P ratio lamps in mesopic zones is not advisable from an energy management perspective. On the other hand, lamps with higher S/P ratios, such as Cool White Light Emitting Diodes (CWLEDs), demonstrate significantly higher L_{mes} values compared to their L_p values. These lamps are exceptionally efficient in the mesopic region, delivering optimal energy performance. It's worth noting that HPSV lamps are frequently chosen for their durable construction, good luminous efficacy, and extended lifespan. Nevertheless, when operating in the mesopic zone, their performance tends to be less effective than LEDs with high S/P ratios.

Future work

Future projects should focus on collecting and standardizing mesopic lighting data for a wider range of light sources and conditions. This will facilitate more accurate and reliable mesopic design in DIALux. User-friendly interface within DIALux can be developed that allows designers to easily switch between photopic and mesopic modes and visualize the impact of mesopic design on their projects. Collaborate with lighting fixture manufacturers to create products specifically designed for mesopic applications, optimizing energy efficiency and performance. Explore the integration of light sensors that can adapt the lighting system in real-time based on mesopic conditions, enhancing energy efficiency and safety.

References

- [1] "Road Lighting: Fundamentals, Technology and Application", Wout van Bommel. Springer, 2015.
- [2] Commission Internationale de l'Eclairage. Recommended System for Visual Performance Based Mesopic Photometry. CIE Publication 191:2010. Vienna: CIE, 2010. 2 Puolakka M, Halonen L. Implementation of CIE 191 mesopic photometry – ongoing and future actions: Proceedings of the CIE, Hangzhou, China, September 19–21: 2012: 64–70.
- [3] Adapted from Encyclopedia Britannica 1994
- [4] O.N.Awasthi, Fundamentals of lighting , ISBN 978-81-8487-347-4; 2014.
- [5] Visibility , Performance and Perception Kenneth Siderius BSc , MIES, LC, LG Cooper Lighting.
- [6] M Eloholma, M Viikari, L Halonen, H Walkey, T Goodman, J Alferdinck, A Freiding, P Bodrogi, G Varady, "Mesopic models-from brightness matching to visual performance in night-time driving: a review". Lighting Res. Technol. 2005; Vol.37; 155-175
- [7] T Uchida and Y Ohno. Simplified field measurement methods for the CIE mesopic photometry system. Panasonic Corporation, Osaka, Japan, National Institute of Standards and Technology, Gaithersburg, MD, USA ; Lighting Res. Technol. 2017; Vol. 49: 774–787.
- [8] Adjustment of Lighting Parameters from Photopic to Mesopic Values in Outdoor Lighting Installations Strategy and Associated Evaluation of Variation in Energy Needs. Enrique Navarrete-de Galvez 1 , Alfonso Gago-Calderon 1,* , Luz Garcia-Ceballos 2, Miguel Angle Contreras-Lopez 2 and Jose Ramon Andres-Diaz
- [9] Simplified field measurement methods for the CIE mesopic photometry system by T Uchida and Y Ohno, Panasonic Corporation, Osaka, Japan, National Institute of

Standards and Technology, Gaithersburg, MD, US;Lighting Res. Technol.2017;Vol.49;774-787

[10] Driver decision making in response to peripheral moving targets under mesopic light levels Yukio Akashi PhD,MS Rea PhD and JD Bullough PhD Lighting Research Center, Rensselaer Polytechnic institute Troy, NY, USA

[11] Defining the visual adaptation field for mesopicphotometry Does surrounding luminance affect peripheral adaptation?T Uchida MEnga,b and Y Ohno PhD Panasonic Corporation, Osaka, Japan National Institute of Standards and Technology, Gaithersburg, MD, USA

[12] CIE Mesopic photometry –implementation for outdoor lighting by Liisa Halonen, Grega Bizjak,laboratory of Lighting & photometry

[13] [Rea et al 2004]: Rea MS, Bullough JD, Freyssinier-Nova JP,And Bierman A.A proposed Unified system of photometry. Lighting Research And Technology,36(2):85-111,2004.

[14] Goodman T, Forbes A, Walkey H, Eloholma M, Halonen L, Alferdinck J, Freiding A, Bodrogi P, Várady G, and Szalmas A. Mesopic visual efficiency IV: a model with relevance to night time driving and other applications. Lighting Research and Technology, 39(4), 2007.

[15] Akashi Y, Rea MS, and Bullough JD. Driver decision making in response to peripheral moving targets under mesopic light levels. Lighting Research and Technology, 39:53–67, 2007.

[16] M Eloholma, M Viikari, L Halonen, H Walkey, T Goodman, J Alferdinck, A Freiding, P Bodrogi, G Varady, “Mesopic models-from brightness matching to visual performance in night-time driving: a review”. Lighting Res. Technol. 2005; Vol.37; 155-175.